Alpine 1/Federal
Final Report - Part 2
Temperature Gradients, Geothermal Potential, and Geology

James C. Witcher[1], W. Richard Hahman[2], and Chandler A. Swanberg[3]

June 1994

ARIZONA GEOLOGICAL SURVEY
CONTRIBUTED REPORT CR-94-F

Prepared for the
Arizona Department of Commerce
Energy Office
Phoenix, Arizona

[1]Geologist, Southwest Technology Development Institute, New Mexico State University, Las Cruces, NM
[2]Consultant-Registered Geologist, Las Cruces, NM
[3]Geothermal Consultant-Geophysicist, Phoenix, AZ

TABLE OF CONTENTS

LIST OF FIGURES

figure **page**

LIST OF TABLES

LIST OF APPENDICES

appendix **page**

ACKNOWLEDGMENTS

The community of Alpine, Arizona is thanked for their friendliness, hospitality, and assistance to the drillers and geologists. The fax machines, good mail service, good meals, hardware and other vendors, and friendly smiles in Alpine all contributed to a successful drilling project. Personnel at the U. S. Forest Service (USFS), Apache-Sitgreaves Forest, Alpine District Office, provided valuable assistance by providing gate keys, locating an acceptable and nearby site to place drilling fluids, and suggesting a very good access from the highway to the drill site. Bob Dyson of the Alpine District Office is especially thanked. John Sass of the U. S. Geological Survey (USGS) is thanked for providing preliminary heat-flow data and discussions on the thermal regime of the area. Chuck Chapin, Director, and Richard Chavez of the New Mexico Bureau of Mines and Mineral Resources (NMBMMR) are thanked for sending a loading crew and a truck to Alpine to pickup the Tertiary core on loan from Larry Fellows, Director, Arizona Geological Survey (AGS). Informal discussions on the geology of the region with Wes Peirce (AGS-Emeritus), Steve Rauzi (AGS), Andre Potochnik (ASU), Steve Cather (NMBMMR), Richard Chamberlin (NMBMMR), and Clay Conway (USGS) are greatly appreciated. Tonto's outstanding drillers and helpers formed a highly proficient and enthusiastic drilling crew. Mike LaOrange, Tonto Drill Forman, and Larry Pisto, Tonto Core Division Manager, are especially thanked for their close coordination and good communications which assisted the geologists tremendously. The staff, secretaries, and students at SWTDI/NMSU are also thanked for their assistance in various phases of this project. Funding for drilling the Alpine 1/Federal corehole was the Arizona Department of Commerce, Energy Office and the U. S. Department of Energy, Geothermal Division.

4.0 PREVIOUS STUDIES

A variety of regional geological, geophysical, and geochemical data indirectly infer geothermal potential. Much of this information is summarized in Stone (1980a); Stone and Witcher (1982). Late Miocene to Pleistocene volcanism in the White Mountains and Springerville volcanic fields is expressed by dominantly alkali basalt and subordinate tholeiite basalt as young as 0.50 my (Laughlin and others, 1979; Laughlin and others, 1980; Aubele and others, 1981; and Cooper and others, 1990). Volcanism of the White Mountains volcanic field is too old (greater than 6 to 8 my; Merrill and Pewe, 1977) to sustain high temperatures at shallow depth. No major differentiation or crustal contamination trends are observed in the younger rocks (<3 my) of the Springerville volcanic field that would indicate large amounts of silicic magmas are being produced (Condit and others, 1989). Over the last million years, volcanism rates for the Springerville field have waned, if not ceased for the last 0.3 my (Condit and others, 1989).

Basalt melts are formed in the mantle. In fact, alkali basalts with zenoliths of the mantle probably travel from the mantle to the surface in an eruption in a matter of days. Magma not erupted is left in the shallow crust as relatively small volume dikes and sills with large surface areas. Depending on magma volume, shape, and burial depth, most dikes and sills will cool to ambient crustal temperatures in a time much less than the youngest dated flows of the Springerville volcanic field (Lachenbruch and others, 1976). With differentiation and crustal melting, large voluminous silicic magma bodies may form as a result of very intense basaltic volcanism in an extensional stress regime (Wohletz and Heiken, 1992. Large silicic magma bodies can sustain high temperatures at shallow levels in the crust. However, there is no evidence for Pleistocene silicic magma formation in lavas erupted on the surface of the area. Also, the maximum volumetric rate of magma extrusion in the Springerville field was 2.8 x 10^{-4} km^3/yr or about half the maximum output rate estimated for the 7 to 9 my Mount Baldy volcano in the adjacent White Mountains volcanic field (Connor and others, 1992). While there is Quaternary basaltic volcanism in the area, it is clear that the type of volcanism, rates of magma input from the mantle, and age of the volcanism do not signify major geothermal resource potential.

One of the first geothermal reconnaissance studies in the region is that of Swanberg and others (1977), using aqueous geothermometry. Geothermometry is based upon temperature-dependent chemical equilibrium of water and rock. Fluids may leak or flow out of a geothermal reservoir or a thermal aquifer in equilibrium, cool and retain the chemical signature of higher temperatures. However, if the waters chemically re-equilibrate, mix, constituents precipitate out of solution, or if highly soluble minerals are dissolved after exiting the reservoir, the technique is not very accurate. The value of the Swanberg and others (1977) approach is that large areas may be filtered for anomalies and potential may be roughly ranked for more detailed exploration.

Witcher and Stone (1983) show that waters with high dissolved carbon dioxide content react with silicate minerals to produce erroneous silica geothermometers that require correction for excess non-temperature dependent dissolved silica. The high silica geothermometers in the Alpine and Nutrioso areas are the result of high dissolved carbon dioxide waters reacting with volcanoclastic rocks and releasing silica and not anomalous geothermal conditions. The high Na/K/Ca geothermometers near St. Johns are the result of calcium carbonate deposition.

A variety of potential field geophysical interpretations of data have implied anomalous subsurface heat in the region (Aiken, 1976; and Byerly and Stolt, 1977). Like all potential field methods, there are any number of configurations that may be modeled with iterative and downward continuation techniques (Nettleton, 1976). Therefore, if there is not adequate subsurface control for the geology or if unrealistic assumptions are made in the place of control, highly misleading models result. Gravity, magnetic, and depth to Curie point magnetic interpretations all fall under the potential field umbrella. Potential field geophysical methods can have value in early reconnaissance to point out possible buried structure. In later stages of exporation, production drilling, and reservoir management, potential field survey results and quantitative models have much value and utility. Also, more is known about subsurface geology to constrain quantitative modeling; therefore, the models more accurately reflect subsurface conditions. The Aiken (1976) gravity low may be a consequence of the thick sequence of Tertiary rocks in the Alpine area rather than a subsurface thermal anomaly or heat source.

Heat flow is also a potential field geophysical method. However, heat flow techniques have an advantage because heat flow directly measures the thermal regime. Where no important vertical ground-water flow occurs (conductive regime), shallow heat-flow information may be used with some confidence to project temperatures at greater depth by making estimates of subsurface thermal conductivities for rocks at greater depth. Where subsurface stratigraphy is well known, such temperaure estimates can be fairly precise.

All considered, published heat-flow information for the area is the only "hard" data available to reliably predict subsurface temperature. Stone (1980b) concluded that the heat flow for the area was somewhat elevated (87 to 115mWm^{-2}); but did not project temperatures to greater depth. An average Colorado Plateau heat flow is 68 mWm^{-2}; while the adjacent Basin and Range has a modal heat flow of 85 mWm^{-2} (Morgan and Gosnold, 1989).

Elsewhere in the region, Minier and Reiter (1991) and Minier and others (1988) describe high heat-flow (>90 mWm^{-2}) areas in a region of overall intermediate heat flow in the Mogollon Slope region just to the east in New Mexico. Minier and Reiter (1991) postulated that the anomalies may result from deep ground-water disturbance in large regional Colorado Plateau structures or from basaltic intrusion of weak zones in the crust. To test these ideas, Minier and others (1988) and Minier and Reiter (1989) present some analytical models for various intrusions. The models show that in order to appreciably affect the thermal regime for a period of time up to a million years, the "instantaneous" intrusions are required to be shallow (<5km depth) and large (1 to 2 km thick and 30 km by 30 km lateral dimensions or have a volume of 900 and 1,800 km^3). In view of the fact that magma extrusion rates are of the order of 10^{-4} km^3/yr for the Springerville volcanic field for the last 3 my and that the magmas, especially zenolith-bearing alkali basalts, probably came up directly from the mantle without storage in a crustal magma chamber, evidence for single basaltic intrusions in the crust with 1,000 km^3 volumes during the last 3 my is lacking in this region. Such a magma body would be larger than the total volume of lava extruded on the surface for the entire Springerville and White Mountains volcanic fields which span a time of 10 to 12 my. Therefore, high heat flow (90 to 120 mWm^{-2}) measurements do not necessarily indicate major Quaternary basaltic magmatic heat sources in the Alpine area.

As will be shown below, it is apparent that some proponents of HDR in the area have not accounted for rock thermal conductivity changes at depth and have uncritically relied heavily on indirect indicators reported in the literature to infer 200 C (400 F) temperatures at 10,000 feet depth or less.

5.0 THERMAL REGIME

5.1 BACKGROUND

Temperature gradients in the earth are the result of several heat transfer processes and properties. In the shallow crust and over relatively short depth intervals, conduction and convection are primary processes. Radiative transfer is not important at typical upper crustal temperatures and rock heat production does not change temperature gradients over short depth intervals. Therefore the magnitude of a temperature gradient in a conductive temperature regime is regulated mostly by rock thermal conductivity and local heat flow from the earth's interior. Heat flow is the product of the rock thermal conductivity and the temperature gradient.

5.2 TEMPERATURE GRADIENTS

On 22 October, 1993, Southwest Geophysical Surveys obtained an equilibrium temperature log of the Alpine 1/Federal borehole. Appendix 10 is a summary table of the Alpine1/Federal temperature log with temperature picks at 25 feet intervals. Figure 12 is a temperature versus depth plot for the Alpine 1/Federal borehole. Overall, temperature gradients decrease with depth in this borehole (Table 11). A relatively high temperature gradient (72 C/km) in the upper 300 to 800 feet depth interval changes to a relatively normal temperature gradient (33 C/km) in the lower 700 feet of the hole. Thermal conductivity variation probably accounts for the temperature gradient differences. Clay-rich sandstones and volcanoclastic sediments in the upper portion of the hole have relatively low thermal conductivity (see Stone, 1980b). Quartzose sandstones and carbonate rocks in the lower portion of the hole typically have high in thermal conductivity. Similar high thermal conductivity rocks will occur downward and deep into the Precambrian basement.

Detailed rock thermal conductivity measurements and heat-flow analysis for the Alpine 1/Federal borehole will be reported by John Sass, U. S. Geological Survey (USGS), an invited participant of the State of Arizona, in a forthcoming USGS Open-File Report.

Table 11. Temperature gradients in the Alpine 1/Federal borehole.

depth (ft)	temperature gradient (C/km)	intercept temperature (C)	correlation	formation
300 to 800	72.1	7.7	0.99970	Pueblo Creek
800 to 1100	64.1	9.7	0.99938	Pueblo Creek
1500 to 2600	57.2	10.8	0.99978	Mogollon Rim
2800 to 3400	47.8	17.8	0.99931	Dakota/San Andres
3800 to 4500	32.8	33.6	0.99920	Corduroy/Ft Apache

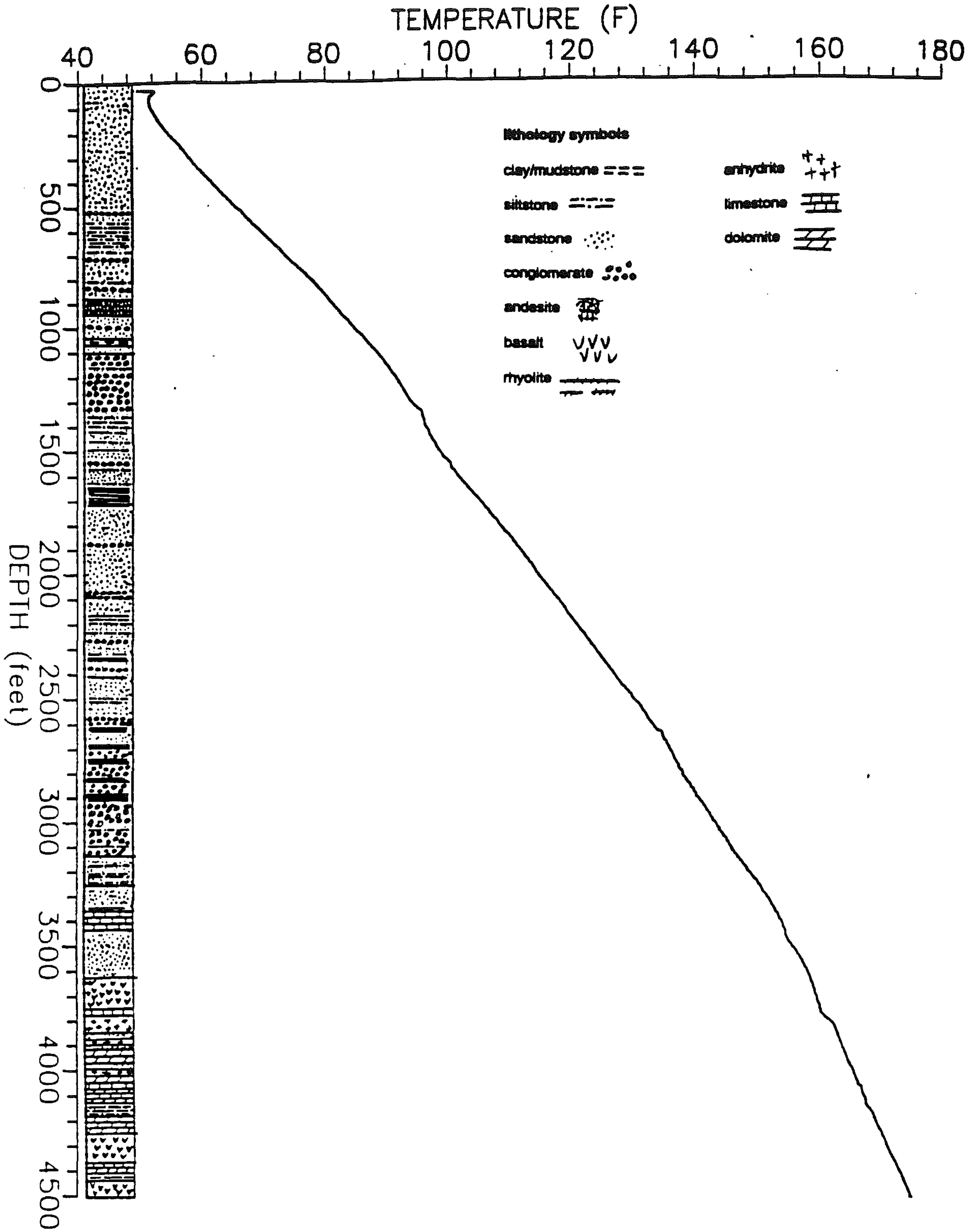

Figure 12. Equilibrium temperature versus depth for the Alpine 1/Federal borehole.

5.3 HEAT FLOW AND SUBSURFACE TEMPERATURE

A preliminary heat-flow estimate is 96 mWm^{-2} (personnel communication, John Sass, USGS/Flagstaff). The Alpine 1/Federal heat flow is practically the same as the SJ-116 measurement of Stone (1980) (115mWm^{-2}) if thermal conductivity measurement errors are considered for both sets of data. Typical thermal conductivity measurement errors are 5 to 15 percent.

Figure 13 is a pre-drilling temperature versus depth projection (solid line) that was based on heat-flow information reported by Stone (1980) for the SJ-116 well at Alpine Divide. Thermal conductivity estimates, used in the temperature projection at depth, were typical generic values for rock types expected at depth (Blackwell and Steele, 1989; and Roy and others, 1981). Actual temperatures measured in the Alpine 1/Federal borehole are shown at 1,000 feet intervals with the "X" symbol. Predicted temperature at 4,500 feet was 76 C and very close to the actual measured temperature of 78.6 C. An average temperature gradient in the Precambrian will range between 30 and 40 C/km. Heat flow and thermal conductivity constraints indicate that a gradient over 40 C/km will not occur.

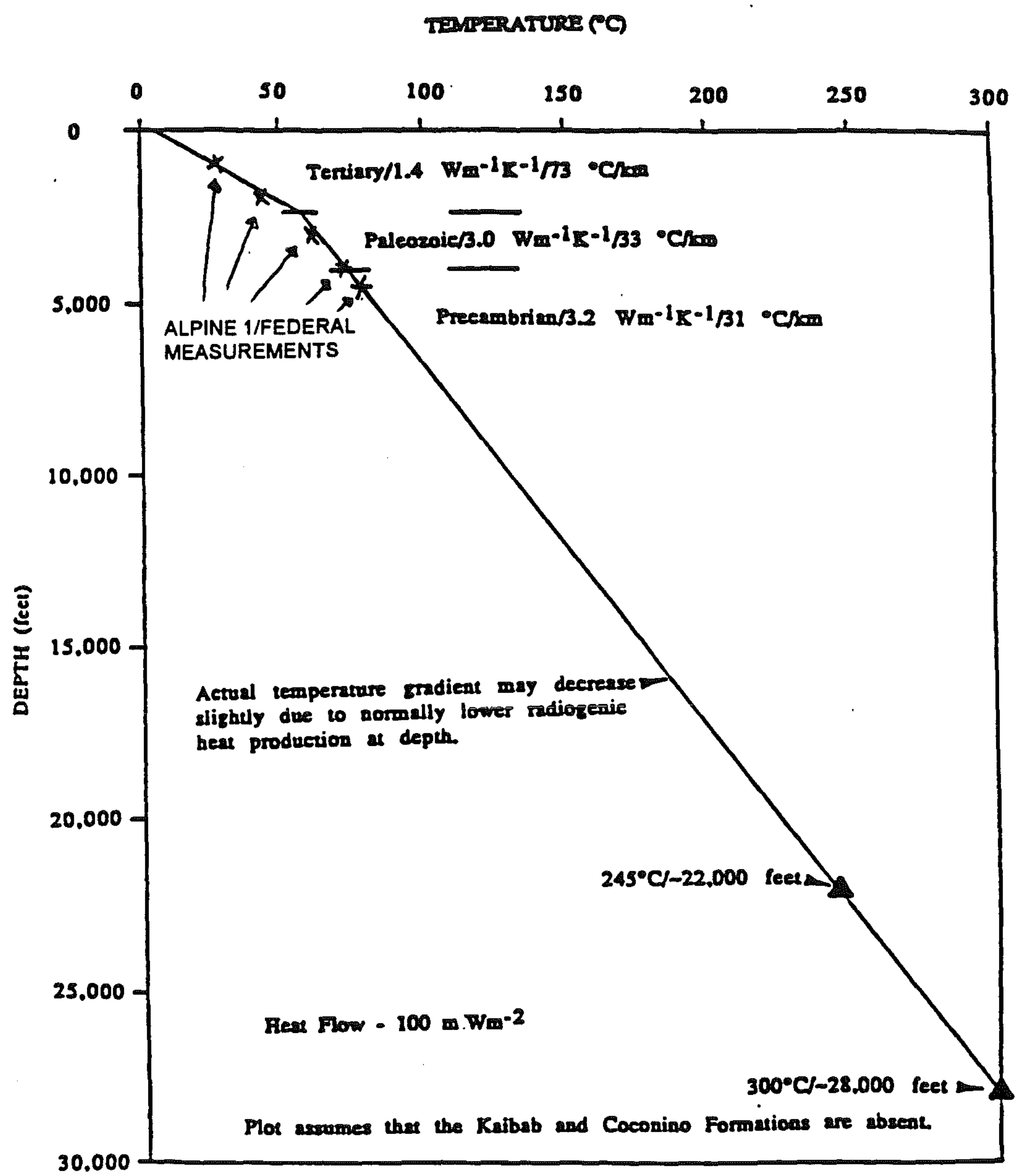

Figure 13. Temperature-depth plot based upon heat-flow data for the Alpine Divide site (SJ-116).

6.0 GEOTHERMAL POTENTIAL

The Alpine 1/Federal borehole is not situated over a convective hydrothermal geothermal system. Convective geothermal systems are generally associated with temperature gradients that greatly exceed 150 C/km. Therefore, any geothermal resource potential in the Alpine-Nutrioso area is conductive hydrothermal (deep confined aquifer) and hot dry rock (HDR) associated with the regional heat flow and accompanying geotherm.

Hot dry rock (HDR) is a technology under development. The concept and a degree of technical feasibility has been demonstrated at Fenton Hill, New Mexico. On the other hand, commercial feasibility has not been demonstrated for the general use of HDR beyond the Federal research effort at Los Alamos National Laboratory. Electrical power production and direct-use geothermal applications are possible end uses of a productive HDR geothermal reservoir. Each will have unique requirements and economics aside from the costs and requirements of the HDR reservoir. Considering current and projected fossil fuel cost, assuming no major unforeseen overseas oil crises, a site with near-term HDR potential should be located in an area with currently high electrical and/or other high utility fuel costs and high demand. In other words, the site should be in a good marketable position. Also, a near-term HDR site should have relatively high resource quality for lower end drill costs and for fewer problems in creating the man-made reservoir that connects the injection and production wells. A readily available and assured water supply is essential.

Because of drilling costs, which currently increase non-linearly with depth, the quality and near-term feasibility of a site will largely depend upon the basement (Precambrian) temperature gradient. This is because the temperature gradient will dictate the depth necessary to drill for temperatures required for economic thermal energy extraction from the HDR reservoir. Armstead and Tester (1987) categorize HDR resources according to quality or grade. Two grades are used, thermal and non-thermal. Thermal grade includes resources characterized by gradients of 38 C/km or greater. Non-thermal grade "resources" have less than 38 C/km gradients. The Alpine-Nutrioso resource is non-thermal.

Recently, Tester and Herzog (1990) define three grades of HDR resources for the purpose of investigating economic feasibility. A high-grade resource has a gradient above 80 C/km; a mid-grade resource has a gradient of 50 C/km; and a low-grade resource has a gradient of 30 C/km. Within the Tester and Herzog (1990) framework, the Alpine-Nutrioso area falls into the low- to mid-grade category. In other words, wells depths of 10,000 to over 20,000 feet are required to obtain usable heat, depending upon whether direct-use or electrical power production is done.

Table 12 summarizes the breakeven cost of electricity with current technology. The Tester and Herzog (1990) model calculates cost on a per KWe installed basis. With a 40 C/km gradient costs for electricity are 12 to 18 cents per kilowatt-hour. These costs are unlikely to be economically attractive to a utility or its customers. The consumers actual costs would be even higher.

Table 12. Economic model costs for HDR electrical power.

temperature gradient (C/km)	electricity breakeven cost ($/w/hr) with current technology
30	0.375 to 0.235
40	0.184 to 0.119
50	0.121 to 0.082

Table 13 summarizes the break even costs for direct-use HDR geothermal utilization with the Tester and Herzog (1990) model. Costs are based upon a supply rate of heat at one million Btu per hour (MMBTU). Costs for direct-use are a little more attractive for HDR in the Alpine area. This is especially true for space heating, using lower temperature fluids. The key parameters involved with direct-use geothermal in the Alpine-Nutrioso area are heating loads and natural gas availibility. Climate in the area requires space heating for much of the year so that potentially large heating loads may exist in the area. Inexpensive natural gas is not available. Direct-use space heating in the Alpine-Nutrioso area, using the 40 C/km gradient model of Tester and Herzog (1990) indicates a $4 to $7 per MMBTU break even cost. This cost may be marginally economic for specific types of large space heating requirements. With natural gas costs in the $3 to $5 MMBTU ($5 to $7 MMBTU with boiler inefficiencies accounted), it is unlikely that commercial enterprises would relocate to the area for industrial process heat or space heat from geothermal resources.

The best potential direct-use HDR geothermal application is likely to be a district heating system for homes, schools, businesses, and government buildings at Alpine. Costs per MMBTU will be higher than model costs because additional costs would be encurred for distribution lines. However, geothermal energy costs could potentially compete with current propane use in Alpine. Such a system could operate as a utility and have initial capital costs subsidized with government aid and matching grants. Detailed study, beyond the scope of this report, is required to obtain specific feasibility for geothermal district heating at Alpine.

Table 13. Economic model costs for HDR direct-use geothermal.

temperature gradient (C/km)	cost high-temp (> 80 C) direct-use for industrial applications ($/MMBTU)	cost low-temp (<80 C) direct-use for space heating ($/MMBTU)
30	16.6 to 9.7	10.6 to 6.3
40	9.7 to 5.7	7.2 to 4.3
50	6.9 to 4.1	5.5 to 3.3

7.0 GEOLOGY

7.1 PREVIOUS STRATIGRAPHIC STUDIES AND NOMENCLATURE

The Alpine 1/Federal borehole is located within 15 miles of the Arizona and New Mexico border. Geologic nomenclature frequently changes across political boundaries. Also, the borehole is located near the transition between the Colorado Plateau and the Basin and Range/Rio Grande rift tectonic provinces, each with different nomenclature. In addition, several regional geologic trends converge in this area to complicate stratigraphic studies. Furthermore, relatively outdated reconnaissance geologic studies are the only available information specific to the Alpine region (Wrucke, 1961; Sirrine, 1956; and Weber and Willard, 1959). Prior to drilling of the Alpine 1/Federal borehole, no hard pre-Tertiary stratigraphic information existed for the Alpine area. On the other hand, many recent studies of the geology of areas surrounding the Alpine region have been published. These studies, when compared to each other and older literature, use widely ranging stratigraphic nomenclature, depending upon location and regional depositional interpretations. This is mainly the result of sparse data and large areas of interpretation. The following discussion outlines the stratigraphic nomenclature used for the Alpine 1/Federal. The discussion will update usage for the area and point out controversial stratigraphic nomenclature.

Outcrops of Tertiary rocks in the Alpine area are frequently designated as the Tertiary Datil Formation or Tertiary Datil Group. However, Osburn and Chapin (1983) restrict the use of Datil in its type locality in the eastern Datil-Mogollon region in New Mexico to volcanic rocks and related sediments beneath the 32 my Hells Mesa Tuff. The Hells Mesa Tuff is not known to extend into the Alpine region or into much of the western Datil-Mogollon region of New Mexico and Arizona. In the Alpine area, rocks similar to the Datil Group extend upward to the base of basaltic rocks which cap Escudilla Mountain. The Escudilla Mountain flows probably represent the Bearwallow Mountain Andesite (personnel communication, Richard Chamberlin, NMBMMR, Socorro, NM). Marvin and others (1987) bracket the Bearwallow Mountain andesite at 23 to 27 my. A sanadine-rich ash-flow tuff outcrops a short distance below the Escudilla Mountain basaltic rocks and near the top of the Tertiary volcanoclastic sedimentary section (Wrucke, 1961). The ash-flow tuff may correlate with the regionally extensive Bloodgood Canyon Tuff that Marvin and others (1987) show is 28 to 29 my. In any case, rocks similar to the Datil in the Alpine area are younger, at least in part, than the 32 my Hells Mesa Tuff. A new formation, defined by recent mapping in the Bull Basin Quadrangle in New Mexico about 15 to 20 miles southeast of Alpine, is probably correlative with the Tertiary rocks encountered in the upper part of the Alpine 1/Federal borehole. Ratte (1989) applies the new name, Pueblo Creek Formation, to a Tertiary volcanic and volcanoclastic unit in the western Datil-Mogollon region which overlies the Eocene-Paleocene Baca Formation. This study uses the Ratte (1989) Pueblo Creek Formation nomenclature.

Early Tertiary sediments beneath the Pueblo Creek Formation that have Precambrian basement and Paleozoic provenance are variously designated in the region as the Baca Formation (Cather and Johnson, 1984), Eager Formation (Sirrine, 1956), Rim Gravels (Cooley and Davidson, 1963), and the Mogollon Rim Formation (Potochnik, 1989). The nearest complete measured section of this unit is that of Potochnik (1989). Potochnik's section also contains intermediate volcanic clasts in the basal conglomerate, which is not a characteristic of the Baca Formation to the east in New Mexico. The Eocene rocks in the Alpine1/Federal corehole also contain andesite clasts in the basal conglomerate. Therefore, the Mogollon Rim Formation nomenclature is used in this report.

The basal Pueblo Creek Formation grades downward into the Mogollon Rim or Baca Formation. Cather and Johnson (1984) define the top of the Baca Formation by a lack of volcanic clasts. This criteria fails to define the lower Tertiary package of rocks in the Alpine 1/Federal borehole. On the other hand, Potochnik (1989) selects the top where volcanic clasts are 50 percent or less in a sandstone or conglomerate. Neither criteria are easily suited to field mapping or easy delineation without petrographic studies.

Ratte (1989) maps a conglomerate with limestone, granite, gneiss, and volcanic clasts in the lower Pueblo Creek Formation below volcanic flows and volcanoclastic sediments. Field inspection of the stratigraphic section along the Red Hill Road between Beaverhead and Blue about 20 miles south of Alpine and 12 miles west of the type section for the Pueblo Creek Formation shows a relationships similar to the type section and the section in the Alpine 1/Federal borehole. Ratte and others (1969) briefly discuss the

Red Hill Road section and mentioned similar gravels east of Milligan Peak about 5 miles northeast of the Red Hill Road occurrence. In the Nutrioso area about 5 miles north of the Alpine 1/Federal borehole, Wrucke (1961) decribes additional gravels with granite and limestone clasts. In any case, conglomerate with Precambrian clasts near the base of the Pueblo Creek Formation is not localized to the Alpine 1/Federal borehole and appears to have regional extent and possibly regional importance. What is not clear is whether the conglomerate observed in the widely separated localities is the same conglomerate unit or actually several discontinous conglomerate lenses with different or similar stratigraphic position.

Muddy sandstones and mudstones with abundant silicic lapilli occur below the lower Pueblo Creek Formation gravels. The top of the Mogollon Rim Formation is picked at the bottom of the last macroscopically visible occurrence of silicic lapilli and silicic air fall tuffs.

A new stratigraphic unit was encountered in the Alpine 1/Federal borehole beneath the Mogollon Rim Formation. This unit is informally named the LaOrange formation. A similar orange and orange red unit was described near Round Top about 55 miles to the west of the Alpine 1/Federal borehole (Potochnik, 1989). The sandstone and siltstones of the LaOrange have different provenance than the unconformably overlying Mogollon Rim Formation basal conglomerate.

The LaOrange formation overlies a probable upper Cretaceous sandstone. This unit may represent the Dakota Formation (see Nations, 1989). The Dakota Formation overlies a Paleozoic limestone. This limestone is assigned to the San Andres Formation rather than the Kaibab

Formation in accordance with Peirce (1989). Likewise, the underlying sandstone unit is called the Glorieta Sandstone (see Peirce, 1989). The Glorieta Sandstone is a time-stratigraphic equivalent to the Coconino Sandstone.

Sandstones, evaporites, and carbonate rocks below the Glorieta Sandstone are the subject of long-standing debate concerning regional correlation and use of nomenclature. Debate will no doubt continue for some time to come. Eastward in New Mexico, rocks below the Glorieta Sandstone are assigned to the Yeso Formation. West of the Alpine borehole site, these rocks are assigned to the Supai Group (Peirce, 1989), Schenebly Hill Formation (Blakey, 1980), and the Supai Formation (Winters, 1963). The nomenclature of Peirce and Blakey is formulated upon regional stratigraphic arguments and interpretations based upon stratigraphic sections far removed from the Alpine area. For simplicity, the member designations of Winters (1963) are used in this report. The measured sections used by Winters are within 50 to 70 miles of the drill site and contain a limestone unit, the Fort Apache Limestone member, that is easily recognized in the Alpine 1/Federal borehole. Gerrard (1966) redefined the Fort Apache Limestone member of Winters (1963) as the Fort Apache member by including all contiguous limestone, dolomite and evaporites at the base of the Corduroy member. This redefinition is based correlations of subsurface well data in the region with the Mogollon rim outcrops of Winters (1963). Gerrard's correlations assume that the lowest and thickest dolomite/evaporite sequence in the Corduroy of subsurface well data is the same laterally continuous unit as the Fort Apache Limestone in outcrop. Because significant depositional environment change is implied between the dolomite/evaporite (possible intertidal to supratidal coastal sabka) and the limestone (restricted shallow marine), we prefer the unambiguous Winters (1963) nomenclature. Blakey retains the Gerrard (1966) Corduroy and Fort Apache member designations in his Schenebly Hill Formation; while Peirce (1989) upgrades the Winters (1963) Corduroy member to formation status in his Supai Group. The Peirce Corduroy Formation includes the Fort Apache Limestone as a member. From top to bottom the Winters (1963) nomenclature for Supai/Yeso units in the Alpine 1/Federal well are the Corduroy member, Fort Apache Limestone member, and the Big A Butte member.

7.2 FORMATION LITHOLOGY AND DISCUSSION

Appendix 8 is a descriptive lithologic log of the Alpine 1/Federal borehole. Appendix 9 is a graphic lithologic log of core from the Alpine 1/Federal borehole. The graphic log is at a scale of 1 inch equals 25 feet. Each 200 feet depth interval is in three parts. The first compares lithology to the penetration rate; the second compares the lithology to the natural gamma log; while the third compares lithology to the neutron log. Figure 14 is a summary graphic log of the penetration rate and lithology; Figure 15 is a summary graphic log of the natural gamma log and lithology; while Figure 16 is a summary graphic log of the neutron log and lithology. Table 14 is a summary of formations encountered in the core hole.

The upper Pueblo Creek Formation was encountered from the surface to 1,093 feet depth. The upper Pueblo Creek Formation consists mostly of

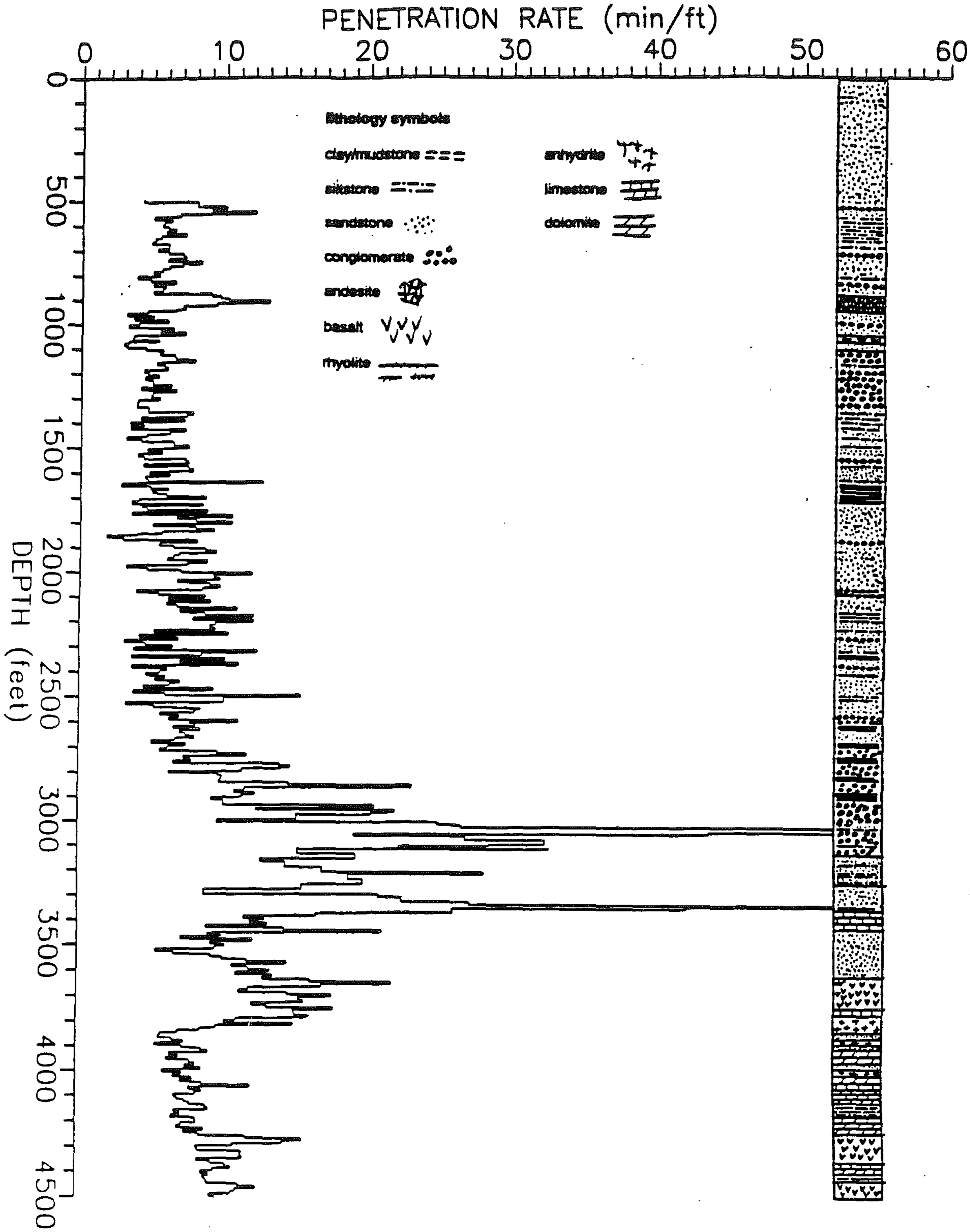

Figure 14. Summary graphic of core penetration rates and lithology.

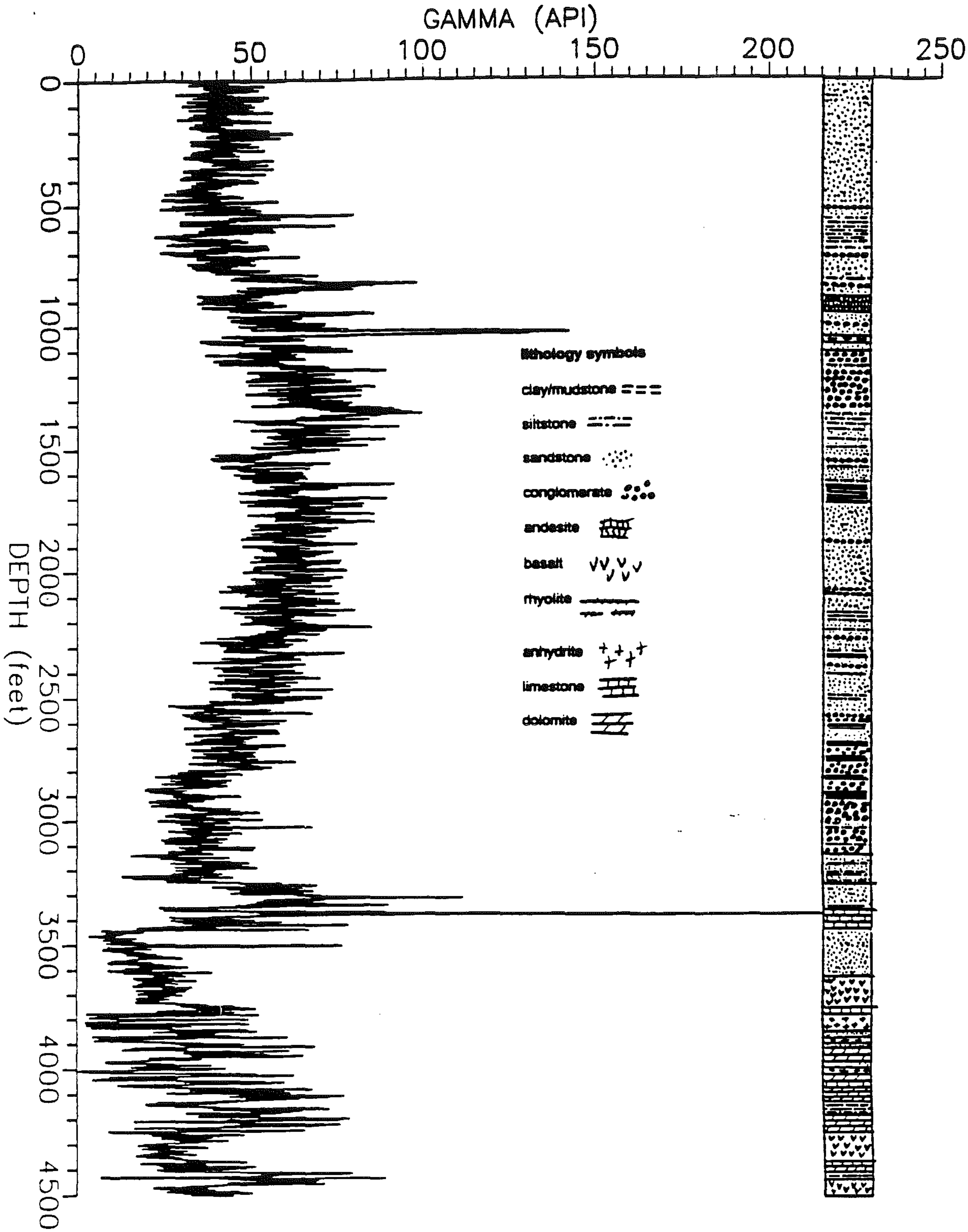

Figure 15. Summary correlation of the natural gamma log and lithology.

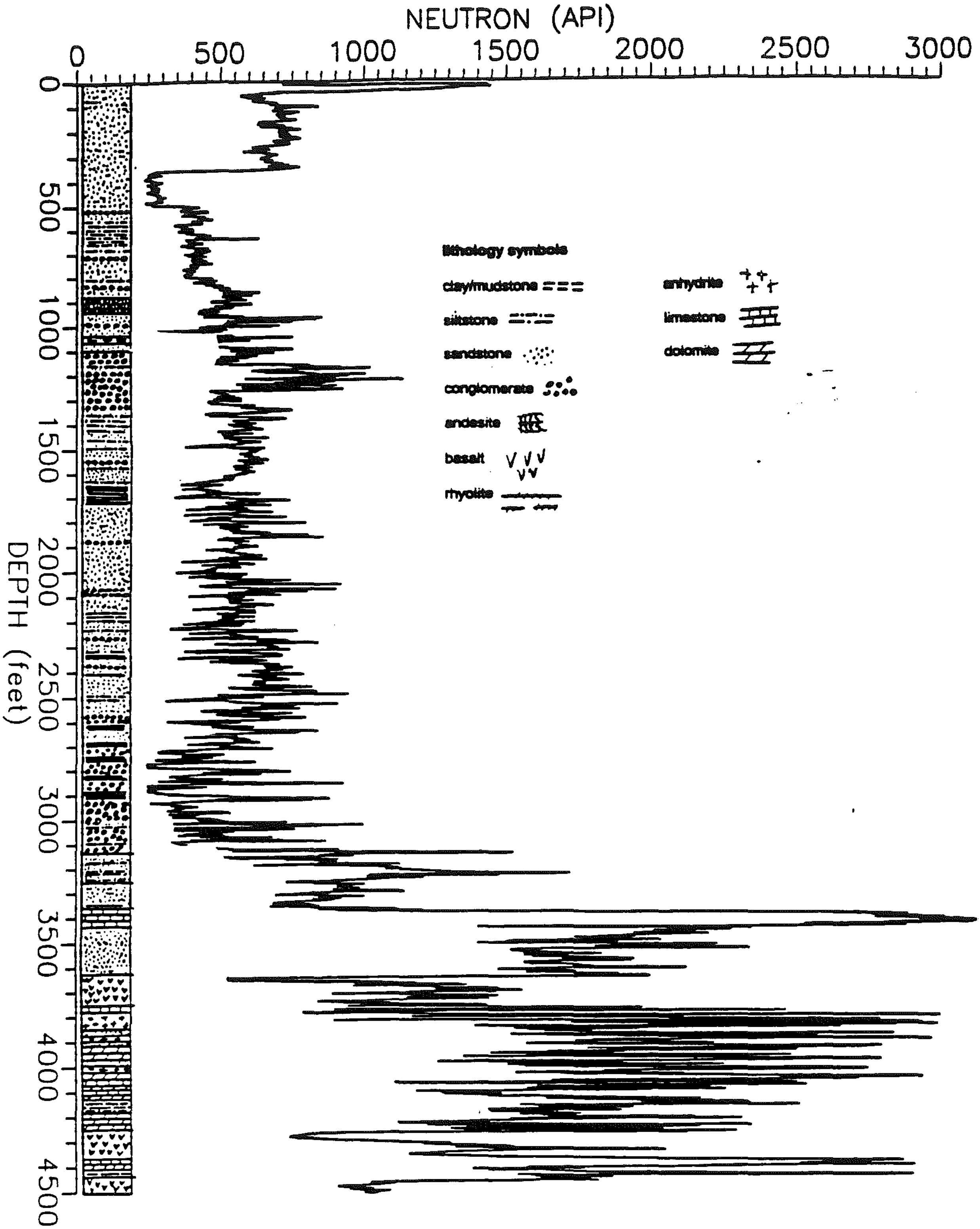

Figure 16. Summary correlation of the neutron log and lithology.

Table 14. Formation summary of the Alpine1/Federal borehole.

Tertiary Pueblo Creek Formation and Mogollon Rim formation
0 to 3,139 feet (0 to 957 m)
thickness 3,139 feet (957 m)
unnamed Tertiary (?)/Cretaceous(?) unit
3,139 to 3,246 feet (957 to 989 m)
thickness 107 feet (32 m)
Cretaceous Dakota (?) Sandstone
3,246 to 3,362 feet (989 to 1,025 m)
thickness 116 feet (36 m)
Permian San Andres Formation
3,362 to 3,436 feet (1,025 to 1,047 m)
thickness 74 feet (22 m)
Permian Glorieta Sandstone
3,436 to 3,639 feet (1,047 to 1,109 m)
thickness 203 feet (62 m)
Quaternary(?)/Tertiary (?) basaltic intrusion
3,639 to 3,751 feet (1,109 to 1,143 m)
thickness 112 feet (34 m)
Permian Corduroy member "Supai Formation" (Winters, 1963)
3,751 to 4,266 feet (1,143 to 1,298 m)
thickness 515 feet (157 m)
Quaternary(?)/Tertiary (?) basaltic intrusion
4,260 to 4,322 feet (1,298 to 1,317 m)
thickness 62 feet (19 m)
Permian Fort Apache Limestone member "Supai Formation" (Winters, 1963)
4,322 to 4,327 feet (1,317 to 1,319 m)
thickness 5 feet (2 m)
Quaternary(?)/Tertiary (?) basaltic intrusion
4,327 to 4,362 feet (1,319 to 1,330 m)
thickness 35 feet (11 m)
Permian Fort Apache Limestone member "Supai Formation" (Winters, 1963)
4,362 to 4,405 feet (1,330 to 1,343 m)
thickness 43 feet (13 m)
Permian Big A Butte member "Supai Formation" (Winters, 1963)
4,405 to 4,454 feet (1,343 to 1,358 m)
thickness 49 feet (15 m)
Quaternary(?)/Tertiary (?) basaltic intrusion
4,454 to 4,505 feet (1,358 to 1,373 m)
thickness 51 feet (15 m)

epiclastic volcanic mudflows and volcanic arenites and conglomerates. Between 854 feet and 942 feet, a dark blue-green to gray blue-green andesite porphry flow-breccia is interbedded in the Pueblo Creek sequence. This unit may be probably a toe-breccia or a volcanic lahar, peripheral to the andesite flow that is mapped at the surface along the northern and eastern flanks of Escudilla Mountain. The andesite in the borehole may be correlative with the Dry Leggett Canyon Andesite of Ratte (1989).

An orange-brown rhyolite lithic-crystal ash-flow tuff between 1,018 feet and 1,038 feet is the only other volcanic flow encounterd in the Pueblo Creek Formation. The ash-flow tuff probably represents the distal outflow from an Oligocene silicic cauldron or silicic dome complex tens of miles southeast and south of the Alpine1/Federal location. This ash-flow tuff is tentatively correlated with the Tuff of Bishop Peak (Ratte, 1989). Marvin and others (1987) give a K-Ar biotite age of 37.1 my for the Tuff of Bishop Peak.

From 1,093 feet to 1580 feet the lower Pueblo Creek Formation is identified. The top of the lower Pueblo Creek Formation is picked at the top of a major conglomerate unit. The conglomerate unit contains the first occurrence of red granite (Precambrian ? clasts). The lower member of the Pueblo Creek Formation from 1,093 feet to 1,580 feet consists of a sandy, granule-to- cobble conglomerate interbedded with coarse-to-medium sandstone and pebbly sandstone. The conglomerates are mainly matrix-supported and contain well-rounded to subrounded clasts of silicic and intermediate volcanics, limestone, and red granite. From 1,266 feet to 1,325 feet the Pueblo Creek Formation consists of siltstone that increases in clast size downward into fine-to-medium sandstone and pebbly sandstone and pumaceous fine-to-medium sandstone. The Pueblo Creek Formation consists of interbedded matrix-supported granule-to-cobble conglomerate and medium-to-coarse sandstone betweeen 1,325 feet and 1,358 feet. Above 1,580 feet, altered pumice lapilli are sometimes observed and many sandstones are noticeably pumaceous. At 1,438 feet, a 2-to-3 inch thick air-fall tuff with distinct biotite crystals was encountered. The interval from 1,093 feet to 1,580 feet in the Pueblo Creek Formation probably records the initiation of silicic volcanism which culminated in the Oligocene 'ignimbrite flareup' in the Datil-Mogollon volcanic field to the south and southeast of the Alpine 1 location. The conglomerate in the lower Pueblo Creek Formation (1,093 feet to 1,266 feet) may indicate thermal tumulscence preceding the Oligocene volcanism, reactivation of older Laramide basement-involved structures, and/or onset of a dryer climate, and/or reworking of lower Mogollon Rim Formation gravel units.

From 1,580 feet to 2,966 feet the Mogollon Rim Formation consists of mostly siltstone and fine-to-medium sandstone with minor interbedded conglomerates and red-brown mudstone. The conglomerate and red-brown mudstone become dominant from about 2,850 feet to 3,139 feet depth.

The Mogollon Rim Formation is predominantly an arkosic litharenite, showing bioturbation, parallel laminations, some ripple cross-lamination, flaser structures, some soft sediment deformation, very thin-to-medium bedding, weak pedogenic and diagenitic calcite, and root casts. The gravels rich in Precambrian lithologies at the base of Mogollon Rim Formation represent the uplift and unroofing of basement-cored uplifts associated with the later phases of the Laramide Orogeny in east central Arizona. In any case, the section of Mogollon Rim Formation encountered in the Alpine 1/Federal core hole is one the thickest Baca Formation equivalent sections in Arizona or New Mexico. The gradational nature of the Pueblo Creek Formation and Mogollon Rim Formation and differences in where the Baca and equivalent tops are picked provide ambiguity on which sections are the thickest. Cather and Johnson (1984) define the top of the Baca where volcanic clasts disappear; Potochnik (1989) picks the top of the Mogollon Rim Formation, a Baca equivalent, where volcanic clasts roughly equal Paleozoic and Precambrian clasts.

At 3,139 feet depth, the basal Mogollon Rim Formation conglomerate rests unconformably upon a orange red and orange siltstone and fine-to-medium silty sandstone with a calcitic cement. This orange sandstone is informally designated as the LaOrange formation. Potochnik (1989) describes a similar unit between the Mogollon Rim Formation and Cretaceous sandstone south of Show Low. The depositional setting of the LaOrange formation is much different than the overlying Baca Formation and minor granule-to-cobble conglomerate beds suggest a much different provenance also. Clasts in the LaOrange are predominantly limestone, with minor intermediate volcanic porphyry clasts, as opposed to gravels rich in Precambrian plutonic and metamorphic clasts. The LaOrange shows both parrallel and cross laminations and some ripple cross-laminated zones. The occurrence of intermediate volcanic clasts may indicate a Late Cretaceous to early Tertiary (early Laramide Orogeny) age. It is possible that the LaOrange is a southern Colorado Plateau equivalent to early Laramide units, the Fort Crittenden and Ringbone Formations of the Basin and Range of southeastern Arizona and southwestern New Mexico (see Dickinson and others, 1989 and Lawton and others, 1993).

Unconformably below the LaOrange formation is a carbonaceous medium-to-coarse sandstone with calcitic cement. This unit is tentatively correlated with Cretaceous Dakota Formation (see Nations, 1989). In the Alpine 1/Federal core hole, the Dakota is cross laminated and has abundant ripple cross-laminated zones with much carbonaceous laminae. This unit is a light-gray, dark-gray and black, moderately well-sorted, quartz arenite. Marcasite or pyrite is abundant, especially in association with carbonaceous-rich zones. Carbonaceous material is concentrated where carbonate cements are lacking, in ripple troughs, and in coarse sand laminae.

The Permian San Andres limestone is a finely crystalline, medium-to-dark gray, and brown limestone with predominant mudstone and uncommon wackestone textures. The San Andres micrites and crinoid biomicrites have black parallel and wavy laminations and dark sutured stylolites are common. Oily films are present along stylolite and fracture surfaces. Vertical fractures and minor small-scale vugs, partially filled with calcite crystals, are common. Several fractures, no doubt, contributed to lost circulation during coring. The lower 3 feet of the San Andres, just above the Glorieta Sandstone, is a probable solution-collapse breccia with a black shale and dark micrite matrix, possibly rich in carbonaceous material.

The Permian Glorieta Sandstone consists of medium-to-fine, well-sorted, light gray and white sandstone with wavy and parallel laminations, ripple cross laminations, cross laminations, and cross bedding. Calcite, quartz, and dolomite (?) cement is present. Reduction spots, generally less than 0.5 inch diameter, contain marcasite or pyrite, vitrinite and other carbonaceous material. Marcasite or pyrite and black carbonaceous material is also common along many wavy laminations. Healed and opened high-angle fractures are present. Open fractures contain calcite crystals and appear to have contributed to lost circulation, especially between 3,455 and 3,465 feet depth. Intergranular porosity is indicated by drill mud sieving (ie mud buildups) on outer core surfaces, except on darker gray "reduction spots." Contact between the Glorieta Sandstone and the underlying Corduroy unit of Winters (1963) is obscurred by a basalt intrusion, a probable dike of late Tertiary age.

The upper 35 feet of the Permian Corduroy member is characterized by a solution-collapse or rubble breccia. Anhydrite dominates the Corduroy member between 3,788 and 3,905 feet depth. Massive, laminar, nodular, and mosaic anhydrite textures are present. Dark gray-to-brown siltstone, sandstone, and sandy dolomite are interbedded in the anhydrite. Bioturbation, rip-up clasts, and scour troughs are common. Soft sediment deformation, along with possible dewatering structures or enterolithic structures are also present. A coastal sabka depositional environment is indicated. Between 3,905 and 4,158 feet, gray-to- dark brown and brown limestone and dolomite predominates in the Corduroy member over a few sandstone and anhydrite beds less than 5 to 15 feet thick. The mostly micritic limestones and dolomites show wavy laminations, bioturbation, flaser, soft sediment deformation. Many units are sandy; while others have blue-gray anhydrite nodules. Light-brown to dark brown, muddy, fine sandstone to siltstone with wavy bedding and laminations, some cross laminations, bioturbation, and soft sediment deformation occurs between 4,158 and 4,226 feet depth. Brown microcrystalline dolomite to calcareous dolomite and some interbedded blue-gray anyhydrite occurs in the Corduroy member between 4,226 and 4,260 feet. Some of the dolomite at 4,228 to 4,231.5 feet is weakly fetid. Altogether 509 feet of the Corduroy member were cored in the Alpine 1/Federal. If basalt intrusions at the base and top of the Corduroy are dikes, the Corduroy member beneath Alpine Divide may have a thickness approaching 680 feet. Winters (1963) reports approximatetly 330 feet of the Corduroy member in the Carrizo Creek area. The Corduroy member in the Alpine area also contains considerably more carbonates and evaporites than measured sections to the west. Greater carbonate and evaporite content, coupled with much greater thickness suggests that the Permian Holbrook basin trends southeastward toward the Alpine region.

The Fort Apache Limestone member, a finely crystalline, dark gray to black, fossiliferous limestone, is found between 4,322 and 4,327 feet and 4,362 and 4,405 feet depth. A basalt dike or sill intrudes the Fort Apache Limestone from 4,327 to 4,362 feet. If the basalt is a sill, the Fort Apache Limestone is thinned to about 50 feet thickness in the Alpine subsurface compared to about 95 to 120 feet in the region around White River west of the borehole. Between 4,399 and 4,402 feet depth the Fort Apache Limestone member shows oily films and staining.

The majority of the Big A Butte member from 4,405 to 4,454 feet depth is a brown very-fine sandstone to siltstone. The cored section of the Big A Butte member represents only the upper part of the unit. A basalt intrusion was cored from 4,454 feet to total depth at 4,505 feet.

Winters (1963) reports the the Big A Butte and Amos Wash members total about 805 feet thickness in the White River region west of the Alpine drill site. Therefore, the bottom of the Alpine 1/Federal borehole may be at least 750 feet above Precambrian basement. If Pennslyvanian Naco Group and older rocks are present, the remaining depth will approach 2,000 feet. The Tenneco 1 Federal B well, 45 miles northwest of the Alpine 1/Federal site has 1,167 feet of Pennslyvanian and older rocks (Peirce and others, 1977) On the other hand, the M. A. Belcher Trust 1 State well, 20 miles northeast of the Alpine drill site, has 1,670 feet of section above Precambrian basement and below the Coconino/Glorieta sandstone (Foster, 1964). The Fort Apache "limestone" is not present in the Belcher well. However, with the Gerrard (1966) Fort Apache member definition, the Belcher well relationships also suggest that the Alpine 1/Federal total depth is about 800 feet above Precambrian basement.

Wrucke (1961) and Weber and Willard (1959) map Pennslyvanian carbonate rocks in isolated exotic outcrops on the northeast side of Escudilla Mountain and just across the New Mexico-Arizona border east of the Alpine drill site. However, these outcrops are highly fractured and allochthonous. Harrison (1989) describes similar exotic Pennslyvanian outcrops in stratigraphically equivalent Tertiary rocks in New Mexico more than 100 miles east the Alpine area. Harrison (1989) postulates that the allochthonous Pennslyvanian limestone outcrops are gravity slide deposits associated with wrench faulting. Individual slide blocks may be tens of miles from their origin as a result of wrench faulting and slide detatchment. Major strike-slip faulting in the region east and south of Alpine is hypothesized by Chamberlin and

Anderson (1989). Therefore, evidence for the occurrence of Naco Group carbonate and older rocks in the subsurface of the Alpine area is tentative without drilling.

7.3 STRUCTURAL IMPLICATIONS

Figure 17 shows a pre-drilling estimate of geology that is based upon the Belcher 1/State well (Foster, 1964), located 21 miles north-northeast from Alpine Divide, and projection of major regional unconformities into the subsurface of the area. No pre-Tertiary information is available for 60 miles to the south and east. The nearest pre-Tertiary well and outcrop data to the northwest and west is over 40 miles distance. Several reasonable assumptions, given the amount and quality of data available, were used to make the pre-drilling estimate. First, no major structures (faults) were assumed between the Belcher well and Alpine Divide. Existing geologic maps for the area show no faults. Structurally, the area north of the Belcher well is relatively flat with minor folds and the Precambrian is generally at higher elevation toward the south. Second, Tertiary sediments and volcanics were assumed to be inset against paleotopography, resulting from major regional unconformities. Inset Tertiary sediments and volcanics along the Mogollon Rim, a mostly late Mesozoic to mid-Tertiary erosional scarp, is common in the region to the west in the Transition Zone between the Colorado Plateau and Basin and Range Provinces (see Elston and Young, 1991; and Peirce and others, 1979). The subsurface model was tested by

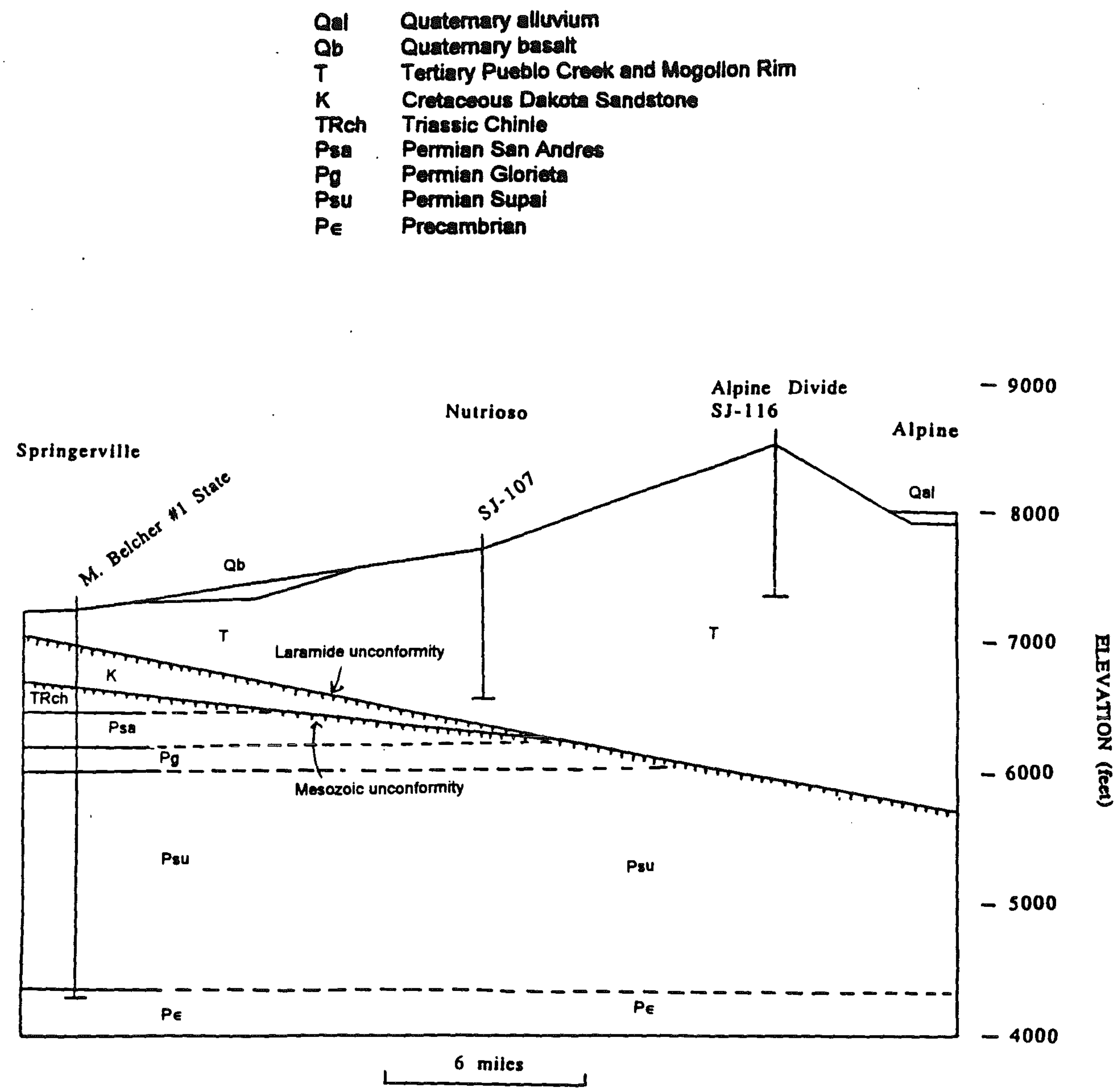

Figure 17. Pre-drilling geologic model of subsurface geology.

comparing it with Tertiary subcrops in the Whiteriver area approximately 50 miles to the west. In the Whiteriver area, the Tertiary Mogollon Rim formation, was observed resting unconformably on Permian Supai equivalent rocks at elevations similar to the pre-drilling model.

Figure 18 shows the actual geology to 4,505 feet depth at Alpine Divide. All of the Triassic Chinle, most of the Permian San Andres, and most of the Cretaceous Dakota sandstone were removed by erosion beneath the two major regional unconformities. However, more than 600 feet of Tertiary sediments were cored than predicted by the pre-drilling model. Also, the unconformity at the top of the Cretaceous Dakota Sandstone is approximately 1,600 feet lower in elevation above sea level in the Alpine 1/Federal than in the Belcher 1/State well. At least of 1,600 feet of structural displacement, faulting (?) down to the south, has occurred after deposition of the LaOrange formation, a probable new formation identified by this project. The LaOrange was deposited on a Dakota Sandstone erosional surface with probable low topographic relief.

7.4 SYNTHESIS OF GEOLOGY FINDINGS

The Alpine 1/Federal drilling provided valuable new information on the geology of the region. Cretacous and Permian hydrocarbon source rocks for petroleum maturation are present. A new and probable lower Tertiary or upper Cretaceous unit was recognized. Several basalt sills or dikes of unknown age intrude the Paleozoic section. Cretaceous rocks rest unconformably on the Permian San Andres Formation. The Corduroy

Qal	Quaternary alluvium
Qb	Quaternary basalt
T	Tertiary Pueblo Creek and Mogollon Rim
T/K	Tertiary (?)/Cretaceous (?) LaOrange
K	Cretaceous Dakota Sandstone
TRch	Triassic Chinle
Psa	Permian San Andres
Pg	Permian Glorieta
Psu	Permian Supai
P€	Precambrian

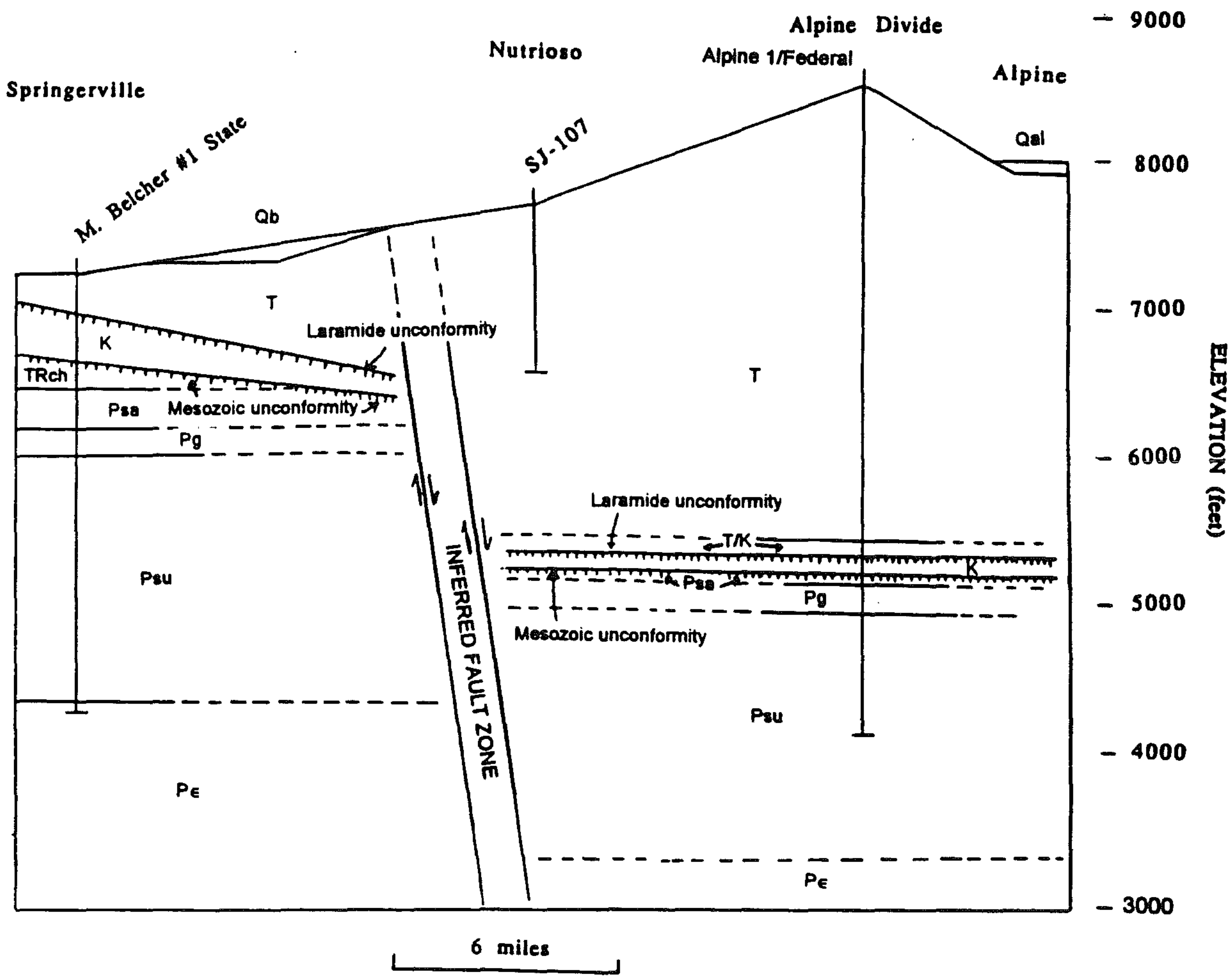

Figure 18. Post-drilling geologic model of subsurface geology.

member is thicker and has greater percentage of carbonate and evaporite rocks than sections east of Springerville and around Whiteriver. The Fort Apache Limestone member is present but thinner than sections near Whiteriver. A thicker than expected Oligocene to Paleocene section is present.

The Alpine 1/Federal borehole failed to reach Precambrian basement at 4,505 feet depth because of previously unidentified major structure that was backfilled with a thicker than expected Tertiary section. The occurrence of a probable new formation and Cretaceous rocks, the preservation of the San Andres and Glorieta Formations below a major unconformity, and basaltic intrusions also contributed to a thicker phanerozoic cover on the Precambrian.

A qualitative petroleum potential apparently exists in the area (Fellows, 1994; Rauzi, 1994a; and Rauzi, 1994b). The organic-rich Dakota Sandstone and fetid and petroliferous dolomites and limestones in the San Andres Formation, Corduroy member, and Fort Apache Limestone member indicate potential as source rocks for petroleum maturation. Detailed petrographic analysis and facies studies of core, hydrocarbon maturation studies, delineation of the burial and thermal history of the Cretaceous and Permian rocks, assessment of the hydrodynamic history of the area, and analysis of potential structural and stratigraphic traps and potential reservoir rocks is required to assess the oil and gas potential of the area. The Alpine 1/Federal core and logs provide key information for an assessment.

8.0 CONCLUSIONS AND RECOMMENDATIONS

The Alpine 1/Federal drilling project provided valuable new information on the geology of the region. Except for drilling into Precambrian rocks, the objectives of the project were accomplished. Sufficient temperature and heat-flow information were obtained to assess the near-term HDR geothermal potential of the eastern White Mountains region. Therefore, the primary mission of the project was successful.

The HDR potential for near-term electrical power production is not economic. Potential for HDR direct-use space heating is marginal at best and should realistically be considered uneconomic.

The Alpine 1/Federal hole should be deepened to Precambrian basement to provide definitive subsurface geological information for this region. Deeper drilling will determine Precambrian lithology and assess if older Paleozoic rock units are present. The hole may be deepened with a BQ drill string. Depth to Precambrian is likely to be between 800 and 2,000 feet below the current 4,505 feet total depth. The failure to reach Precambrian basement due to a previously unknown and unmapped major structural offset highlights the need for detailed surface geological mapping in this poorly understood region.

9.0 REFERENCES

Aiken, C. L. V., 1976, The analysis of the gravity anomalies of Arizona: unpublished PhD dissertation, University of Arizona, Tucson, 127 p.

Armstead, H. C. H., and Tester, J. W., 1987, Heat Mining: E. F. Spon, London, 478 p.

Aubele, J. C., Crumpler, L. S., and Shafiquallah, M., 1981, K-Ar ages of late Cenozoic rocks of the central and eastern parst of the Springerville volcanic field, east-central Arizona: Isochron/West, no. 46, p. 3-5.

Blackwell, D. D. and Steele, J. L., 1989, Thermal conductivity of sedimentary rocks: measurement and significance, in Naeser, N. D., McCulloh, T. H., eds., Thermal History of Sedimentary Basins, p. 13-36.

Blakey, R. C., 1980, Pennslyvanian and early Permian paleogeography, southern Colorado Plateau and vicinity in Fouch, T. D. and Magathan, E. R., eds., Paleozoic Paleogeography of West-Central United States: Society of Economic Paleontologists and Mineralogists, Denver, p. 239-257.

Byerly, P. E., and Stolt, R. H., 1977, An attempt to define the Curie point isotherm in northern and central Arizona: Geophysics, v. 42, p. 1394-1400.

Cather, S. M., and Johnson, B. D., 1984, Eocene tectonics and depositional setting of west-central New Mexico and eastern Arizona: New Mexico Bureau of Mines and Mineral Resources Circular 192, 33 p.

Chamberlin, R. M, and Anderson, O. J., 1989, The Laramide Zuni uplift, southeastern Colorado Plateau: a microcosm of Eurasian-style indentation-extrusion tectonics? in Anderson, O. J., Lucas, S. G., Love, D. W., and Cather, S. M., eds., Southeastern Colorado Plateau: New Mexico Geological Society Fortieth Field Conference Guidebook, p. 81-90.

Condit, C. D., Crumpler, L. S., Aubele, J. C., and Elston, W. E., 1989, Patterns of volcanism along the southern margin of the Colorado Plateau - the Springerville field: Journal of Geophysical Research, v. 94, no. B6., p 7,975-7,986.

Connor, C. B., Condit, C. D., Crumpler, L. S., and Aubele, J. C., 1992, Evidence of regional structural controls on vent distribution - Springerville volcanic field, Arizona: Journal of Geophysical Research, v. 97, no. B9, p. 12,349-12,359.

Cooley M. E. and Davidson, E. S., 1963, The Mogollon highlands - their influence on Mesozoic and Cenozoic erosion and sedimentation: Arizona Geological Society Digest, v. 6, p. 7-35.

Cooper, J. L., Aronson, J. L., Condit, C. D., and Hart, W. K., 1990, New K-Ar ages of lavas from the Colorado Plateau-Basin and Range transition zone, east-central Arizona: Isochron/West, no. 55, p. 28-31.

Dickinson, W. R., Fiorillo, A. R., Hall, D. L., Monreal, R., Potochnik, A. R., and Swift, P. N., 1989, Cretaceous strata of southern Arizona in Jenny, J. P., and Reynolds, S. J., eds., Geologic Evolution of Arizona: Arizona Geological Society Digest 17, p. 447-461.

Elston, D. P., and Young, R. A., 1991, Cretaceous-Eocene (Laramide) landscape development and Oligocene-Pliocene reorganization of Transition zone and Colorado Plateau, Arizona: Journal of Geophysical Research, v. 96, no. B7, p. 12,389-12,406.

Fellows, L. D. 1994, Oil show in geothermal test: Arizona Geology, v. 24, no. 1, p. 1-4

Foster, R. W., 1964, Stratigraphy and Petroleum possibilities of Catron County, New Mexico: New Mexico Bureau of Mines and Mineral Resources Bulletin 85, 55 p.

Gerrard, T. A. , 1966, Environmental studies of Fort Apache Member, Supai Formation, east-central Arizona: Bulletin of the Amerian Association of Petroleum Geologists, v. 50, no. 11, p. 2434-2463.

Harrison, R. W., 1989, Exotic blocks with the early Tertiary Rubio Peak Formation in the north-central Black Range, New Mexico: occurence, insights into post-emplacement tectonic activity, economic implications and emplacement hypothesis in Anderson, O. J., Lucas, S. G., Love, D. W., and Cather, S. M., eds., Southeastern Colorado Plateau: New Mexico Geological Society Fortieth Field Conference Guidebook, p. 99 -106.

Laughlin, A. W., Brookins, D. G., Damon, P. E., and Shafiqullah, M., 1979, Late Cenozoic volcanism of the central Jemez zone, Arizona-New Mexico: Isochron/West, no. 25, p. 5-8.

Laughlin. A. W., Damon, P. E., and Shafiqullah, M., 1980, K-Ar dates from the Springerville volcanic field, central Jemez zone, Apache County, Arizona: Isochron/West, no. 29, p. 3-4.

Lawton, T. F., Basabilvazo, G. T., Hodgson, S. A., Wilson, D. A., Mack, G. H., Mcintosh, W. C., Lucas, S. G., and Kietzke, K. K., 1993, Laramide stratigraphy of the Little Hatchet Mountains, southwestern New Mexico: New Mexico Geology, v. 15, no. 1, p. 9-15.

Marvin, R. F., Naeser, C. W., Bikerman, M., Mehnert, H. H., and Ratte, J. C., 1987, Isotopic ages of post-Paleocene igneous rocks within and bordering the Clifton 1 degree by 2 degree quadrangle, Arizona-New Mexico: New Mexico Bureau of Mines and Mineral Resources Bulletin 118, 63 p.

Merrill, R. K., and Pewe, T. L., 1977, Late Cenozoic geology of the White Mountains, Arizona: Arizona Bureau of Geology and Mineral Technology Special Paper 1, 65 p.

Minier, J., and Reiter, M., 1989, Coal maturation and geothermal history, west-central New Mexico, in Anderson, O. J., Lucas, S. G., Love, D. W., and Cather, S. M., eds., Southeastern Colorado Plateau: New Mexico Geological Society Fortieth Annual Field Conference, p. 127-133.

Minier, J., and Reiter, M., 1991, Heat flow on the southern Colorado Plateau: Tectonophysics, v. 200, p. 51-66.

Minier, J., Reiter, M., Shafiqullah, M., and Damon, P. E., 1988, Geothermal studies in the Quemado area, New Mexico: Geothermics, v. 17, no. 5/6, p. 735-755.

Morgan, P., and Gosnold, W. D., 1989, Heat flow and thermal regimes in the continental United States, in Pakiser, L. C. and Mooney, W. D., eds., Geophysical Framework of the Continental United States: The Geological Society of America Memoir 172, p. 493-522.

Nations, J. D., 1989, Cretaceous history of northeastern and east-central Arizona in Jenny, J. P., and Reynolds, S. J., eds., Geologic Evolution of Arizona: Arizona Geological Society Digest 17, p. 435-446.

Nettleton, L. L., 1976, Gravity and Magnetics in Oil Prospecting: McGraw-Hill, New York, 464 p.

Osburn, G. R., and Chapin, C. E., 1983, Nomenclature for Cenozoic rocks of northeast Mogollon-Datil volcanic field, New Mexico: New Mexico Bureau of Mines and Mineral Resources Stratigraphic Chart 1.

Peirce, H. W., 1989, Correlation Problems of Pennslyvanian-Permian strata of the Colorado Plateau of Arizona in Jenny, J. P., and Reynolds, S. J., eds., Geologic Evolution of Arizona: Arizona Geological Society Digest 17, p. 349-368.

Peirce, H. W., Jones, N., and Rogers, R., 1977, A survey of uranium favorability of Paleozoic rocks in the Mogollon rim and slope region-east central Arizona: Arizona Bureau of Geology and Mineral Technology Circular 19, 60 p.

Peirce, H. W., Damon, P. E., and Shafiqullah, M., 1979, An Oligocene (?) Colorado Plateau edge in Arizona: Tectonophysics, v. 61, p. 1-24.

Potochnik, A. R., 1989, Depositional style and tectonic implications of the Mogollon Rim formation (Eocene), East-Central Arizona, in Anderson, O. J., Lucas, S. G., Love, D. W., and Cather, S. M., eds., Southeastern Colorado Plateau: New Mexico Geological Society Fortieth Field Conference Guidebook, p. 107-118.

Ratte, J. C., 1989, Geologic map of the Bull Basin Quadrangle, Catron County, New Mexico: U. S. Geological Survey Geologic Quadrangle Map GQ-1651, 1:24,000 scale.

Ratte, J. C., Landis, E. R., Gaskill, D. L., Raabe, R. G, and Eaton, G. P., 1969, Mineral Resources of the Blue Range Primitive area Greenlee County, Arizona, and Catron County, New Mexico with a section on Aeromagnetic Interpretation: U. S. Geological Survey Bulletin 1261-E, 91 p.

Rauzi, S. L., 1994a, Geothermal test hints at oil potential in eastern Arizona volcanic field: Oil and Gas Journal, Jan 3, 1994, p. 52-54.

Rauzi, S. L., 1994b, Implications of live oil shows in eastern Arizona geothermal test: Arizona Geological Survey Open-File Report 94-1, 16 p.

Sirrine, G. K., 1956, Geology of the Springerville-St Johns area, Apache County, Arizona: Unpublished PhD dissertation, University of Texas, Austin, 248 p.

Stone, C., 1980a, Springerville geothermal project, geology, geochemistry, geophysics-final report: Arizona Bureau of Geology and Mineral Technology Open File Report 80-4, 23 p.

Stone, C., 1980b, Springerville-Alpine geothermal project, results of heat flow drilling: Arizona Bureau of Geology and Mineral Technology Open-File Report 79-17, 21 p.

Stone, C., and Witcher, J. C., 1982, Geothermal Energy in Arizona: Arizona Bureau of Geology and Mineral Technology Open-File Report 83-12, 398 p.

Tester, J. W., and Herzog, H. J., 1990, Economic predictions for heat mining: A review and analysis of Hot Dry Rock (HDR) geothermal energy technology: Massachusetts Institute of Technology, Energy Laboratory, Report MIT-EL 80-001, prepared for the U. S. Department of Energy, Geothermal Technology Division, 180 p.

Weber, R. H., and Willard, M. E., 1959, Reconnaissance geologic map of Reserve thirty-minute quadrangle: New Mexico Bureau of Mines and Mineral Resources Geologic Map 12, 1:126,720 scale.

Winters, S. S., 1963, Supai Formation (Permian) of eastern Arizona: Geological Society of America Memoir 89, 99 p.

Witcher, J. C., and Stone, C., 1983, A CO2 - silica geothermometer for low temperature geothermal resource assessment, with application to resources in the Safford basin, Arizona: Stone and Witcher consulting geologists, prepared for Arizona Solar Energy Commission and U. S. Department of Energy, 91p.

Wohletz, K. H., and Heiken, G., 1992, Volcanology and Geothermal Energy: University of California Press, 432 p.

Wrucke, C. T., 1961, Paleozoic and Cenozoic rocks in the Alpine-Nutrioso area Apache County, Arizona: U. S. Geological Survey Bulletin 1121-H, 26 p.

APPENDIX 8

DESCRIPTIVE FIELD GEOLOGIC LOG OF CORE FROM THE ALPINE 1/FEDERAL BOREHOLE

KEY

1st column depth interval (feet)

2nd column core lithology description

DESCRIPTIVE FORMATS

clastic

Basic lithology and grain size: color, cements, bedding thickness, depositional structures, clast composition, other notable features.

carbonate

Basic lithology and grain size: color, depositional structures, other textures and features, Folk's classification.

igneous

Composition name: color, pyroclastic name (if applicable), textures, notable mineralogy, other important features.

500 to 554	Clayey, pebbly fine to coarse sandstone and fine to coarse sandstone: red brown to light brown, parallel laminated, cross laminated, ripple cross laminations, scour, rip-up clasts, minor granule to pebble conglomerate with intermediate and silicic volcanic clasts.
554 to 564	Siltstone and mudstone: red brown, parallel laminated, thin bedded.
564 to 700	Siltstone to coarse sandstone: red brown to brown, parallel laminated, cross laminated, rip-up clasts, minor granule to cobble conglomerate and laminated mudstone.
700 to 713	Fine to coarse sandstone: brown to red brown, clayey, tuffaceous.
713 to 719	Mudstone and siltstone: red brown, thin bedded.
719 to 808	Fine to coarse sandstone: red brown and brown, clayey, minor pebble conglomerate as scour fill.
808 to 824	Siltstone to coarse sandstone: light gray to brown
824 to 828	Mudstone: gray to red brown, soft sediment deformation.
828 to 854	Fine to medium sandstone and minor clayey pebble conglomerate: brown to yellow brown, calcitic, parallel laminated.
854 to 900	Andesite porphyry breccia: gray green to dark blue green, breccia blocks may be largely matrix-supported, matrix is light-gray tuffaceous sandstone, unit may represent an andesite flow toe breccia or a volcanic lahar.
900 to 942	Andesite porphyry breccia: gray green to dark blue green, breccia blocks may be largely matrix-supported, matrix is light-gray tuffaceous sandstone, unit may represent an andesite flow toe breccia or a volcanic lahar.
942 to 952	Siltstone to coarse sandstone: gray brown, calcitic, thin-bedded, small-scale, graded bedding, some mudstone laminae.
952 to 955	Pebbly coarse sandstone and pebble conglomerate: tuffaceous.
955 to 982	Tuffaceous fine to medium sandstone: gray to gray brown, a few thin to medium interbeds of mudstone, parallel laminated.
982 to 997	Muddy and sandy granule to pebble conglomerate: gray to gray green, tuffaceous.
997 to 1000	Siltstone: light brown.
1000 to 1010	Fine to medium sandstone: brown to gray, calcitic, tuffaceous.
1010 to 1018	Fine to coarse granular and pebbly sandstone: dark gray to gray brown, clayey, flaser, parallel laminated.
1018 to 1038	Rhyolite: orange brown, lithic-crystal ash-flow tuff, weak eutaxitic textures, minor biotite and quartz crystal fragments.
1038 to 1052	Fine to coarse sandstone: dark gray, calcitic and clayey, parallel and cross laminated, flaser.

1052 to 1056	Sandy granule to pebble conglomerate: dark gray, calcitic, smaller clasts are intermediate volcanics, larger clasts are silicic volcanics.
1056 to 1084	Fine to coarse sandstone: dark gray, clayey to calcitic, parallel and cross laminated.
1084 to 1091	Pebble to granule fine to coarse sandstone: dark blue gray, calcitic, parallel and cross laminated, flaser.
1091 to 1100	Granule to cobble conglomerate: gray, calcitic, intermediate volcanics and minor limestone and red granite clasts.
1100 to 1199	Sandy granule to cobble conglomerate with minor interbeds of mudstone, fine to coarse sandstone and pebbly sandstone: gray to gray brown, calcitic,clast compostion is mostly silicic and intermediate volcanics with significant limestone and red granite.
1199 to 12321	Sandy granule to cobble conglomerate: calcitic, clasts are well rounded (limestone and granite) and subangular (volcanics), clasts are predominantly intermediate and silicic volcanics with subordinate limestone and red granite.
1232 to 1243	Fine to coarse sandstone and siltstone: red gray and brown, calcitic, parallel and cross laminated, flaser, wavy bedding, granule to pebble conglomerate from 1233 to 1336 feet.
1243 to 1249	Sandy granule to pebble conglomerate: brown, calcitic.
1249 to 1260	Fine to coarse sandstone and pebbly sandstone: brown, calcitic, parallel and cross laminated, wavy flaser, ripple cross laminations.
1260 to 1266	Sandy granule to pebble conglomerate: brown, calcitic, clasts show slight imbrication.
1266 to 1300	Siltstone and mudstone: yellow brown and brown, calcitic, parallel laminations, thin bedded.
1300 to 1325	Fine to medium sandstone: brown, calcitic, tuffaceous, minor granule to pebble conglomerate beds.
1325 to 1358	Granule to pebble conglomerate and fine to medium sandstone: brown, calcitic, clasts of red granite, limestone, and silicic volcanics, rip-up clasts of mudstone.
1358 to 1400	Tuffaceous siltstone, mudstone and minor tuffaceous fine sandstone: gray to light pink gray, clayey and siliceous, parallel laminated, thin bedded, lapilli altered to "clay."
1400 to 1414	Tuffaceous siltstone: light gray to gray white, clayey, parallel laminated, dark brown mottled zones (bioturbation?), soft sediment deformation.
1414 to 1425	Fine to medium sandstone and minor siltstone: gray green to gray brown, clayey, parallel laminated, ripple cross laminated, some laminae are graded, some bioturbation, soft sediment deformation, tuffaceous.

1425 to 1500	Tuffaceous fine sandstone and siltstone: mostly light brown to gray brown, minor blue gray, clayey, parallel laminations, cross laminated, lapilli altered to white "clay", soft deformation, two inch air fall tuff at 1438 feet.
1500 to 1502	Mudstone: brown, tuffaceous, parallel laminated, thin bedded.
1502 to 1543	Fine to medium sandstone: gray, gray green and brown, clayey, tuffaceous, rip-up clasts, parallel and cross laminated.
1543 to 1557	Fine sandstone to siltstone: gray brown to gray green, clayey, tuffaceous, parallel laminated, some soft sediment deformation.
1557 to 1574	Fine to coarse sandstone: gray green, clayey and calcitic, tuffaceous, rip-up clasts, some cross laminations.
1574 to 1611	Fine to medium sandstone: gray to gray brown, clayey, thin to medium bedded, parallel laminated, rip-up clasts, some thin interbeds and laminae of brown mudstone, soft sediment deformation, calcite filled fractures and very small-scale normal faults.
1611 to 1630	Fine sandstone: blue gray, clayey parallel laminated, minor thin-bedded mudstone.
1630 to 1670	Mudstone: gray brown to red brown, calcitic, fissile, numerous calcite-filled fractures.
1670 to 1694	Fine to coarse sandstone: gray brown to brown, calcitic, minor pedogenic calcite, mudstone rip-up clasts.
1694 to 1700	Mudstone: red brown, calcitic.
1700 to 1709	Mudstone to siltstone: red brown, calcitic, fractured.
1709 to 1725	Sandstone and siltstone:
1725 to 1731	Mudstone to siltstone: brown, calcitic.
1731 to 1758	Medium to coarse sandstone with interbedded siltstone and mudstone: brown, calcitic, bioturbated, rip-up clasts, parallel laminations.
1758 to 1773	Medium to coarse sandstone: brwon, calcitic, mudstone rip-up clasts, bioturbated, small-scale normal faults at 1763 and 1765 feet.
1773 to 1776	Mudstone: brown, calcitic, brittle, pedogenic calcite.
1776 to 1790	Fine to medium sandstone: gray, calcitic, bioturbation, pedogenic calcite.
1790 to 1792	Mudstone: brown, calcitic.
1792 to 1794	Fine to medium sandstone: brown, calcitic.
1794 to 1804	Siltstone to mudstone: brown, calcitic, pedogenic calcite, bioturbated.
1804 to 1814	Fine to coarse sandstone: gray to brown, calcitic, interbeds of coarse sandstone grading downward into fine sandstone.

1814 to 1819	Siltstone
1819 to 1835	Fine sandstone to siltstone: gray brown, calcitic, parallel laminations, thin-bedded, bioturbated, root casts and pedogenic calcitic.
1835 to 1838	Siltstone:
1838 to 1854	Fine to coarse sandstone: calcitic, mudstone rip-up clasts.
1854 to 1858	Siltstone:
1858 to 1886	Fine to coarse sandstone: calcitic, bioturbation, mudstone rip-up clasts.
1886 to 1887	Mudstone: brown, calcitic, pedogenic calcite.
1887 to 1892	Fine sandstone: brown, calcitic, bioturbated.
1892 to 1900	Siltstone: brown, calcitic, pedogenic calcite.
1900 to 1918	Fine sandstone: light brown to yellow brown, calcitic, massive, some bioturbation.
1918 to 1929	Siltstone, mudstone, and fine sandstone, interbeded: yellow brown to gray brown, calcitic, bioturbation, pedogenic calcite.
1929 to 1952	Fine to coarse sandstone: gray, calcitic, pedogenic calcite, bioturbation, mostly massive, minor parallel laminations, generally grades downward from coarse sandstone to fine sandstone at base of unit.
1952 to 1962	Medium sandstone: calcitic, parallel laminations, bioturbated, flaser, pedogenic calcite, minor interbeds of mudstone and siltstone.
1962 to 1964	Mudstone to siltstone: red brown, calcitic, parallel laminated, bioturbated, pedogenic calcite.
1964 to 2012	Fine to coarse sandstone: gray, calcitic, parallel laminations, bioturbated, pedogenic calcite, root casts, one to three feet interbeds of red brown mudstone at 1977 feet and 2004 to 2007 feet.
2012 to 2014	Sandy mudstone: reddish orange, calcitic, pedogenic calcite.
2014 to 2024	Fine to medium sandstone brown to yellow brown, calcitic, bioturbated, parallel laminations, thin bedded, pedogenic calcite.
2024 to 2026	Siltstone to mudstone: yellow brown to red brown.
2026 to 2033	Fine to coarse sandstone: brown, calcitic, bioturbated, root casts, pedogenic calcite.
2033 to 2036	Siltstone: brown, calcitic.
2036 to 2039	Coarse sandstone: brown, calcitic.
2039 to 2044	Sandy pebble conglomerate: calcitic, clasts are granite, limestone, intermediate volcanics, and assorted metamorphics.

2044 to 2058	Fine sandstone: gray yellow brown, calcitic.
2058 to 2061	Mudstone: red brown, calcitic, parallel laminations, bioturbations, root casts, pedogenic calcite.
2061 to 2100	Siltstone and fine sandstone grading downward into pebbbly coarse sandstone: light gray, yellow brown, gray brown, calcitic, mudstone rip-up clasts, some rip-up clasts are crudely imbricated in the middle of the unit, root casts, bioturbation.
2100 to 2106	Siltstone to fine sandstone: dark to light gray, calcitic, thin bedded, parallel laminations, bioturbated, root casts.
2106 to 2148	Fine sandstone to coarse sandstone: gray, calcitic, thin to medium bedded, parallel laminations, bioturbated, minor thin beds of brown siltstone and mudstone, pedogenic calcite.
2148 to 2204	Siltstone with minor interbedded fine sandstone: yellow brown, brown, and gray, calcitic, thin bedded, bioturbation, pedogenic calcite.
2204 to 2211	Fine sandstone to siltstone: gray, calcitic, bioturbated, minor thin beds of red brown mudstone, pedogenic calcite.
2211 to 2213	Mudstone to siltstone: red brown.
2213 to 2226	Fine to medium sandstone: gray to dark gray, calcitic, bioturbated, parallel laminations, thin bedded, minor thin beds of siltstone and mudstone.
2226 to 2237	Mudstone to siltstone: gray, calcitic, thin bedded, parallel laminations, red brown mudstone laminae and very thin beds, pedogenic calcite (?).
2237 to 2241	Coarse sandstone: gray
2241 to 2246	Conglomerate:
2246 to 2252	Mudstone and siltstone: red brown, calcitic, parallel laminations, mudstone is moderately fissile.
2252 to 2270	Siltstone to coarse sandstone: gray, calcitic, grades from fine sandstone downward to coarse sandstone in lower 4 feet.
2270 to 2275	Mudstone and siltstone: dark brown to red brown.
2275 to 2294	Coarse sandstone and pebble conglomerate: gray to gray brown, calcitic, brown mudstone rip-up clasts, conglomerate clasts are limestone, red granite, and assorted metamorphics.
2294 to 2300	Mudstone to siltstone: red brown to brown, calcitic, pedogenic calcite.
2300 to 2317	Coarse sandstone and pebbly coarse sandstone: brown and gray, calcitic, parallel laminations, mudstone rip-up clasts.
2317 to 2332	Sandy mudstone and siltstone: brown, calcitic, bioturbated, pedogenic calcite.
2332 to 2345	Coarse sandstone interbedded with granule and pebble coarse sandstone: gray, calcitic, clasts of red granite, limestone, and intermediate volcanics.

2345 to 2352	Mudstone and siltstone: red brown, calcitic, parallel laminated, thin bedded, pedogenic calcite.
2352 to 2361	Medium to coarse sandstone: gray, calcitic, abundant mudstone rip-up clasts.
2361 to 2365	Fine sandstone and siltstone: gray to brown, calcitic, thin-bedded, parallel laminated, bioturbated.
2365 to 2369	Siltstone: red brown.
2369 to 2386	Fine sandstone: gray, grades into coarse sandstone with siltstone rip-up clasts at base of unit.
2386 to 2388	Siltstone: red brown.
2388 to 2396	Fine sandstone and coarse sandstone: gray brown, fine sandstone grades downward into coarse sandstone.
2396 to 2401	Siltstone: brown, flaser.
2401 to 2414	Fine to medium sandstone: yellow brown and brown, calcitic, bioturbation.
2414 to 2419	Sandy mudstone: brown, calcitic, thin bedded, bioturbation, pedogenic calcite.
2419 to 2425	Fine sandstone: yellow brown, calcitic.
2425 to 2428	Mudstone: brown, calcitic, thin bedded, bioturbated.
2428 to 2438	Medium to coarse sandstone: calcitic, bioturbated.
2438 to 2441	Mudstone to siltstone: brown, calcitic, pedogenic calcite.
2441 to 2464	Fine sandstone to siltstone: light brown to yellow brown, calcitic, some parallel laminations, bioturbated, mudstone rip-up clasts in middle of unit.
2464 to 2465	Mudstone and siltstone: red brown.
2465 to 2495	Fine sandstone and siltstone grading downward into coarse sandtone with interbedded granule to pebble conglomerate: gray to light gray, calcitic, thin bedded, parallel laminations, wavy laminations, cross laminations, mudstone rip-up clasts in lower units.
2495 to 2500	Siltstone: red brown, parallel laminations.
2500 to 2506	Fine sandstone and siltstone: red brown and gray, calcitic, parallel laminations.
2506 to 2513	Mudstone and siltstone: red brown, calcitic, wavy laminations.
2513 to 2525	Fine sandstone grading downward into coarse sandstone: gray, calcitic, parallel laminations.
2525 to 2552	Pebble to cobble conglomerate interbedded with siltstone and sandstone: red brown to gray brown, calcitic, mudstone rip-up clasts.
2552 to 2566	Fine and coarse sandstone: gray brown, calcitic, bioturbation, mudstone rip-up clasts, thin bedded with mudstone laminae, upper part of unit is mudstone and

siltstone that grades downward into sandstone, pedogenic and root casts in the upper mudstone and siltstone.

2566 to 2570	Coarse sandstone and interbedded pebble conglomerate: brown, calcitic, contains red granite clasts.
2570 to 2581	Siltstone to coarse sandstone: gray, calcitic, parallel laminations, some thin bedded mudstone interlayers, siltstone and fine sandstone grade downward into coarse sandstone, bioturbation, soft sediment deformation in upper finer grained units.
2581 to 2594	Gravely coarse sandstone and granule to cobble conglomerate: gray, calcitic, fine to medium bedded, conglomerate is matrix supported, well rounded clasts of red granite, also limestone and intermediate volcanic clasts, "running sand" at 2587.5 feet.
2594 to 2601	Mudstone and interbedded siltstone: gray, dark gray, and red brown (mudstone), calcitic, parallel laminated, pedogenic calcite.
2601 to 2605	Coarse sandstone: calcitic.
2605 to 2617	Siltstone: dark gray to red brown, calcitic, parallel laminated.
2617 to 2622	Coarse sandstone and pebble conglomerate: calcitic, clasts of red granite and intermediate volcanics.
2622 to 2635	Siltstone to pebbly coarse sandstone: red brown to gray brown, calcitic.
2635 to 2638	Cobble conglomerate: calcitic.
2638 to 2649	Coarse sandstone and pebble conblomerate: red brown, calcitic.
2649 to 2653	Mudstone and siltstone: brown, calcitic, pedogenic calcite.
2653 to 2661	Pebbly coarse sandstone: brown to red brown, calcitic, bioturbated.
2661 to 2663	Siltstone and mudstone: brown, calcitic, pedogenic calcite.
2663 to 2670	Fine and coarse sandstone.
2670 to 2673	Granule and pebble conglomerate: calcitic.
2673 to 2682	Siltstone to coarse sandstone: gray and red gray, calcitic, mudstone rip-up clasts, mudstone laminae.
2682 to 2685	Pebble to cobble conglomerate: calcitic, poorly indurated.
2685 to 2694	Sandy mudstone and siltstone: brown to red brown, calcitic, bioturbated, pedogenic calcite.
2694 to 2700	Fine sandstone and siltstone: purple gray brown, calcitic, cross laminations, parallel laminations.
2700 to 2710	Fine sandstone to siltstone: purple gray to gray brown, calcitic, cross laminations, parallel lamintions, pebble and granule conglomerate at 2702 to 2703 feet.

2710 to 2714 Sandy granule to cobble conglomerate: gray, calcitic, matrix supported.

2714 to 2727 Mudstone and sandy siltstone: red brown, calcitic, parallel laminations, root casts and pedodenic calcite.

2727 to 2754 Fine sandstone to siltstone: gray brown to dark brown, calcitic, ripple cross laminations, parallel laminations, flaser, sand lenses.

2754 to 2758 Mudstone: red brown, calcitic, parallel laminated.

2758 to 2764 Siltstone to coarse sandstone: gray, calcitic, siltstone grades downward into sandstone.

2764 to 2768 Coarse sandy granule and pebble conglomerate: calcitic, sandy and clayey poorly indurated matrix, clasts of red granite, limestone, assorted metamorphics, and intermediate volcanics.

2768 to 2791 Mudstone: brown to red brown, calcitic, brittle and slightly fissile, root casts and pedogenic calcite, core condition poor, no core recovery 2786 to 2788 feet.

2791 to 2803 Medium to coarse granular and pebbly sandstone: gray,calcitic, thin to medium bedded, cross laminated, parallel laminated.

2803 to 2806 Granule to boulder conglomerate: calcitic, some clast imbrication, matrix supported, matrix is sandy mudstone.

2806 to 2832 Granule and pebble medium to coarse sandstone with interbedded pebble to cobble conglomerate: calcitic, medium bedded, cross laminations, parallel laminations, conglomerates show weak imbrication, clasts are red granite, limestone, assorted metamorphics, and intermediate volcanics.

2832 to 2840 Pebble to cobble conglomerate: calcitic, poorly indurated, sandy and muddy matrix, clasts are well rounded limestone, red granite, and intermediate volcanics.

2840 to 2847 Mudstone: red brown, calcitic, parallel laminations, pedogenic calcite and root casts.

2847 to 2858 Pebble to cobble conglomerate: calcitic, poorly indurated muddy coarse sand matrix.

2858 to 2862 Mudstone: red brown, calcitic, pedogenic calcite.

2862 to 2867 Muddy medium to coarse sandstone: brown, calcitic, poorly indurated, core is eroded.

2867 to2870 Pebble to cobble conglomerate: calcitic, poorly indurated muddy coarse sand matrix.

2870 to 2877 Granule and pebble medium to coarse sandstone with interbedded pebble to cobble conglomerate: calcitic, medium bedded, cross laminations, parallel laminations, conglomerates show weak imbrication, clasts are red granite, limestone, assorted metamorphics, and intermediate volcanics.

2877 to 2885	Granule to boulder conglomerate: calcitic, poorly indurated muddy sandstone matrix, clasts of red granite, limestone, and intermediate volcanics.
2885 to 2900	Granule and pebble medium to coarse sandstone with interbedded pebble to cobble conglomerate: calcitic, medium bedded, cross laminations, parallel laminations, conglomerates show weak imbrication, clasts are red granite, limestone, assorted metamorphics, and intermediate volcanics.
2900 to 2908	Mudstone: red brown, calcitic, moderately fissile, pebble to cobble conglomerate at 2902 to 2903 feet.
2908 to 2934	Pebble to boulder, mostly cobble, conglomerate: red brown to gray brown, calcitic, matrix supported, poorly indurated muddy coarse sandstone matrix, clasts of limestone red granite, assorted metamorphics, and intermediate volcanics.
2934 to 2937	Sandstone:
2937 to 2939	Mudstone: red brown, partial core recovery.
2939 to 2950	Muddy medium to coarse sandstone: brown to gray, calcitic, parallel laminations, cross laminations, poorly indurated.
2950 to 2953	Conglomerate:
2953 to 2969	Clayey medium to coarse sandstone: brown to gray, calcitic, parallel laminations, cross laminations.
2969 to 2986	Pebble to boulder conglomerate: gray to gray brown, clasts various colors, calcitic, matrix supported, poorly indurated, muddy sandstone matrix, clasts of red granite, limestone, assorted metamorphics, intermediate and silicic volcanics.
2986 to 3000	Muddy granule coarse sandstone: gray, calcitic, granule and pebble conglomerate at 2993 feet.
3000 to 3016	Pebble to boulder conglomerate: gray to gray brown, clasts various colors, calcitic, matrix supported, poorly indurated, muddy sandstone matrix, clasts of red granite, limestone, assorted metamorphics, intermediate and silicic volcanics.
3016 to 3018	Muddy medium to coarse sandstone: brown, calcitic, poorly indurated.
3018 to 3041	Pebble to boulder conglomerate: gray to gray brown, clasts various colors, calcitic, matrix supported, poorly indurated, muddy sandstone matrix, clasts of red granite, limestone, assorted metamorphics, intermediate and silicic volcanics.
3041 to 3044	Muddy medium to coarse sandstone: brown, calcitic, poorly indurated.
3044 to 3063	Pebble to boulder conglomerate: gray to gray brown, clasts various colors, calcitic, matrix supported, poorly indurated, muddy sandstone matrix, clasts of red granite, limestone, assorted metamorphics, intermediate and silicic volcanics.

3063 to 3096	Pebble to boulder conglomerate interbedded with muddy medium to coarse sandstone: gray to gray brown, clasts various colors, calcitic, matrix supported, poorly indurated, muddy sandstone matrix, clasts of red granite, limestone, assorted metamorphics, intermediate and silicic volcanics.
3096 to 3100	Mudstone and sandy mudstone: red brown to orange, calcitic, pedogenic calcite.
3100 to 3130	Muddy fine sandstone to sandy mudstone: orange to red brown, calcitic, eroded core, pedogenic calcite and root casts, conglomerate at 3116 feet.
3130 to 3139	Pebble to boulder conglomerate: gray to gray brown, clasts various colors, calcitic, matrix supported, poorly indurated, muddy sandstone matrix, clasts of red granite, limestone, assorted metamorphics, intermediate and silicic volcanics.
3139 to 3166	Fine sandstone and siltstone: red to orange, calcitic, limestone granule to pebble conglomerate with minor intermediate volcanic clasts 3154 to 3155 feet.
3166 to 3177	Fine sandstone: orange to orange brown, calcitic, cross laminated, scour.
3177 to 3216	Fine sandstone and siltstone: yellow gray to red brown, calcitic, thin bedded, parallel laminations, bioturbated, fining upward sequences 1 to 2 feet thick, ripple cross laminations. root casts and pedogenic calcite 3183 to 3187 feet.
3216 to 3222	Pebble to cobble conglomerate: calcitic, matrix supported, clasts are limestone with very minor intermediate volcanics.
3222 to 3246	Fine sandstone to siltstone: orange gray to red brown, calcitic, bioturbated, cross laminated, ripple cross laminated, minor interbedded sandy granule limestone conglomerate, sedlitharenite.
3246 to 3256	Fine to coarse sandstone: yellow brown to red brown, calcitic and silicic, cross laminated, ripple cross laminated, bioturbated, quartz arenite, unit may represent a weathered zone.
3256 to 3300	Carbonaceous fine to coarse sandstone: light gray to very dark gray, calcitic and silicic, cross laminated, ripple cross laminated with black carbonaceous laminae in ripple roughs, bioturbated, quartz arenite.
3300 to 3362	Carbonaceous fine, medium and coarse sandstone: light gray to very dark gray, calcitic, dolomitic, silicic, clayey below 3330 feet, cross laminated, abundant ripple cross laminations, black carbonaceous laminae and carbonacous ripple troughs, pyrite or marcasite disseminated in dark laminae, four inch clay (bentonite) bed at 3309 feet, laminated coal and carbonaceous shale at 3339 feet, relatively well sorted quartz arenite.
3362 to 3372	Sandy siltstone, no core recovery 3366 to 3369 feet, drill string differential stuck at 3369 feet.
3372 to 3425	Finely crystalline fossiliferous limestone: dark to medium gray, some parallel laminated beds, thin to massive bedding, wackestone and mudstone textures, numerous dark styolites, oil films on stylolite surfaces, vuggy and pinpoint porosity, numerous open vertical fractures with calcite crystals and minor oil films, brown and fetid from 3419 to 3432 feet with minor breccia zones and oil films, micrite, pelmicrite, and biomicrite.

3425 to 3436	Breccia: dark gray limestone breccia in black carbonaceous micritic matrix, may represent a solution collapse breccia.
3436 to 3500	Medium to fine sandstone: light gray to gray white, calcitic, generally well sorted, wavy and parallel laminations, ripple cross laminations, some laminations filled with pyrite or marcasite, sparsely disseminated pyrite or marcasite and "vitrinite", cross bedding and laminations, open high angle fractures from 3247 to 3462 and partially filled with calcite crystals, quartz arenite.
3500 to 3639	Medium to fine sandstone: mostly light gray to gray white, minor light gray brown and light blue gray beds, generallly well sorted, wavy and parallel laminations, some ripple cross laminations, cross laminations and thin to medium cross bedding, numerous high angle fractures partially to completely filled with calcite. minor disseminated pyrite or marcasite and "vitrinite", some laminae contain much pyrite or marcasite, quartz arenite.
3639 to 3700	Andesite or basalt: round calcite vesicle fillings or zenoliths, calcite and chlorite alteration of phenocrysts.
3700 to 3751	Andesite or basalt: round calcite vesicle fillings or zenoliths, calcite and chlorite alteration of phenocrysts.
3751 to 3759	Breccia: black dolomitic limestone, may represent a solution collapse breccia or fault zone.
3759 to 3761	Dolomitic limestone: black, fractured.
3761 to 3775	No core recovery, core barral mislatch and differential stuck.
3775 to 3785	Breccia: dolomite, limestone, anhydrite, unit may represent solution collapse breccia.
3785 to 3795	Dolomite, anhydrite, siltstone: dolomitic unit is very vuggy with dolomite crystals, anhydrite is fractured and white to blue gray with a nodular texture.
3795 to 3834	Fine to medium crystalline anhydrite interbedded with siltstone and fine sandstone: anhydrite is light gray to gray with laminated, massive, and nodular textures, minor stylolites are present, siltstones and sandstones are dark gray to brown with rip-up clasts, scour, and dewatering structures.
3834 to 3861	Fine sandstone to siltstone: dark brown, dolomitic to anhydritic, soft sediment deformation, anhydrite nodules, rip-up clasts, scour.
3861 to 3876	Anhydrite: gray, laminated, massive, and nodular.
3876 to 3880	Siltstone to fine sandstone: brown to light brown.
3880 to 3988	Anhydrite: gray, sandy, laminated.
3988 to 3900	Siltstone to fine sandstone: mottled red brown to gray, dolomitic and anhydritic, soft sediment deformation.
3900 to 3906	Siltstone to fine sandstone: mottled red brown to gray, dolomitic and anhydritic, soft sediment deformation, some anhydrite.

3906 to 3913	Dolomitic limestone: mottled gray to light brown, laminated, black carbonaceous shale laminae, bioturbated, stylolites, micrite.
3913 to 3922	Finely crystalline limestone: mottled gray to brown, slightly fetid, laminated, black carbonaceous shale laminae, bioturbated, stylolites, micrite.
3922 to 3935	Sandy and silty finely crystalline limestone: gray to dark gray, very thin bedded, wavy laminations and flaser, sandy and silty micrite.
3935 to 3947	Siltstone to fine sandstone: red brown, calcitic, wavy thin bedded with wavy laminations, flaser, scour and rip-up clasts.
3947 to 3957	Sandy medium to fine crystalline limestone and dolomite: white limestone grading upward into brown and dark gray dolomite, medium bedded, wavy laminations, bioturbated, sandy micrite.
3957 to 3974	Finely crystalline limestone: dark gray to dark gray brown, wavy laminations, thin to medium bedded, black shale laminae, stylolites, micrite and intramicrite.
3974 to 3987	Medium crystalline dolomite: light gray to white, sucrosic texture, mostly massive, minor parallel laminations.
3987 to 3996	Fine sandstone: brown, dolomitic, some soft sediment deformation, upper part of unit is massive, lower unit is wavy laminated.
3996 to 3999	Sandy finely crystalline dolomite: brown, laminated, micrite.
3999 to 4009	Anhydrite: brown and gray, massive, nodular, and laminated, shale laminae.
4009 to 4022	Medium crystalline to finely crystalline dolomite: light gray to gray, laminated, bioturbated, micrite and minor biomicrite.
4022 to 4023	Anhydrite: blue gray, laminated and nodular.
4023 to 4027	Finely crystalline dolomite: brown, fetid, micrite.
4027 to 4031	Limestone: laminated, black shale laminae, fetid, micrite.
4031 to 4038	Anhydrite: blue gray, massive to weakly laminated, upper 2 feet is brown dolomite with blue gray anhydrite nodules.
4038 to 4060	Sandy finely crystalline dolomite: gray to dark gray, wavy and parallel laminations, flaser, soft sediment deformation, sandy micrite.
4060 to 4065	Silty finely crystalline dolomite with anhydrite: light brown, blue gray anhydrite nodules, parallel laminations, silty micrite.
4065 to 4070	Finely crystalline dolomite: gray to blue gray, wavy laminations, micrite.
4070 to 4087	Finely crystalline dolomite: brown, bioturbated, micrite.
4087 to 4090	Limestone: gray, laminated, black shale laminae, micrite.
4090 to 4100	Silty finely crystalline dolomite: dark brown, micrite.

4100 to 4118	Sandy finely crystalline, finely crystalline and medium crystalline dolomite: dark brown, gray 4112 to 4115 feet, some beds weakly calcareous, medium crystalline beds are sucrosic, lower half of unit is sandy, micrite, minor biomicrite.
4118 to 4128	Finely crystalline calcareous dolomite to dolomitic limestone: gray to gray brown, parallel laminations, thin bedded, black shale laminae, bioturbated, micrite and minor biomicrite.
4128 to 4145	Finely crystalline fossiliferous limestone: gray brown to brown, black shale laminae most abundant in lower half of unit, calcite filled fractures, micrite and biomicrite.
4145 to 4158	Finely crystalline dolomite: gray (upper unit), light gray brown (lower unit), parallel laminated, bioturbation, lower part of unit is sandy, blue gray coarse sand-sized to granule-sized anhydrite at 4147 feet, black laminated shale at 4153 feet, micrite to biomicrite (?).
4158 to 4226	Fine sandstone to muddy siltstone: light brown to dark brown, dolomitic, wavy laminations, minor cross laminations, bioturbation, soft sediment deformation, rip-up clasts, anyhydrite at 4203 feet.
4226 to 4228	Sandy anhydrite: blue gray, weakly laminated, some nodular textures.
4228 to 4242	Finely crystalline dolomite: gray, fetid, anhydrite grains and small nodules, blue gray anhydrite bed at 4235 feet, micrite.
4242 to 4244	Anhydrite: blue gray with brown finely crystalline dolomite intraclasts.
4244 to 4260	Finely crystalline calcareous dolomite: some beds are fetid, thin bedded, wavy laminations, black shale laminae, scattered blue gray anhydrite grains, laminae, and nodules, soft sediment deformation.
4260 to 4300	Olivine basalt: blue black to green black, high and low angle calcite filled fractures, round calcite and dolomite vesicle fillings or zenoliths, chloritic and serpentine-like alteration zones, most olivine is altered.
4300 to 4322	Olivine basalt: blue black to green black, high and low angle calcite filled fractures, round calcite and dolomite vesicle fillings or zenoliths, chloritic and serpentine-like alteration zones, most olivine is altered.
4322 to 4327	Finely crystalline fossilerferous limestone: dark gray to black, micrite and biomicrite.
4327 to 4362	Olivine basalt: blue black to green black, high and low angle calcite filled fractures, round calcite and dolomite vesicle fillings or zenoliths, chloritic and serpentine-like alteration zones, most olivine is altered.
4362 to 4400	Finely crystalline fossiliferous limestone: dark gray to black, medium bedded, mudstone and wackstone textures, fetid, hydrocarbon stains, vuggy porsity and possible moldic porosity, micrite and biomicrite.
4400 to 4405	Finely crystalline dolomite: gray and brown, vuggy porosity, hydrocarbon stains (?), lower part of unit is sandy.
4405 to 4407	Siltstone: gray, calcitic, parallel laminated.

4407 to 4411	Sandy finely crystalline limestone: gray, parallel laminated, black shale laminae, micrite.
4411 to 4416	Siltstone: gray and red brown, parallel laminated, black and brown shaly laminae.
4416 to 4421	Fine sandstone: red brown, calcitic, parallel laminated, black shale laminae, healed vertical hairline fractures.
4421 to 4427	Fine to medium crystalline anhydrite: mostly blue gray, minor brown, nodular textures.
4427 to 4428	Finely crystalline dolomite: gray with black shale laminations, some soft sediment deformation.
4428 to 4454	Fine sandstone to siltstone: light brown to dark brown, calcitic and dolomitic, wavy laminations, rip-up clasts, scour, ripple cross laminations, flaser.
4454 to 4505	Pyroxene basalt: black green, rounded calcite vesicle fillings or zenoliths, chalcedony or opal in fractures at 4486 feet, minor altered olivine.

APPENDIX 9

GRAPHIC GEOLOGIC AND GEOPHYSICAL LOGS OF THE ALPINE 1/FEDERAL BOREHOLE

section 1 penetration rate/lithology
section 2 natural gamma/lithology
section 3 neutron log/lithology

KEY

grain size/weathering profile

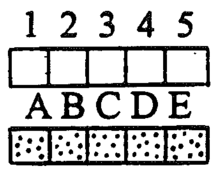

1	mudstone/clay	**A**	basalt/andesite/rhyolite
2	siltstone/fine sandstone	**B**	dolomite
3	medium to coarse sandstone	**C**	dolomitic limestone
4	granule to pebble conglomerate and gravelly sandstone	**D**	limestone
5	cobble to boulder conglomerate	**E**	anhydrite

lithology symbols

clay/mudstone 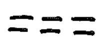

siltstone 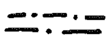

sandstone 

conglomerate 

andesite 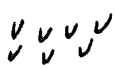

basalt 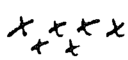

rhyolite 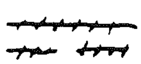

anhydrite 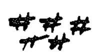

limestone 

dolomite 

dolomitic limestone 

sandy/silty/clayey limestone 

sandy/silty/clayey dolomite 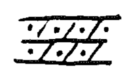

breccia 

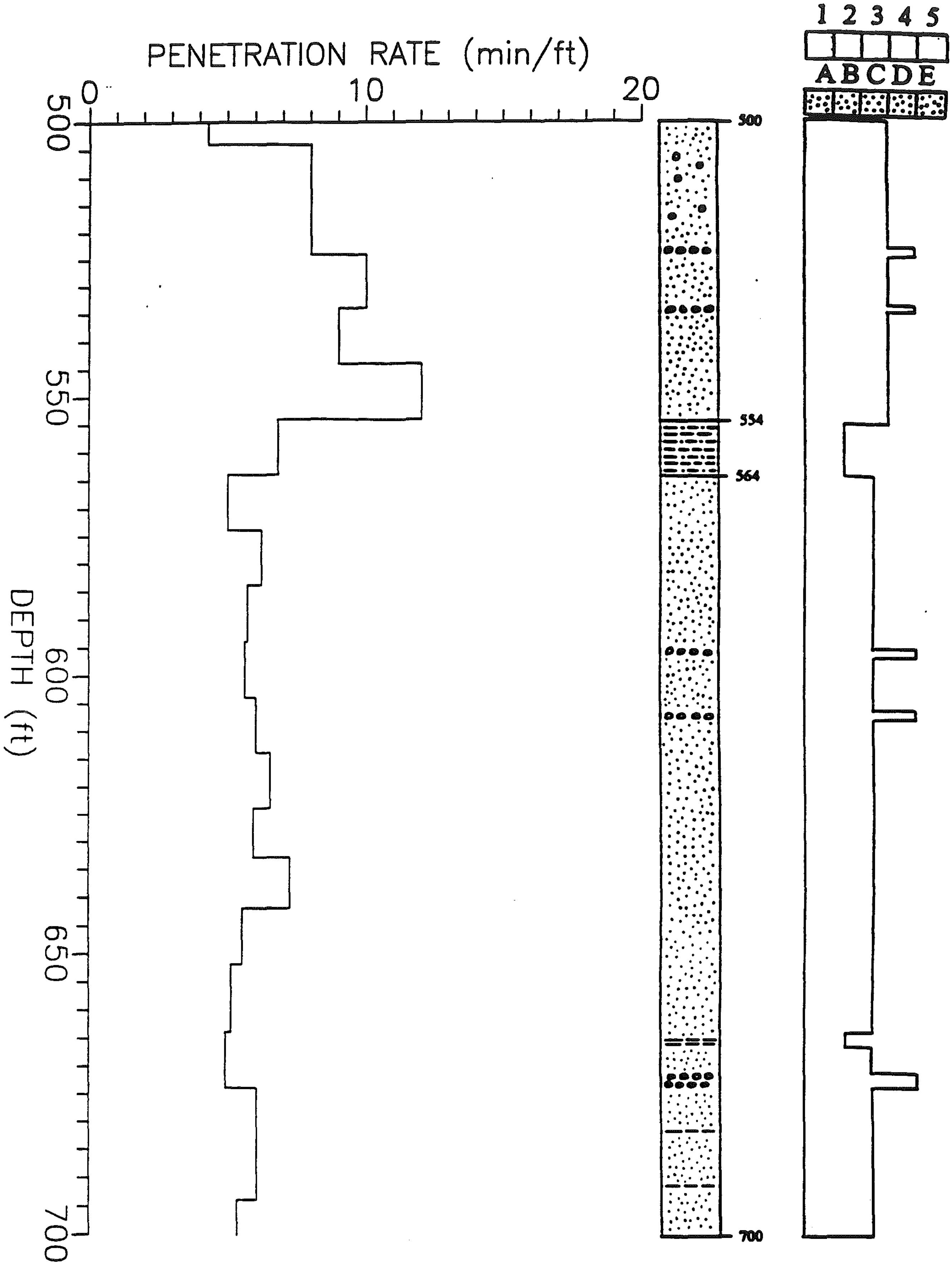
PENETRATION RATE (min/ft)
0
10
20
DEPTH (ft)
500
550
600
650
700
554
564
1 2 3 4 5
A B C D E

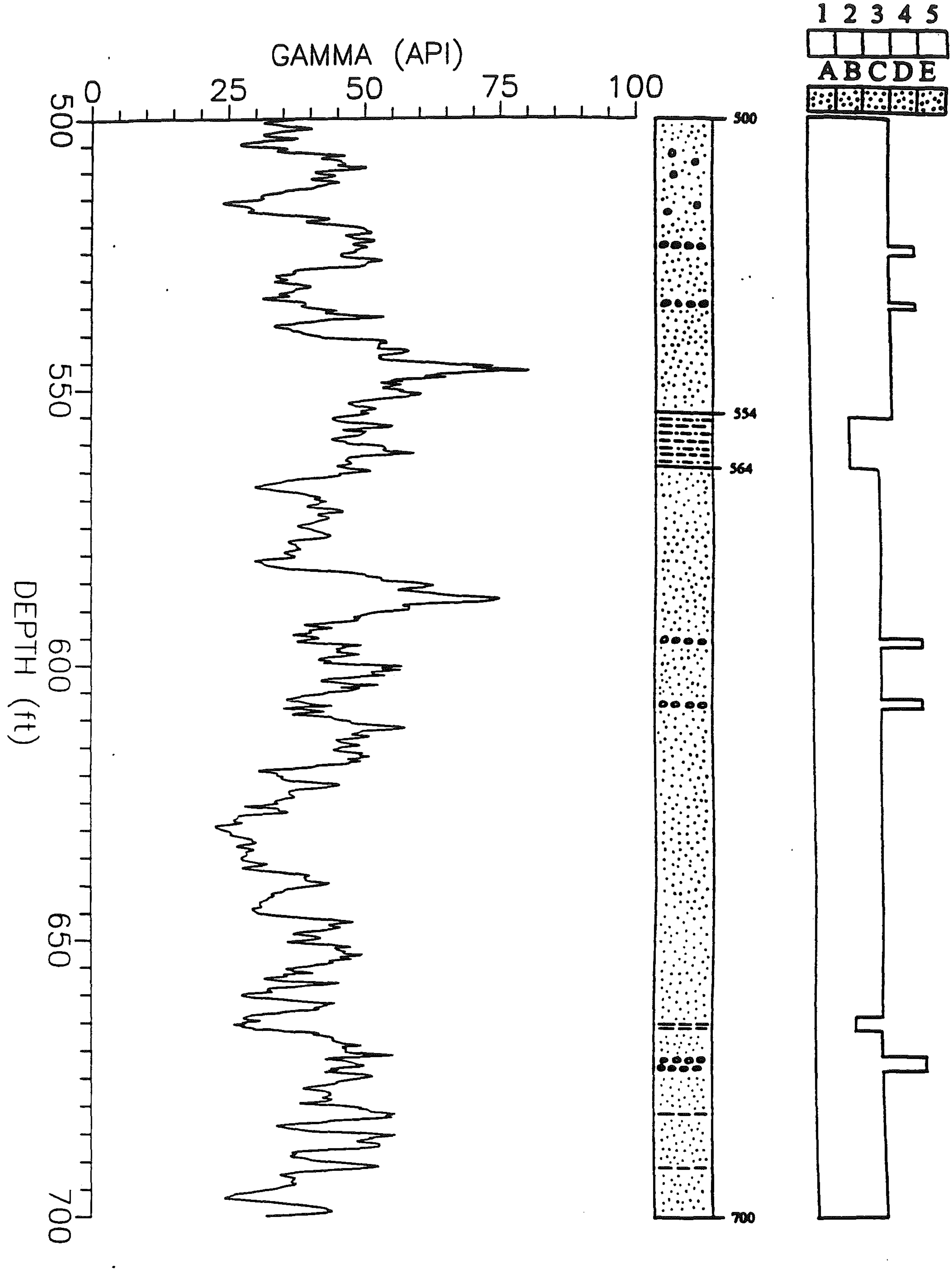
GAMMA (API)
0
25
50
75
100
DEPTH (ft)
500
550
600
650
700
500
554
564
700
1 2 3 4 5
A B C D E

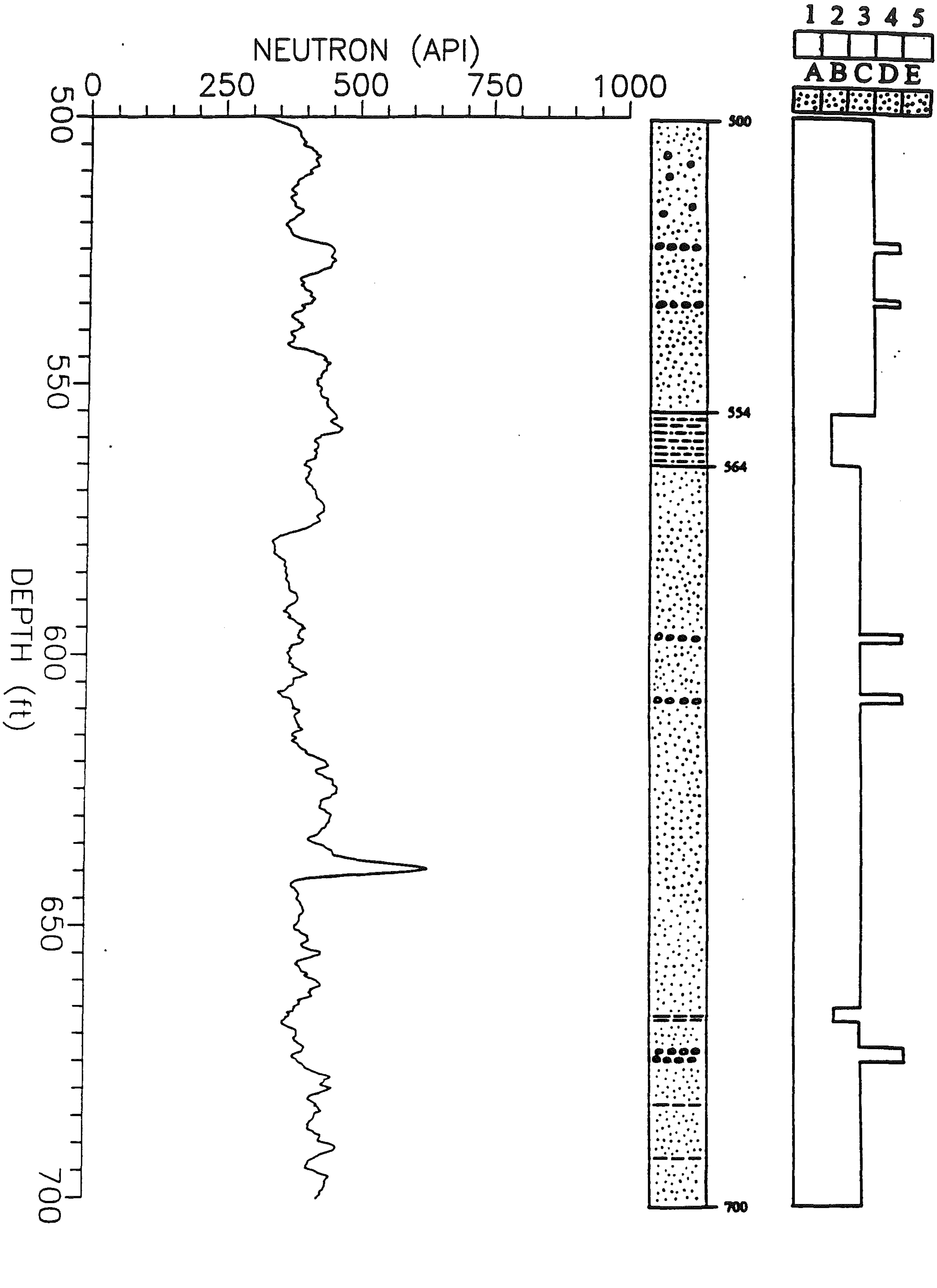
NEUTRON (API)
0
250
500
750
1000
500
550
600
650
700
DEPTH (ft)
500
554
564
700
1 2 3 4 5
A B C D E

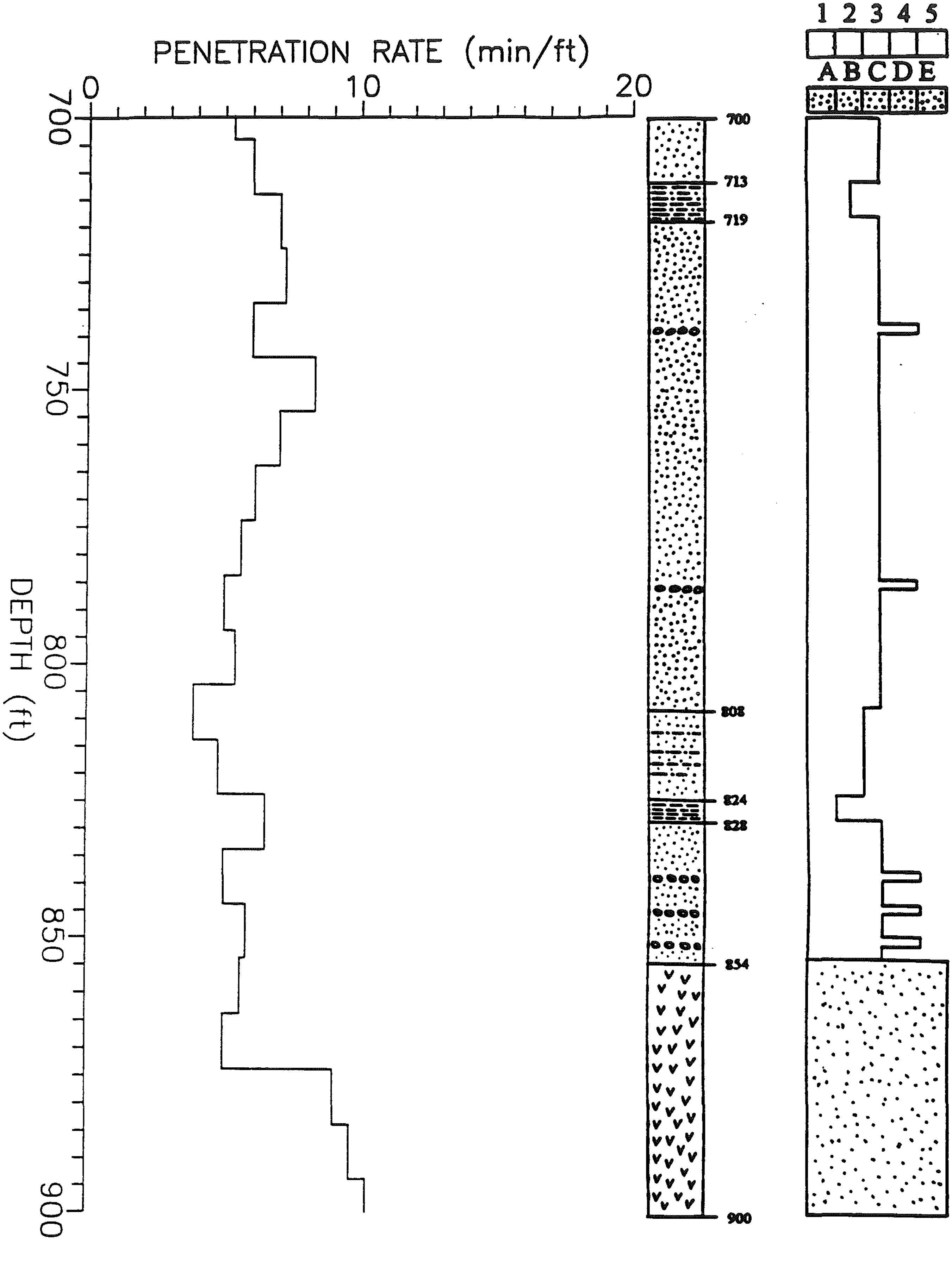
PENETRATION RATE (min/ft)
0
10
20
DEPTH (ft)
700
750
800
850
900
713
719
808
824
828
854
1 2 3 4 5
A B C D E

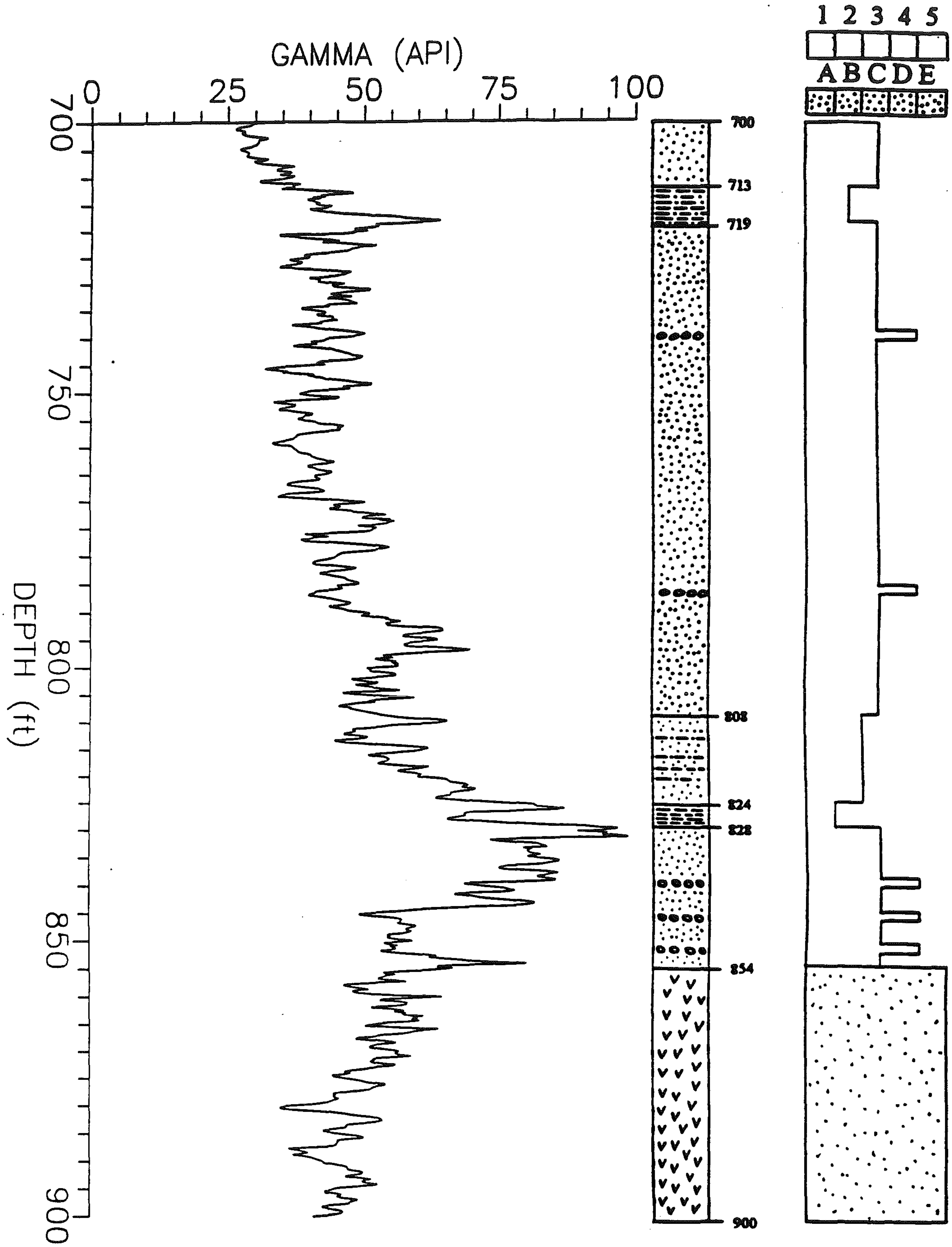
GAMMA (API)
0
25
50
75
100
DEPTH (ft)
700
750
800
850
900
713
719
808
824
828
854
1 2 3 4 5
A B C D E

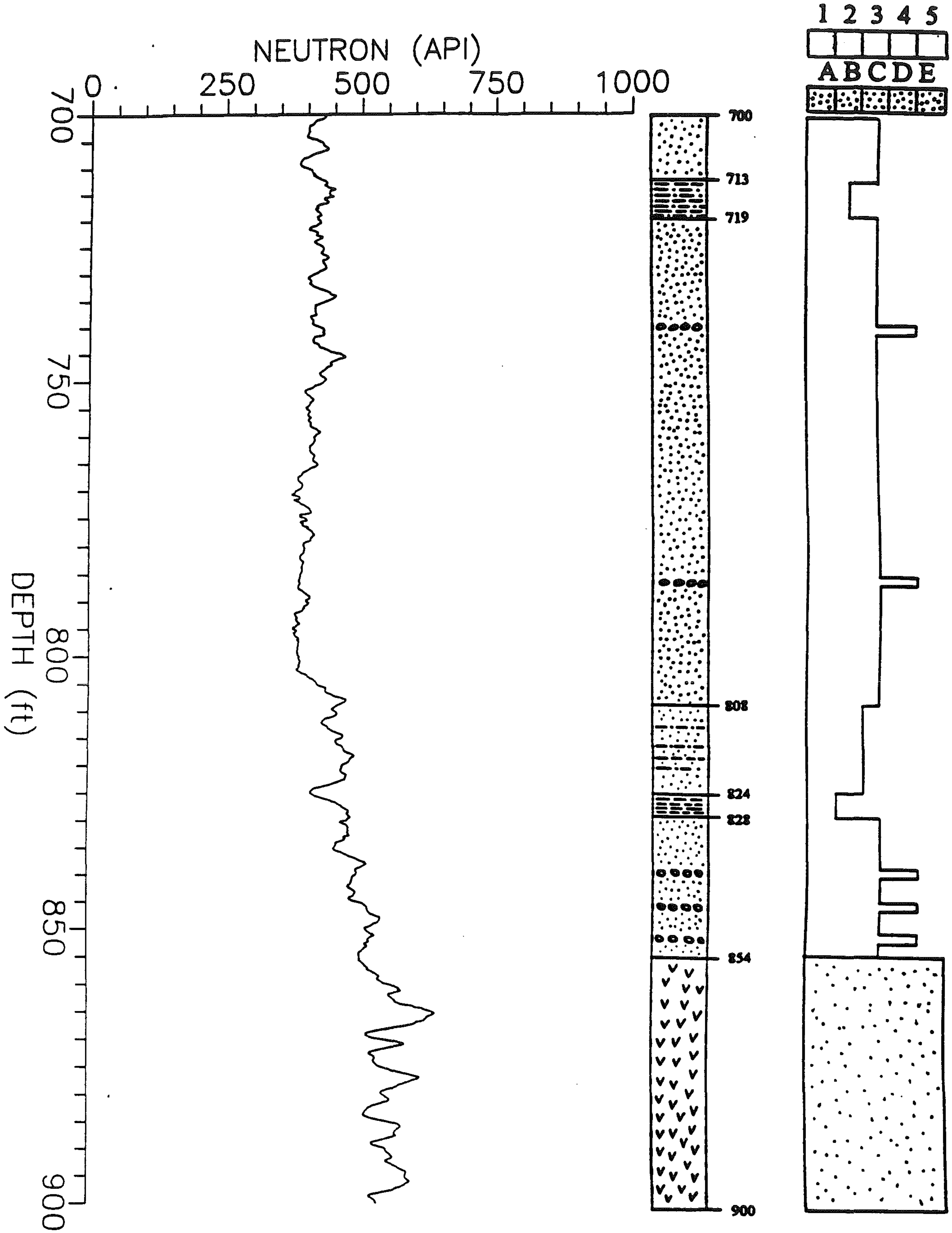

NEUTRON (API)
0
250
500
750
1000
700
750
800
850
900
DEPTH (ft)
700
713
719
808
824
828
854
900
1 2 3 4 5
A B C D E

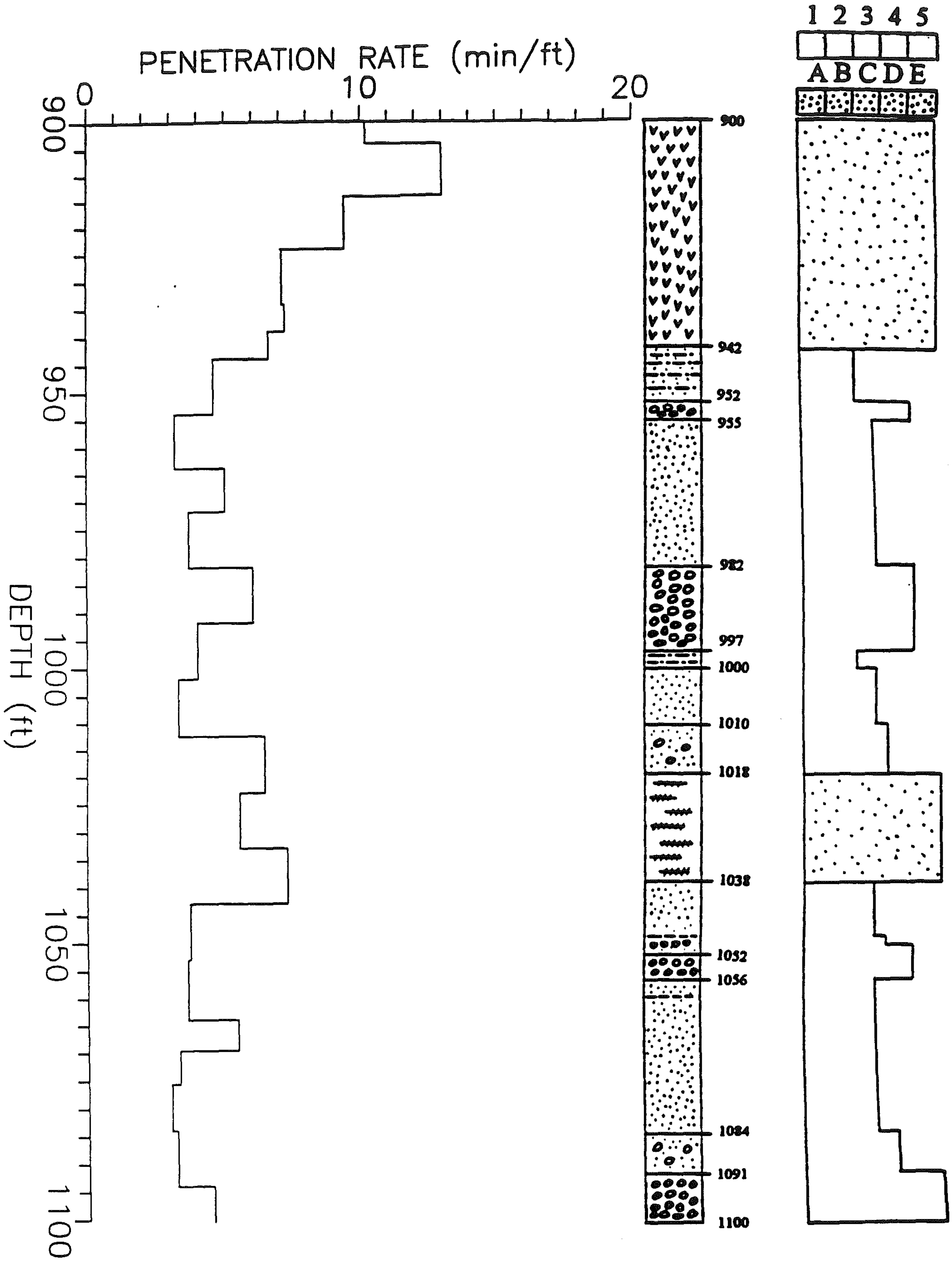

PENETRATION RATE (min/ft)
0
10
20
DEPTH (ft)
900
950
1000
1050
1100
900
942
952
955
982
997
1000
1010
1018
1038
1052
1056
1084
1091
1100
1 2 3 4 5
A B C D E

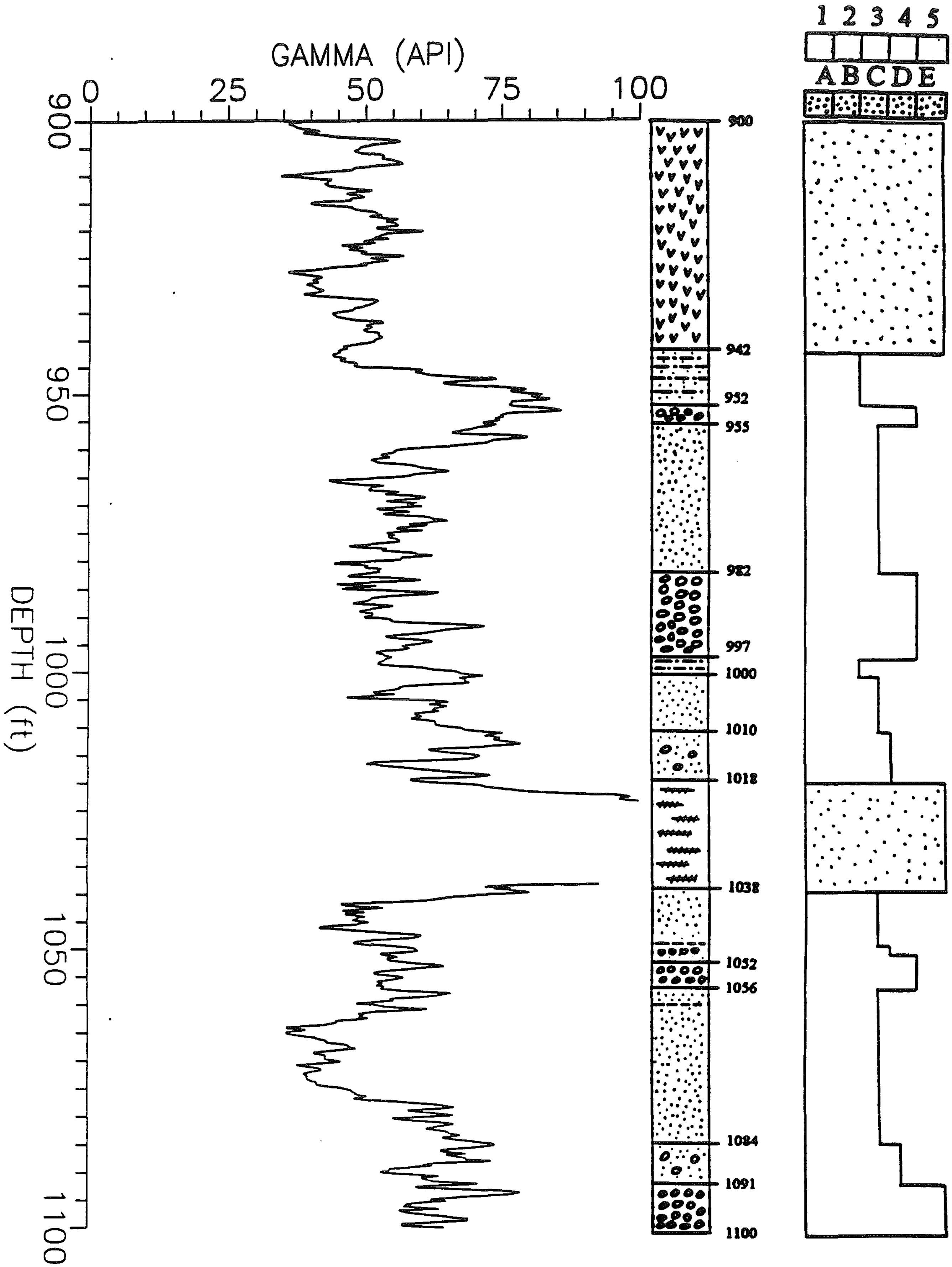
GAMMA (API)
0
25
50
75
100
DEPTH (ft)
900
950
1000
1050
1100
942
952
955
982
997
1000
1010
1018
1038
1052
1056
1084
1091
1 2 3 4 5
A B C D E

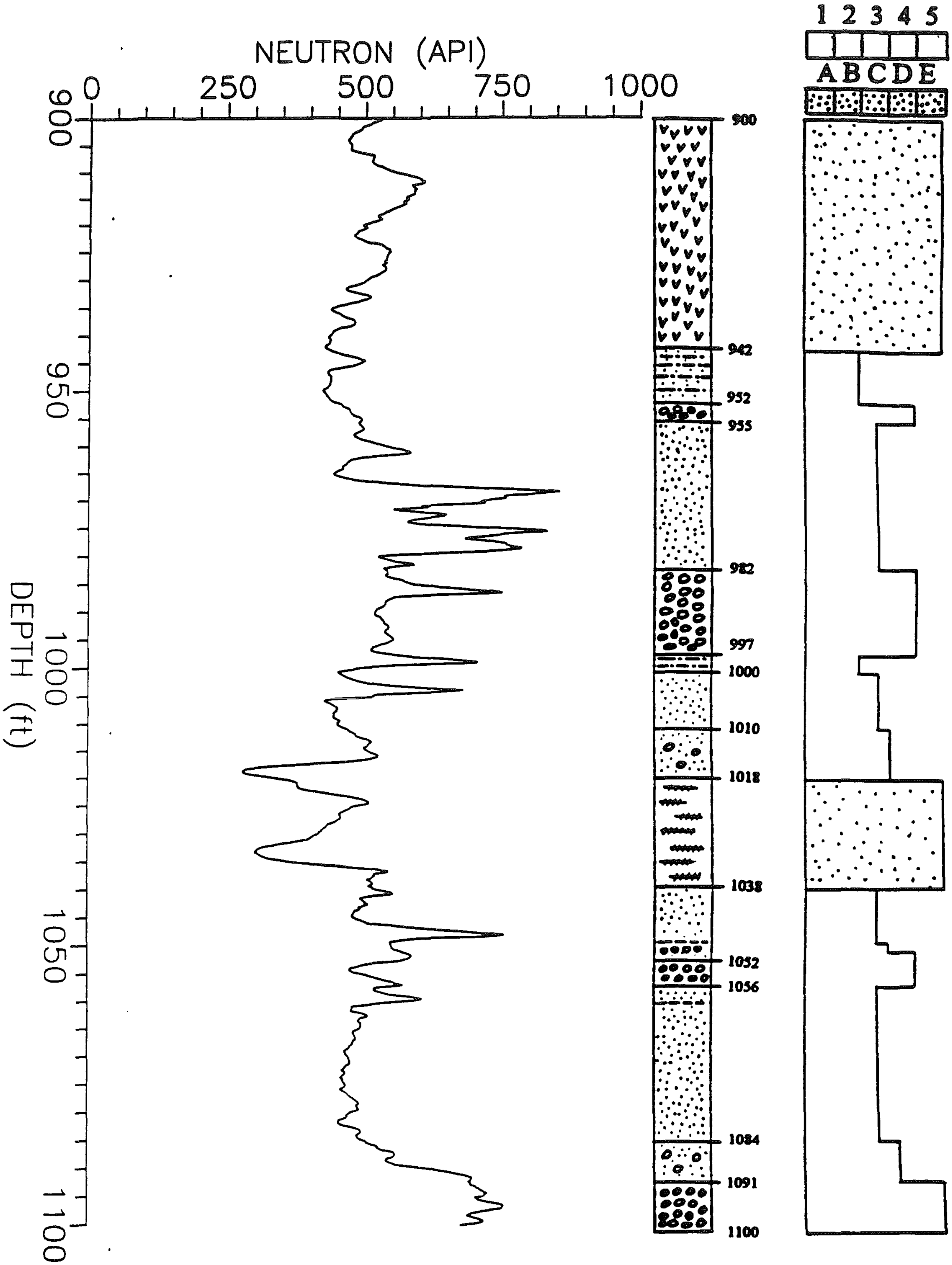
NEUTRON (API)
0
250
500
750
1000
900
950
1000
1050
1100
DEPTH (ft)
900
942
952
955
982
997
1000
1010
1018
1038
1052
1056
1084
1091
1100
1 2 3 4 5
A B C D E

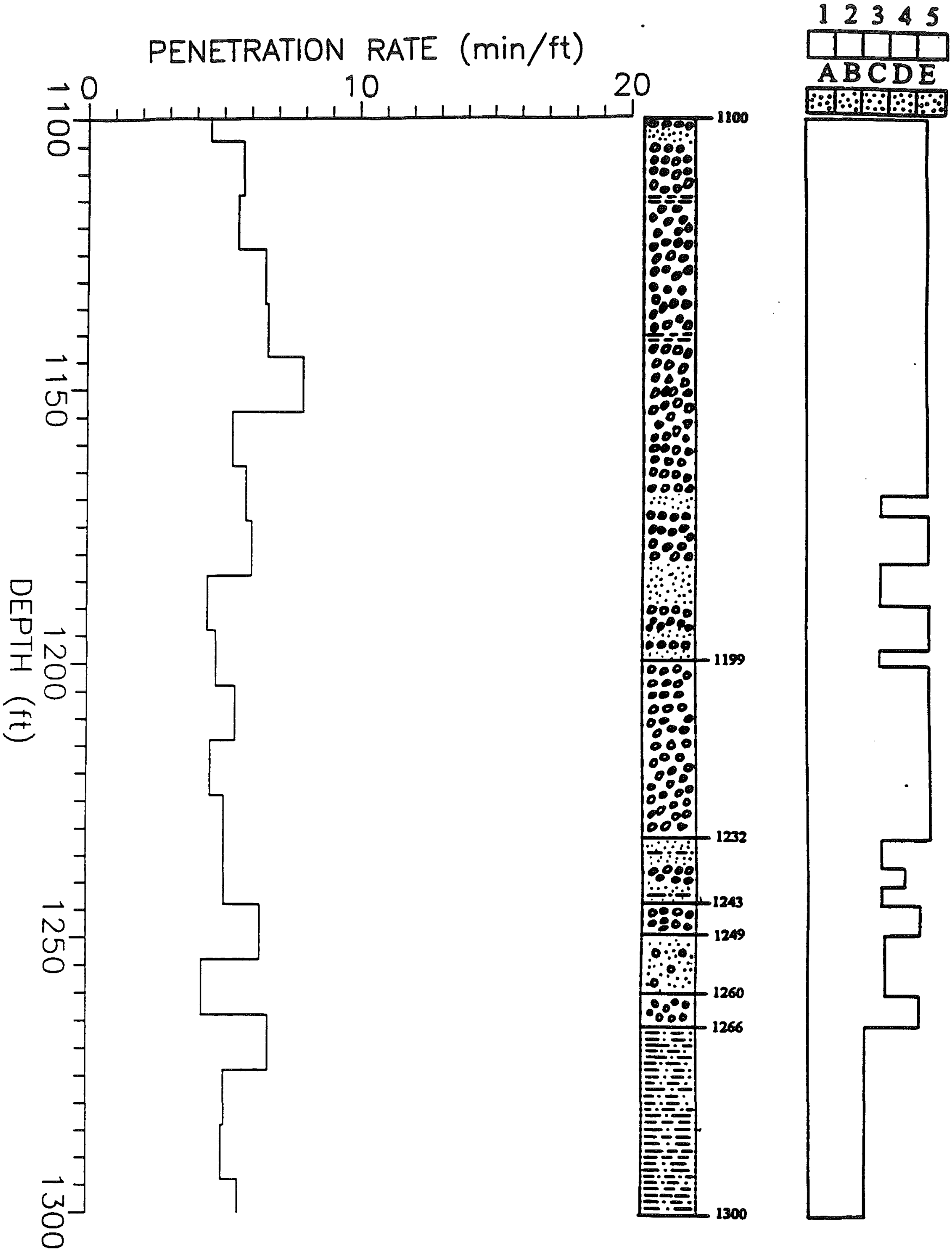
PENETRATION RATE (min/ft)
0
10
20
DEPTH (ft)
1100
1150
1200
1250
1300
1100
1199
1232
1243
1249
1260
1266
1300
1 2 3 4 5
A B C D E

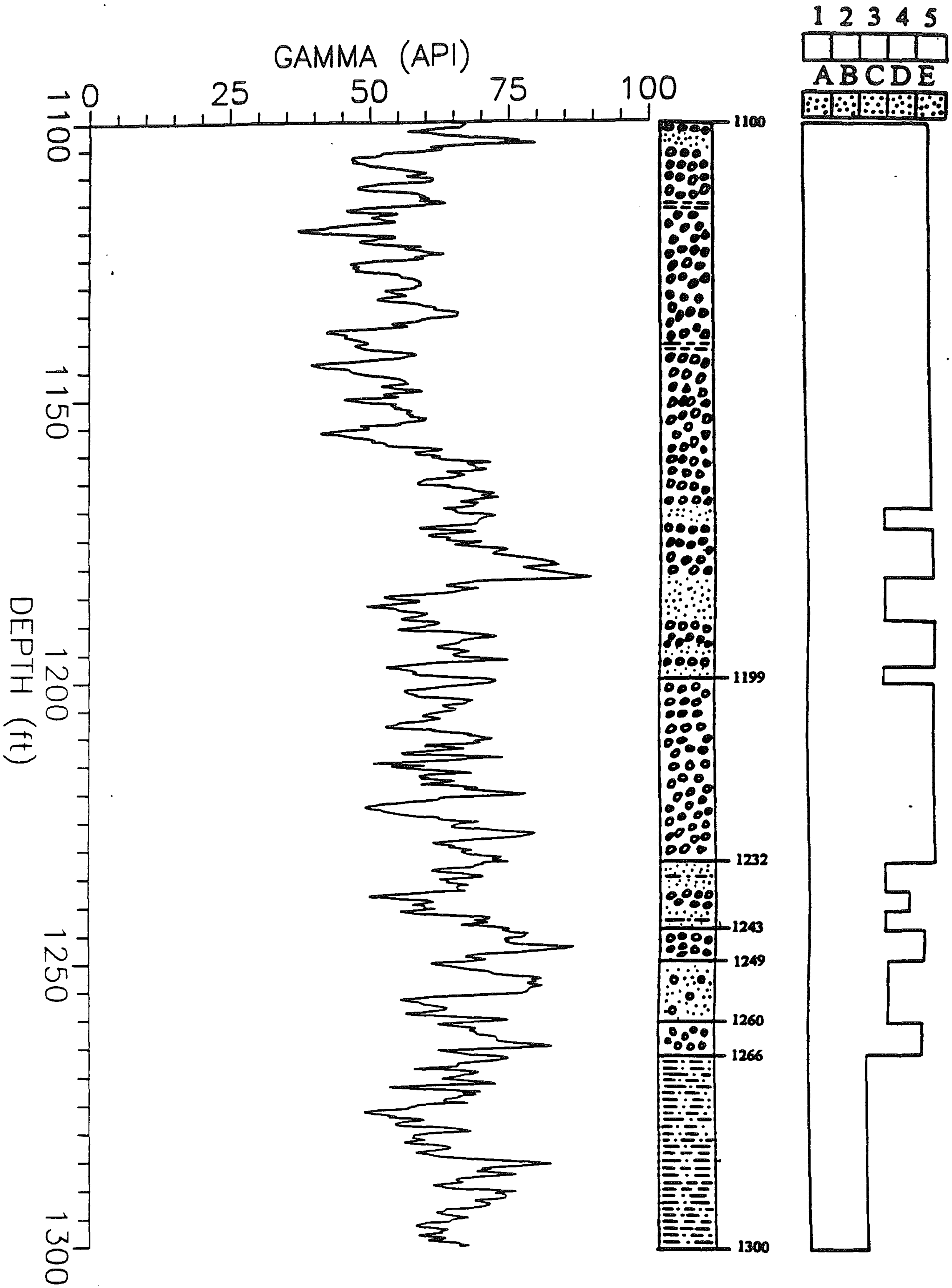

GAMMA (API)
0
25
50
75
100
1100
1150
1200
1250
1300
DEPTH (ft)
1100
1199
1232
1243
1249
1260
1266
1300
1 2 3 4 5
A B C D E

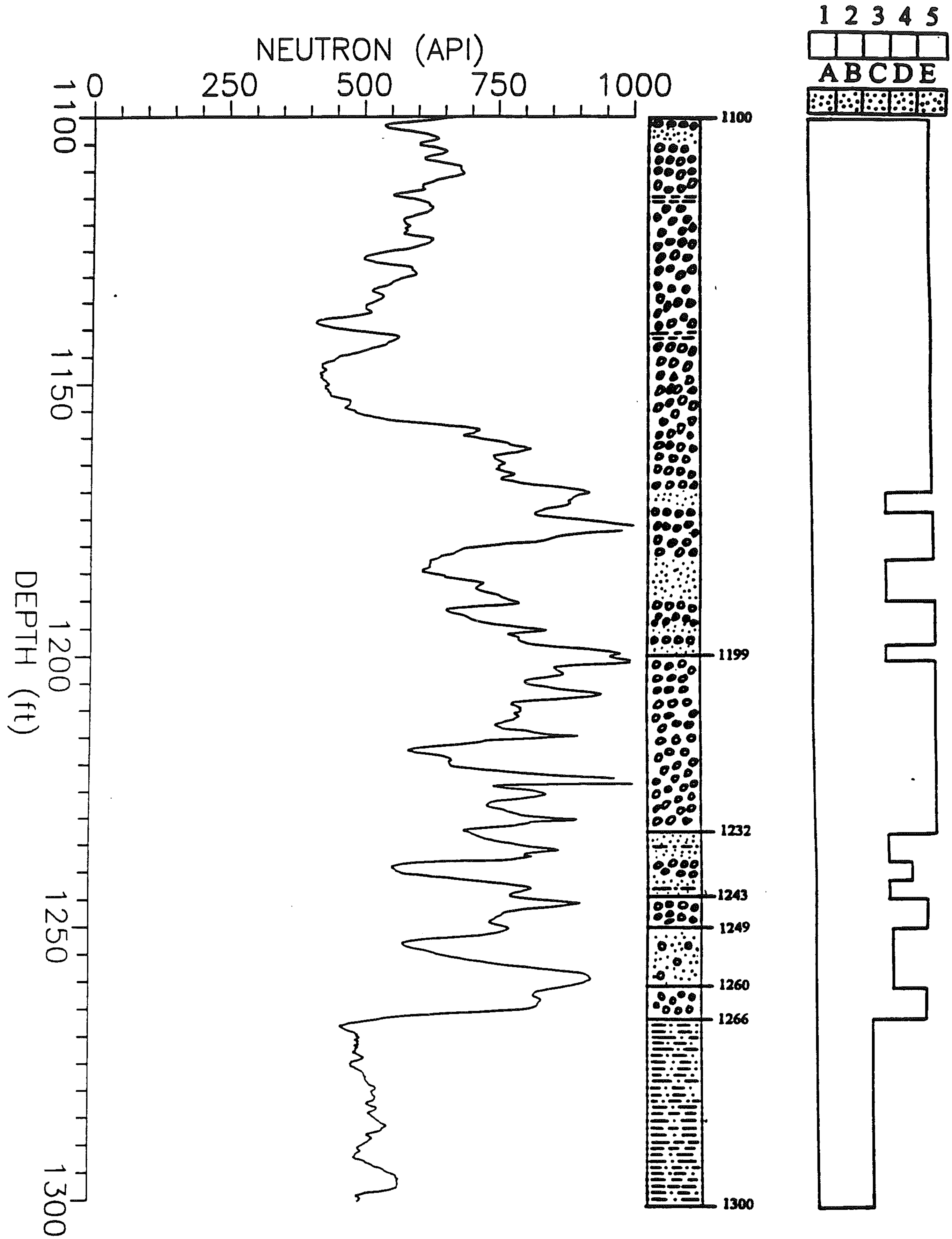
NEUTRON (API)
0
250
500
750
1000
1100
1150
1200
1250
1300
DEPTH (ft)
1100
1199
1232
1243
1249
1260
1266
1300
1 2 3 4 5
A B C D E

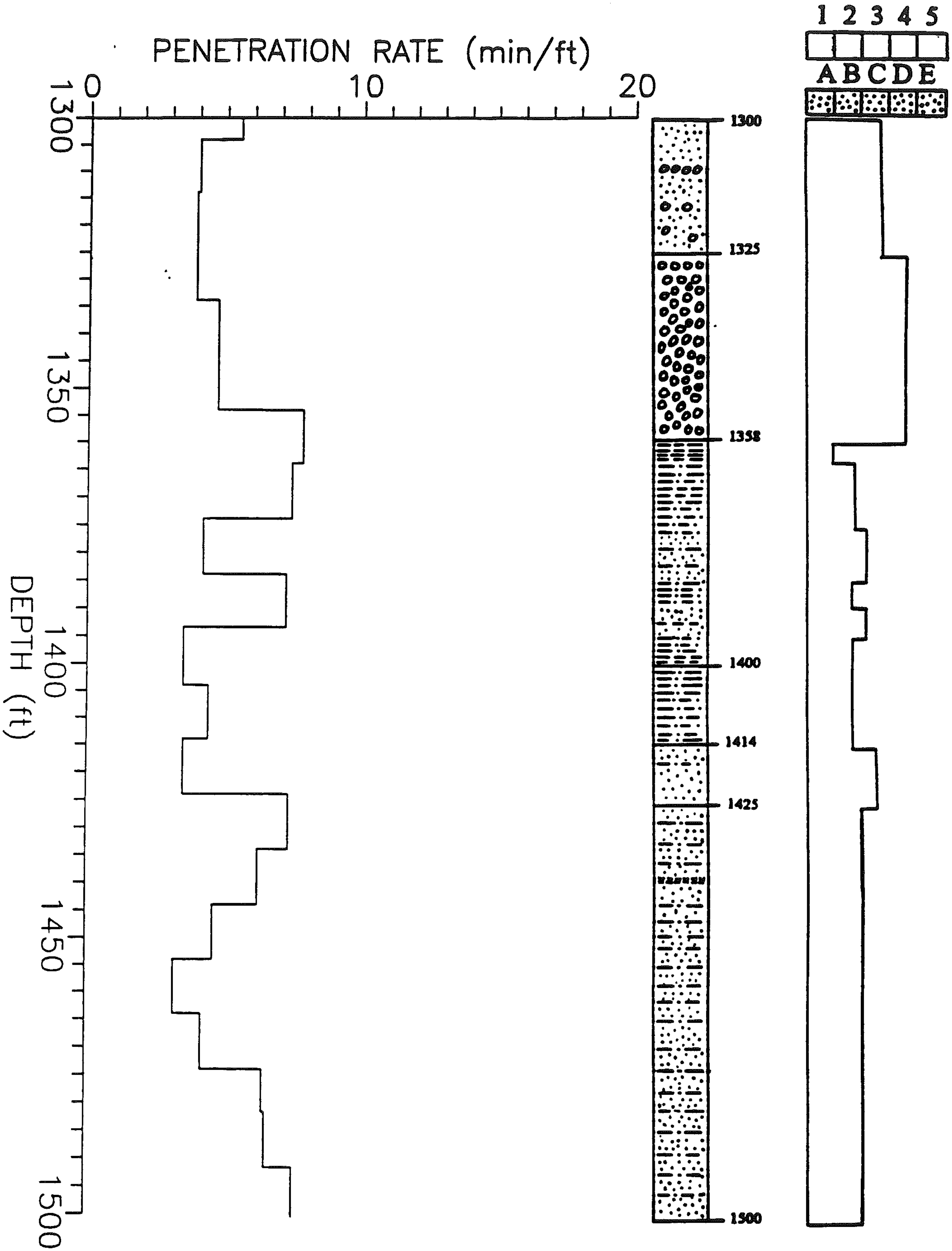
PENETRATION RATE (min/ft)
0
10
20
DEPTH (ft)
1300
1350
1400
1450
1500
1300
1325
1358
1400
1414
1425
1500
1 2 3 4 5
A B C D E

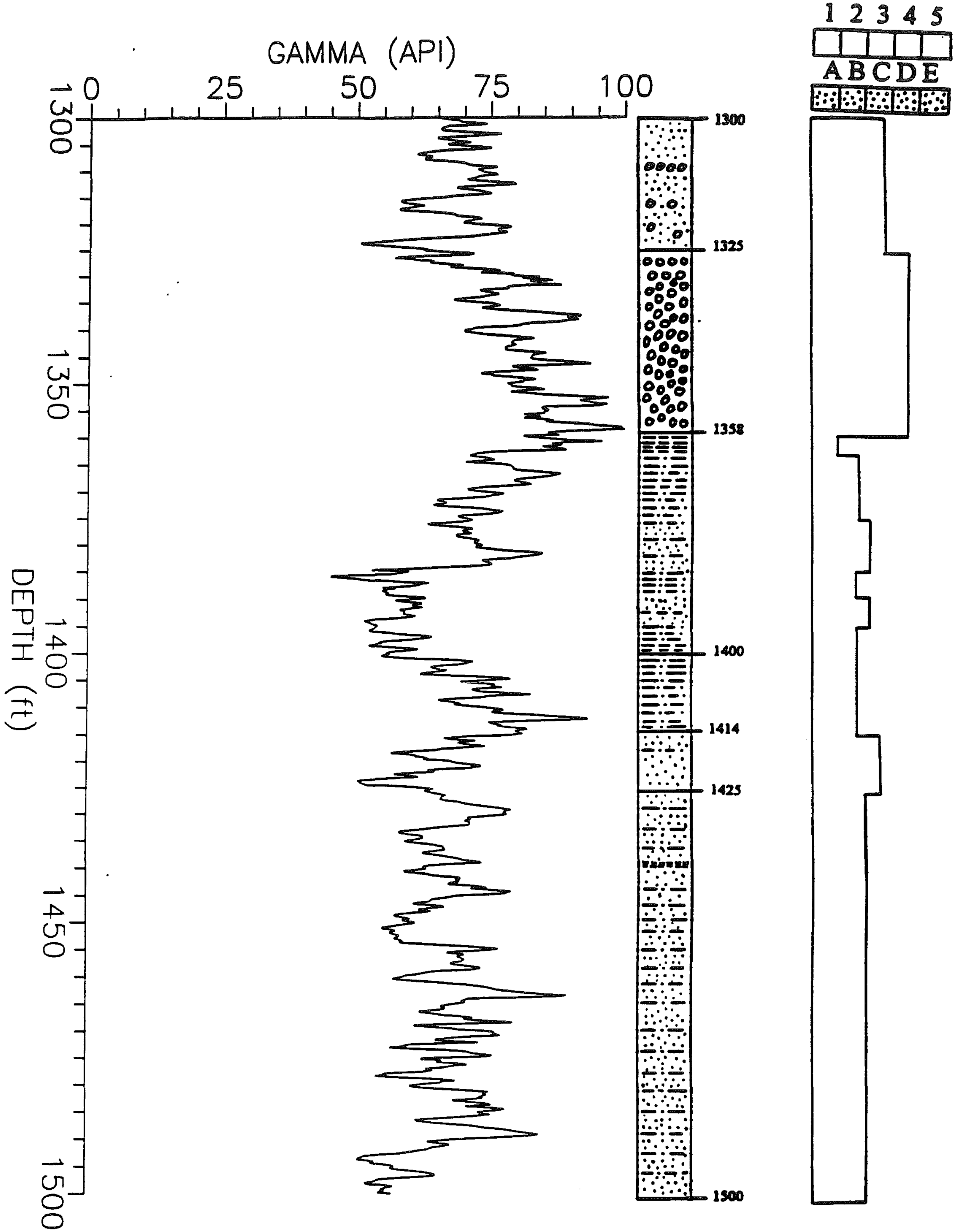

GAMMA (API)
0
25
50
75
100
1300
1350
1400
1450
1500
DEPTH (ft)
1300
1325
1358
1400
1414
1425
1500
1 2 3 4 5
A B C D E

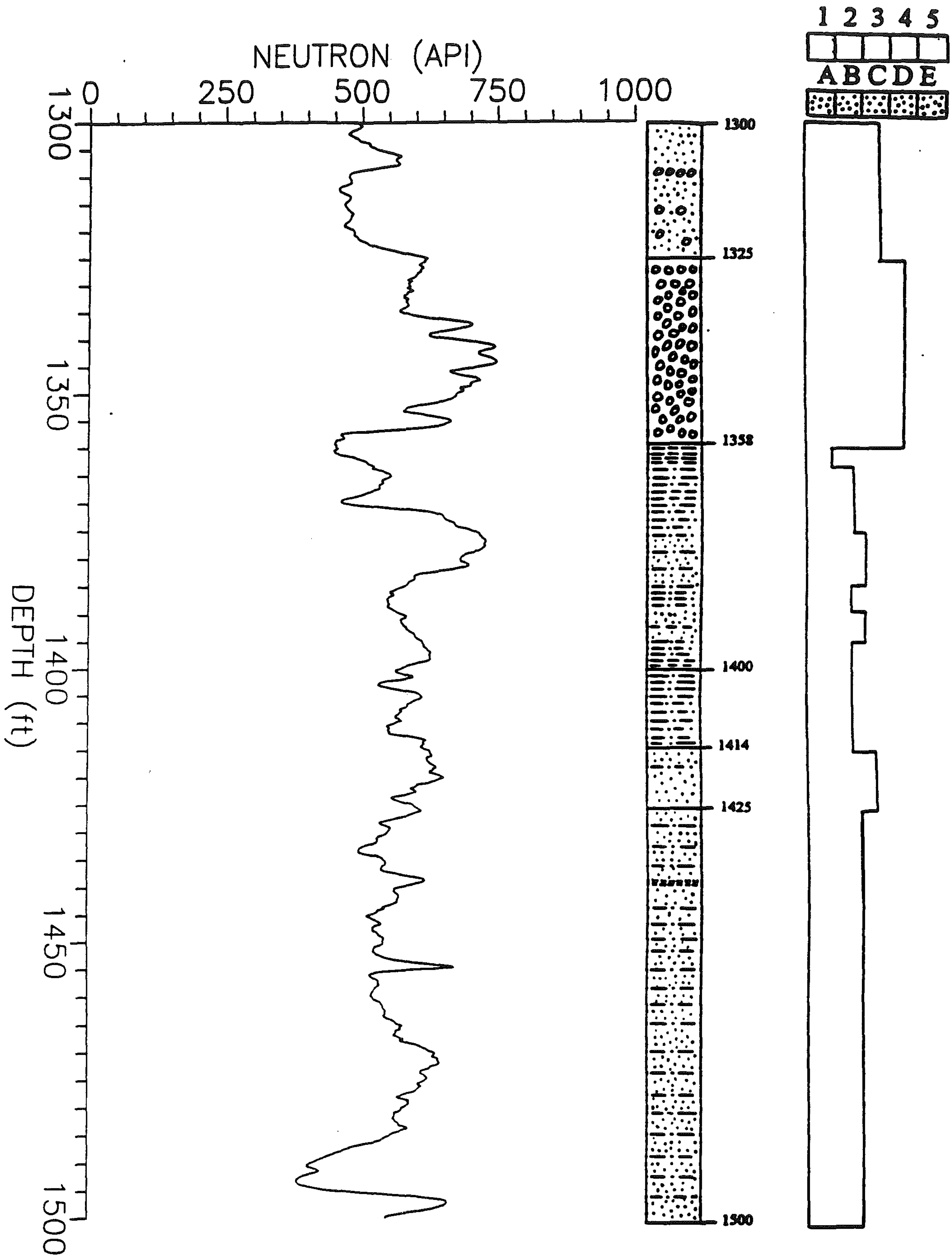

NEUTRON (API)
0
250
500
750
1000
1300
1350
1400
1450
1500
DEPTH (ft)
1300
1325
1358
1400
1414
1425
1500
1 2 3 4 5
A B C D E

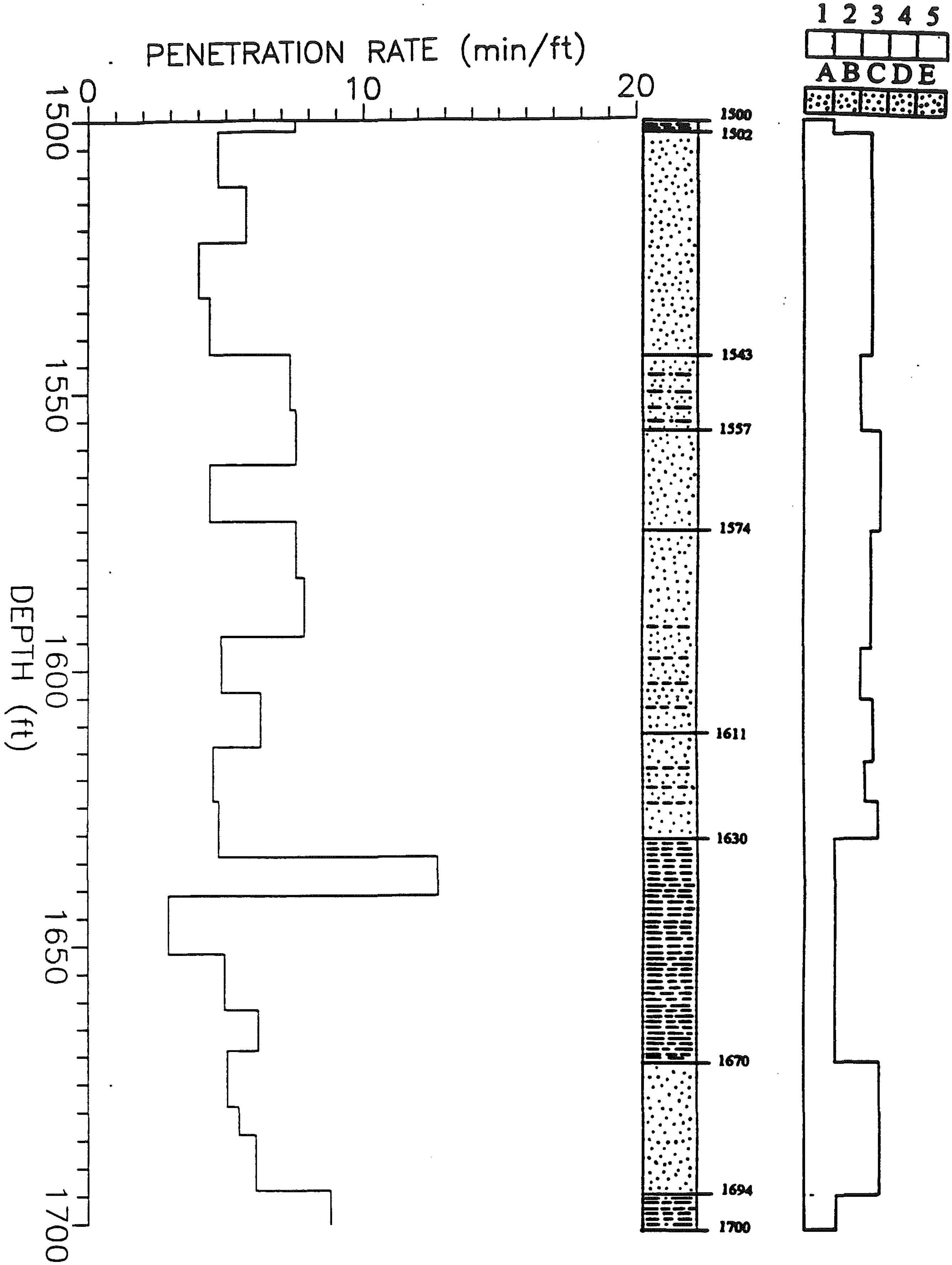

PENETRATION RATE (min/ft)
0
10
20
1500
1550
1600
1650
1700
DEPTH (ft)
1500
1502
1543
1557
1574
1611
1630
1670
1694
1700
1 2 3 4 5
A B C D E

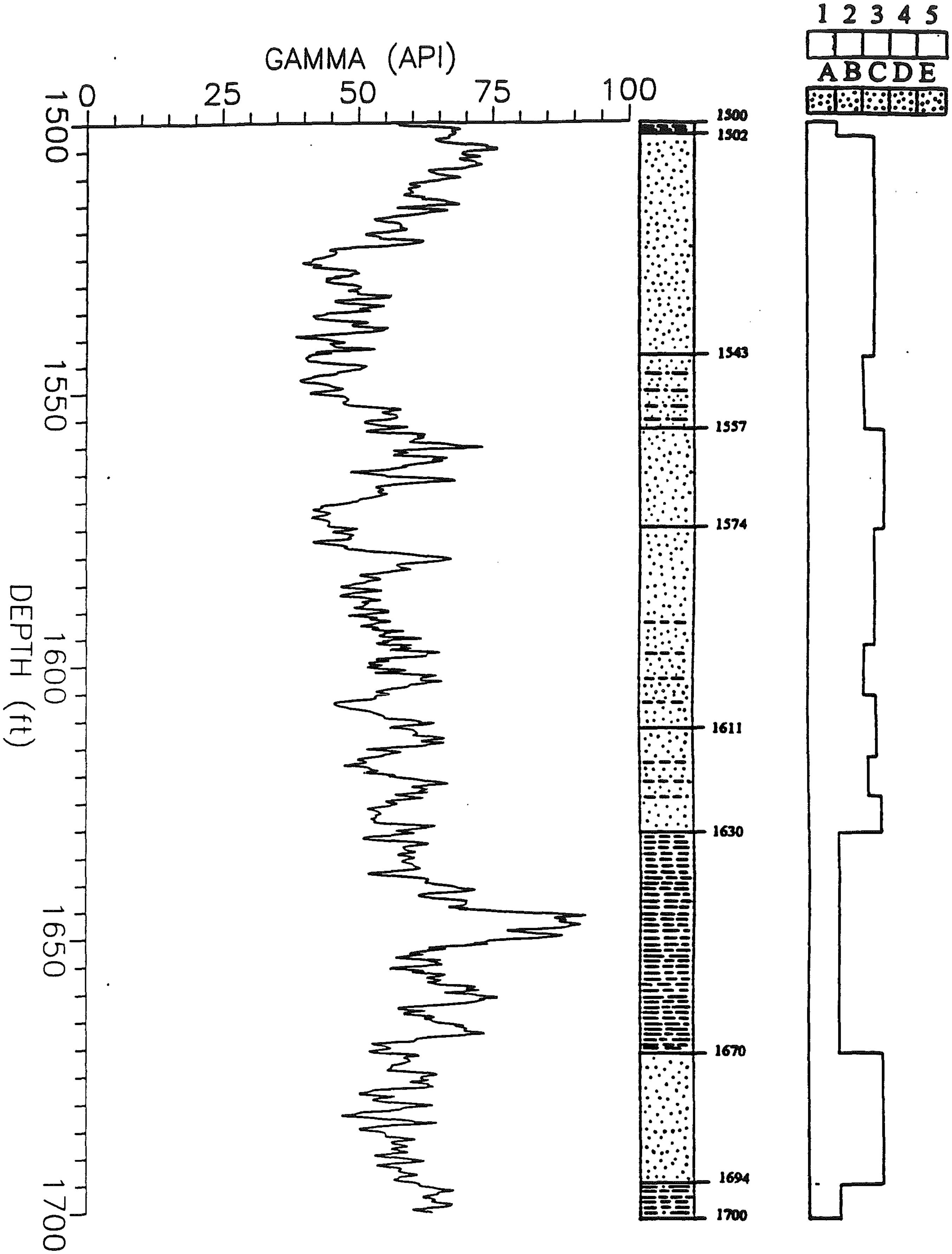
GAMMA (API)
0
25
50
75
100
1500
1550
1600
1650
1700
DEPTH (ft)
1500
1502
1543
1557
1574
1611
1630
1670
1694
1700
1 2 3 4 5
A B C D E

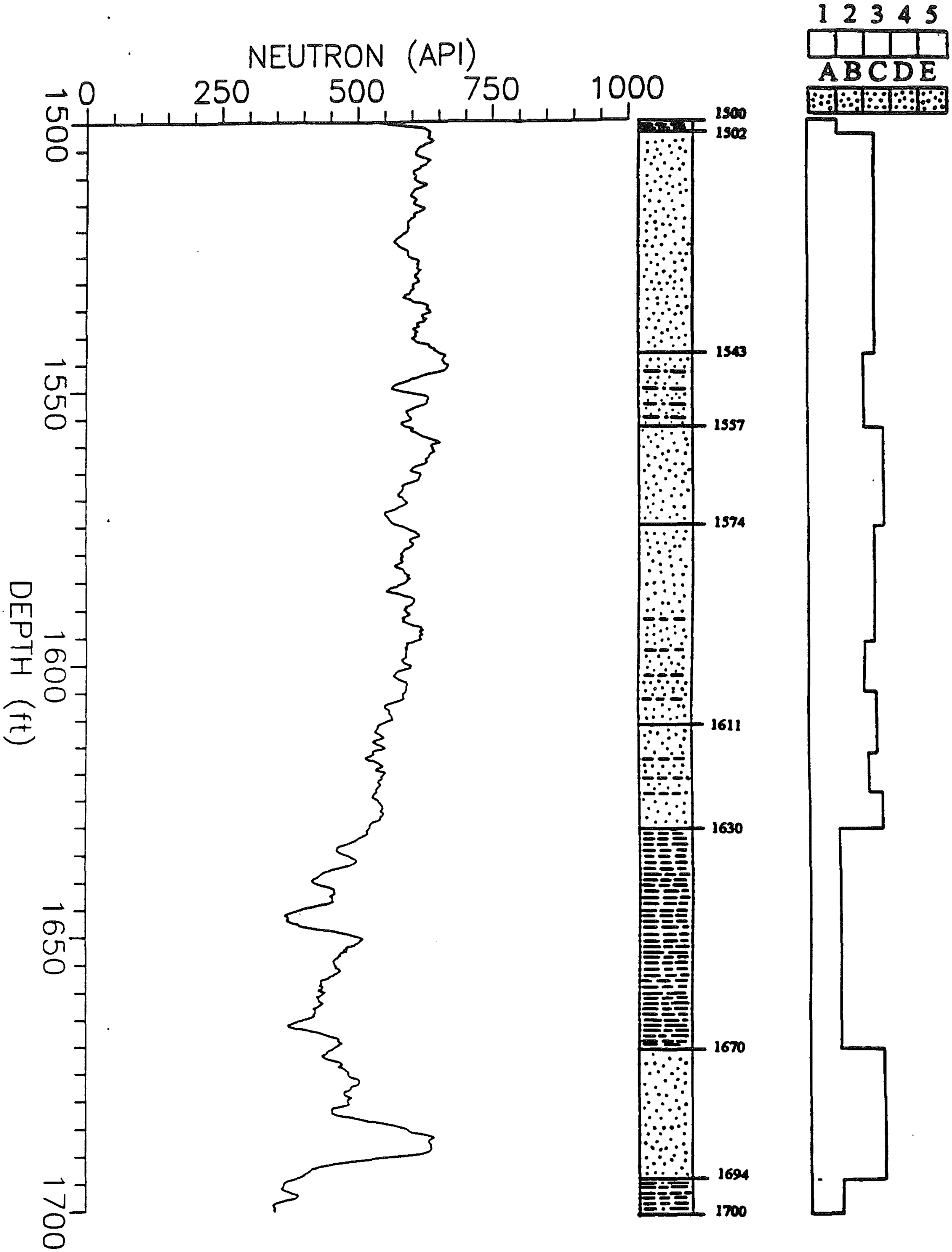
NEUTRON (API)
0
250
500
750
1000
1500
1550
1600
1650
1700
DEPTH (ft)
1500
1502
1543
1557
1574
1611
1630
1670
1694
1700
1 2 3 4 5
A B C D E

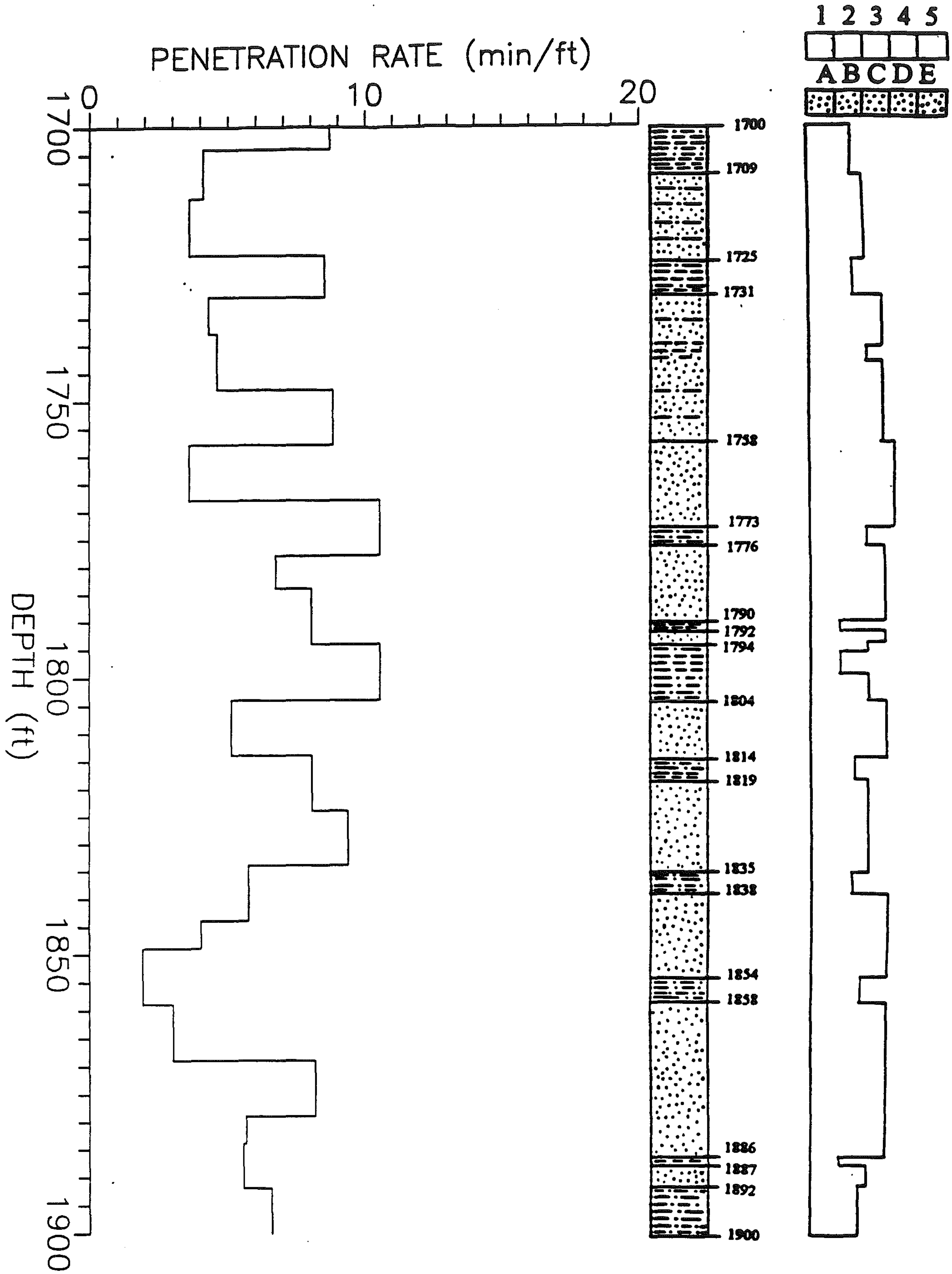
PENETRATION RATE (min/ft)
0
10
20
1700
1750
1800
1850
1900
DEPTH (ft)
1700
1709
1725
1731
1758
1773
1776
1790
1792
1794
1804
1814
1819
1835
1838
1854
1858
1886
1887
1892
1900
1 2 3 4 5
A B C D E

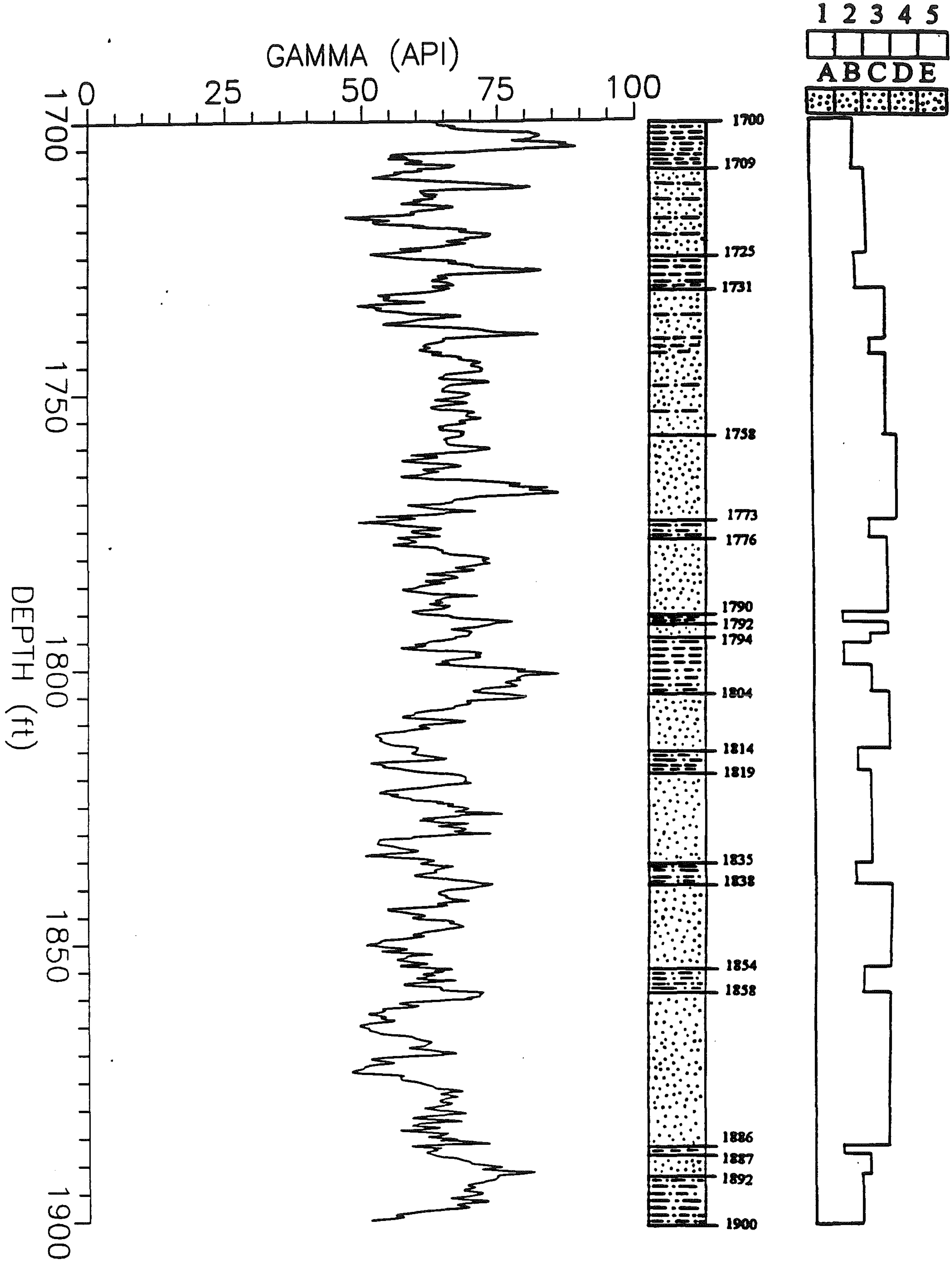
GAMMA (API)
0
25
50
75
100
DEPTH (ft)
1700
1750
1800
1850
1900
1700
1709
1725
1731
1758
1773
1776
1790
1792
1794
1804
1814
1819
1835
1838
1854
1858
1886
1887
1892
1900
1 2 3 4 5
A B C D E

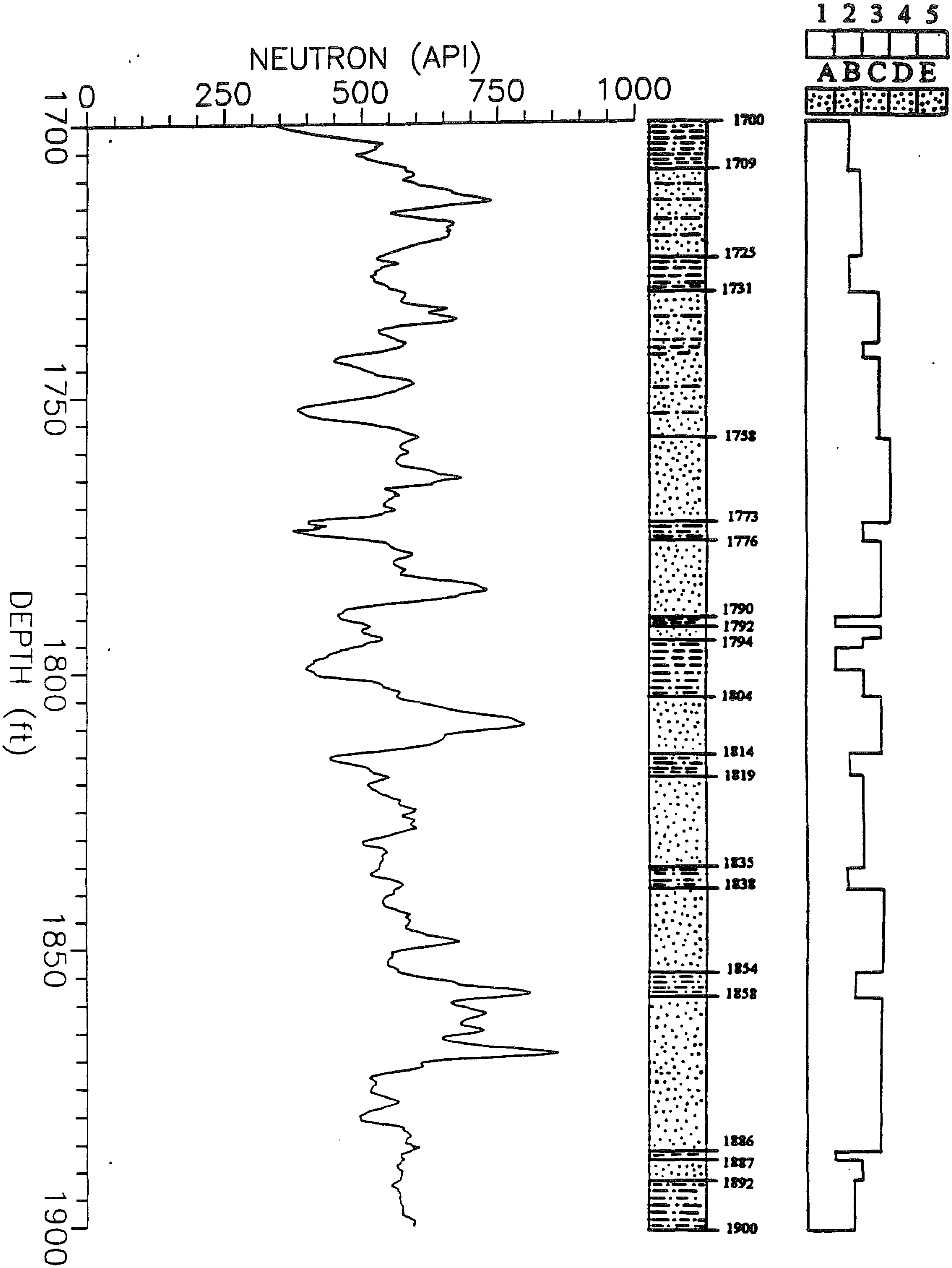

NEUTRON (API)
0
250
500
750
1000
DEPTH (ft)
1700
1750
1800
1850
1900
1700
1709
1725
1731
1758
1773
1776
1790
1792
1794
1804
1814
1819
1835
1838
1854
1858
1886
1887
1892
1900
1 2 3 4 5
A B C D E

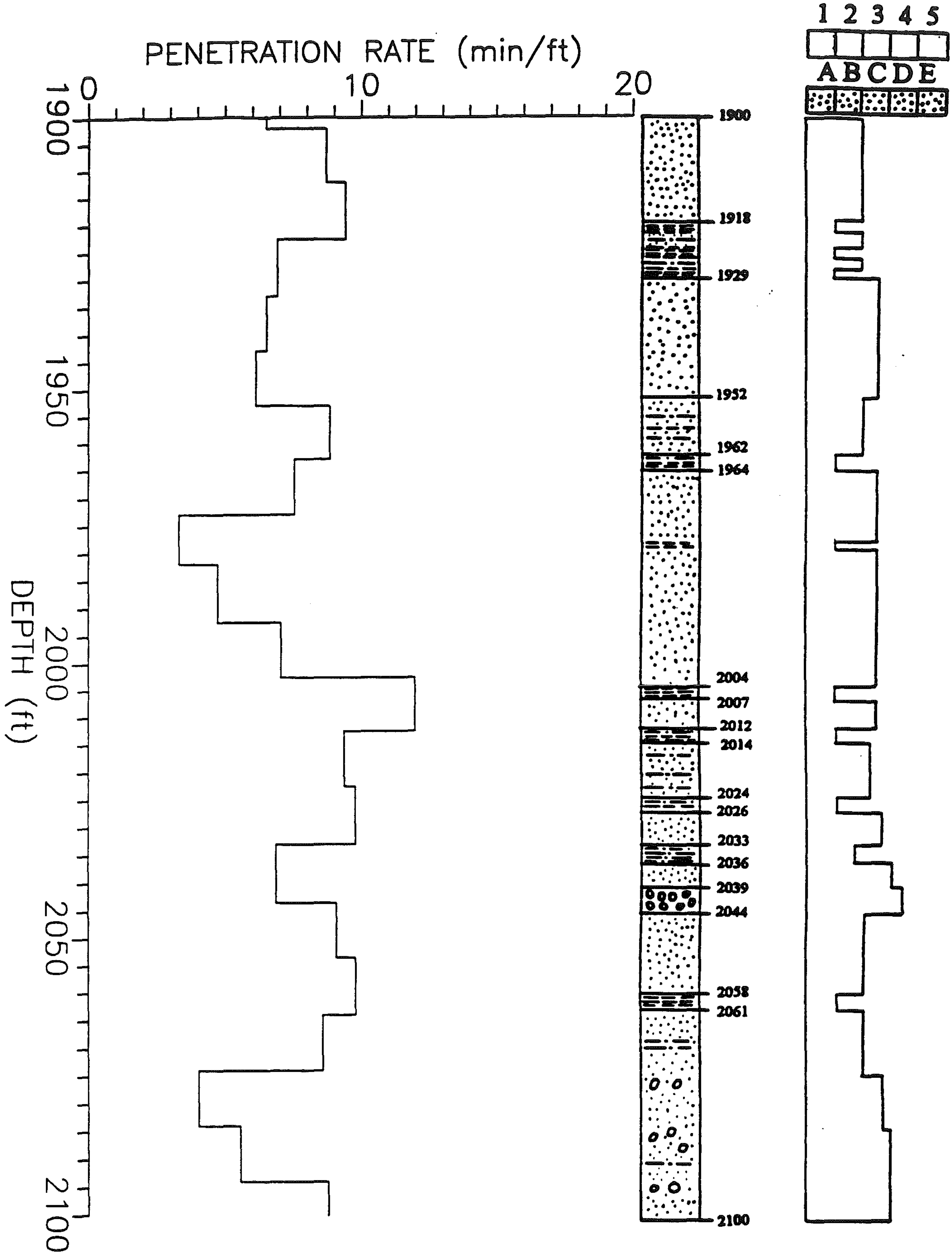
PENETRATION RATE (min/ft)
0
10
20
DEPTH (ft)
1900
1950
2000
2050
2100
1900
1918
1929
1952
1962
1964
2004
2007
2012
2014
2024
2026
2033
2036
2039
2044
2058
2061
2100
1 2 3 4 5
A B C D E

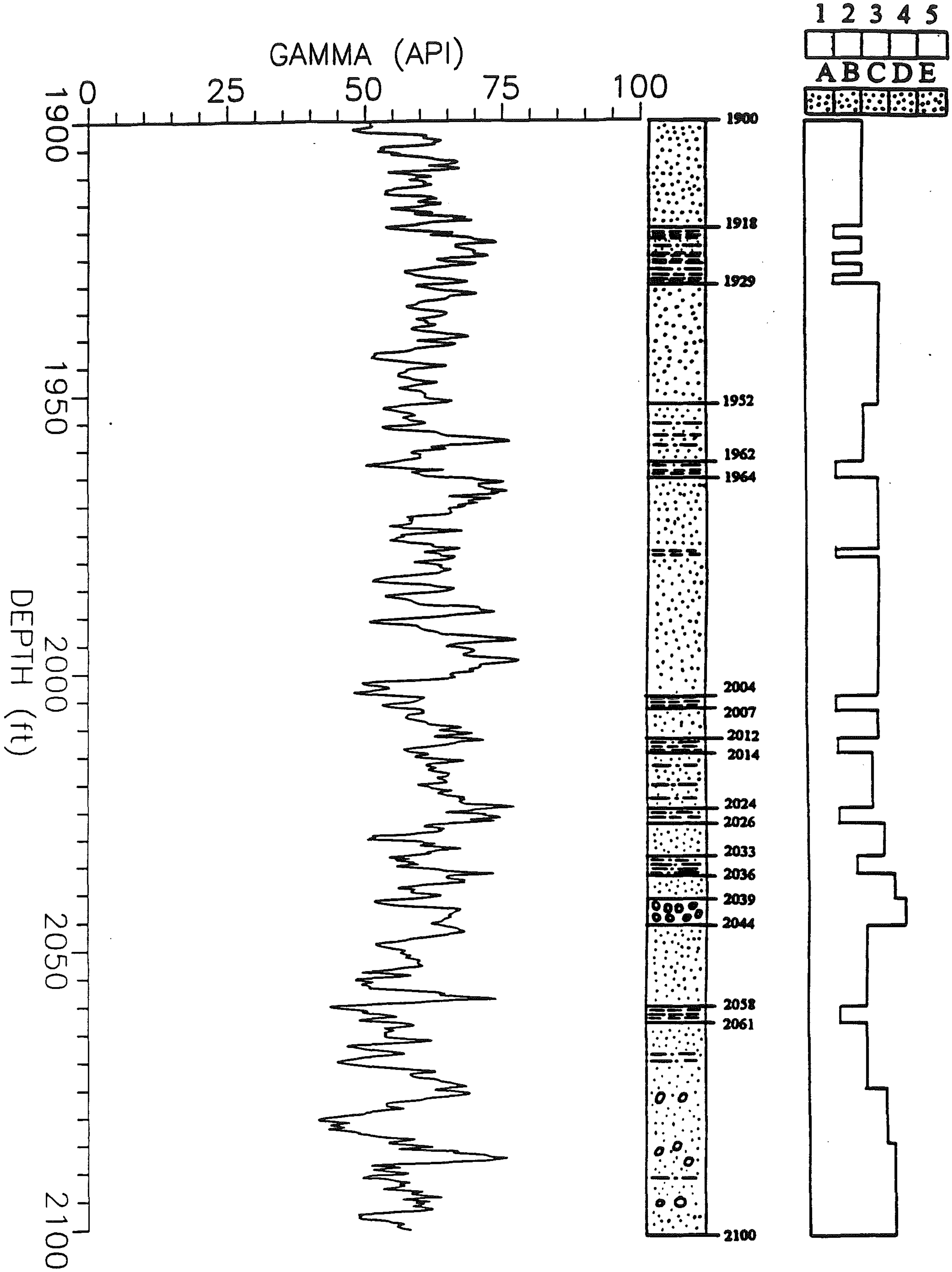

GAMMA (API)
0
25
50
75
100
1900
1950
2000
2050
2100
DEPTH (ft)
1900
1918
1929
1952
1962
1964
2004
2007
2012
2014
2024
2026
2033
2036
2039
2044
2058
2061
2100
1 2 3 4 5
A B C D E

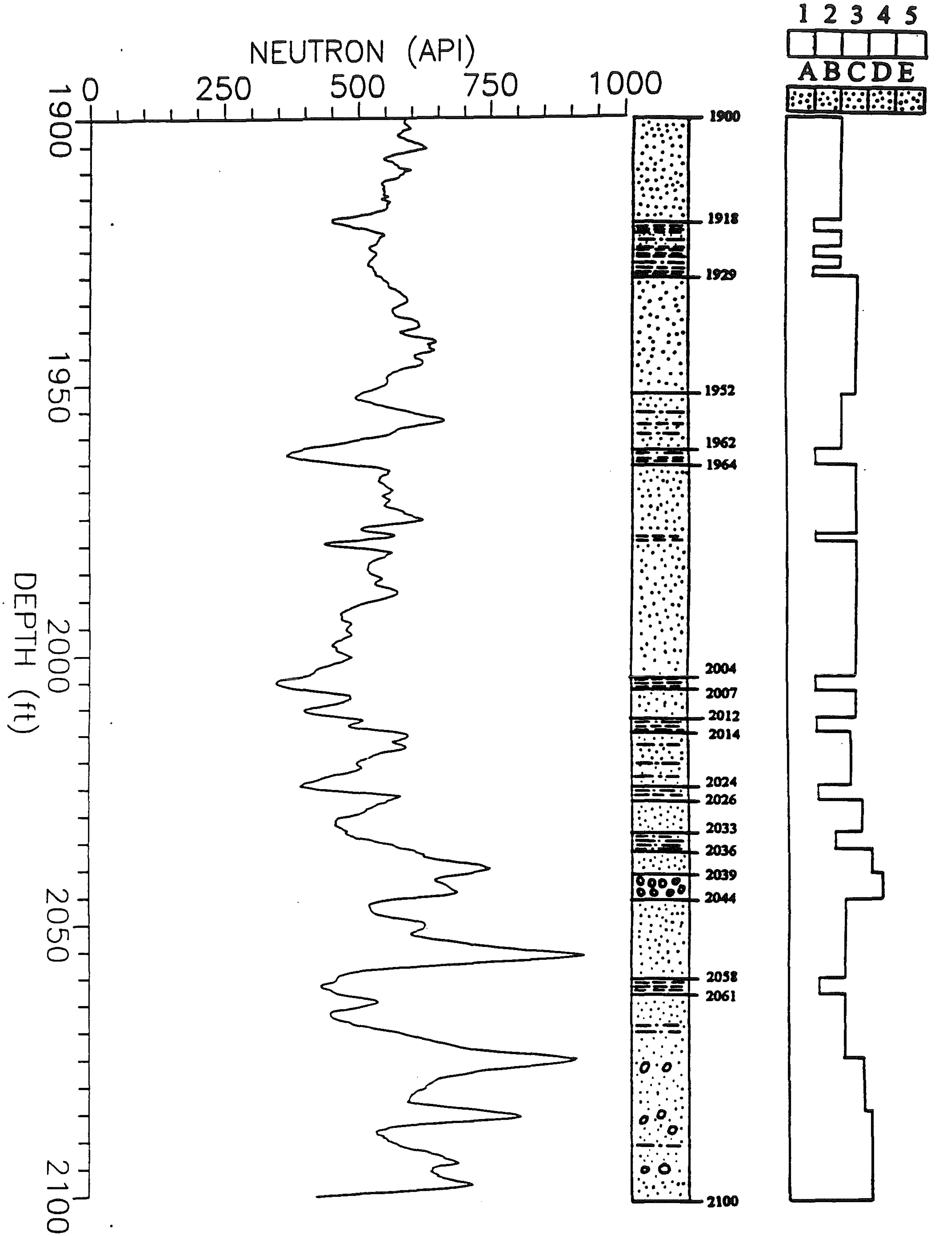

NEUTRON (API)
0
250
500
750
1000
DEPTH (ft)
1900
1950
2000
2050
2100
1900
1918
1929
1952
1962
1964
2004
2007
2012
2014
2024
2026
2033
2036
2039
2044
2058
2061
2100
1 2 3 4 5
A B C D E

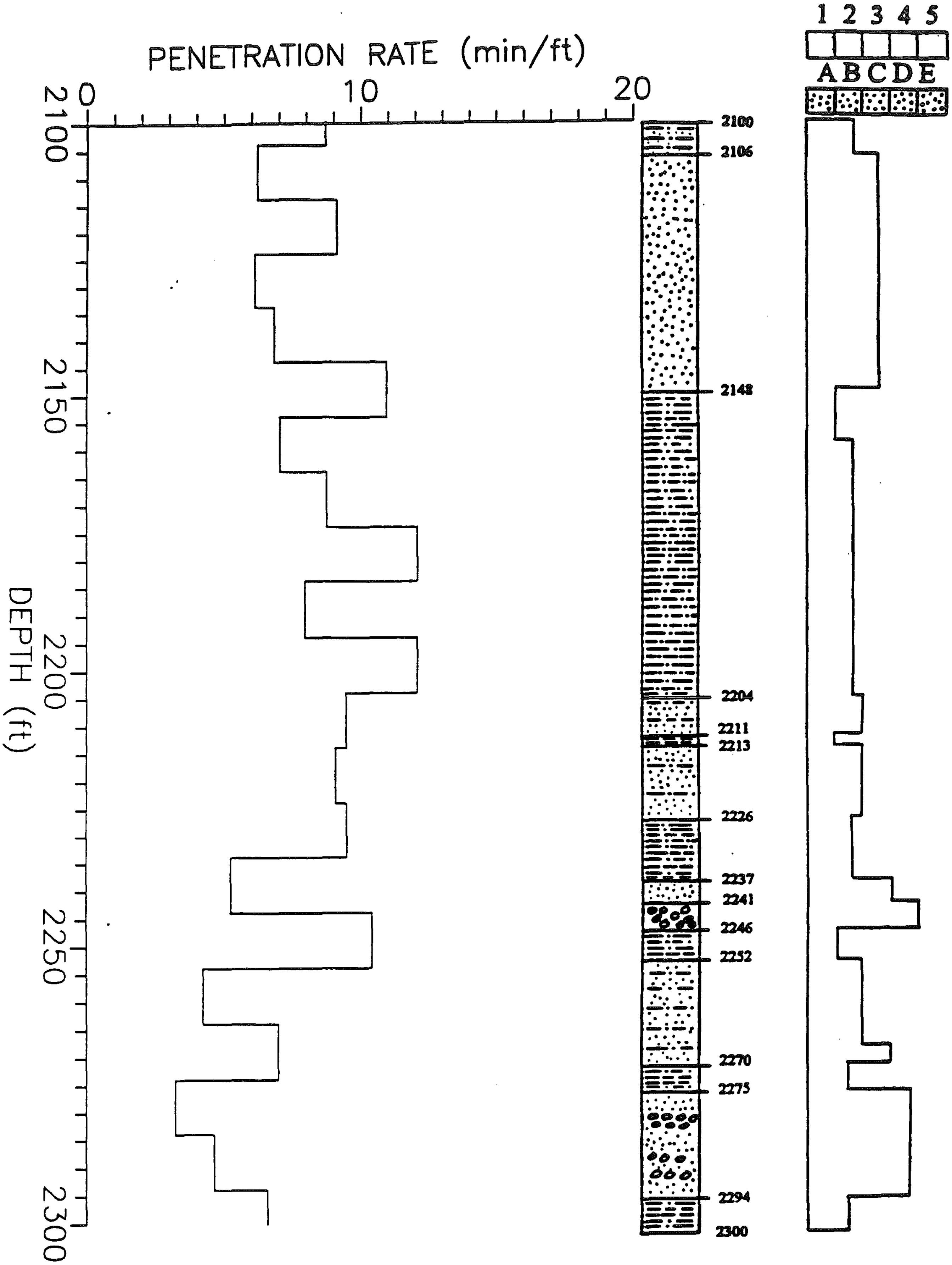

PENETRATION RATE (min/ft)
0
10
20
2100
2150
2200
2250
2300
DEPTH (ft)
2100
2106
2148
2204
2211
2213
2226
2237
2241
2246
2252
2270
2275
2294
2300
1 2 3 4 5
A B C D E

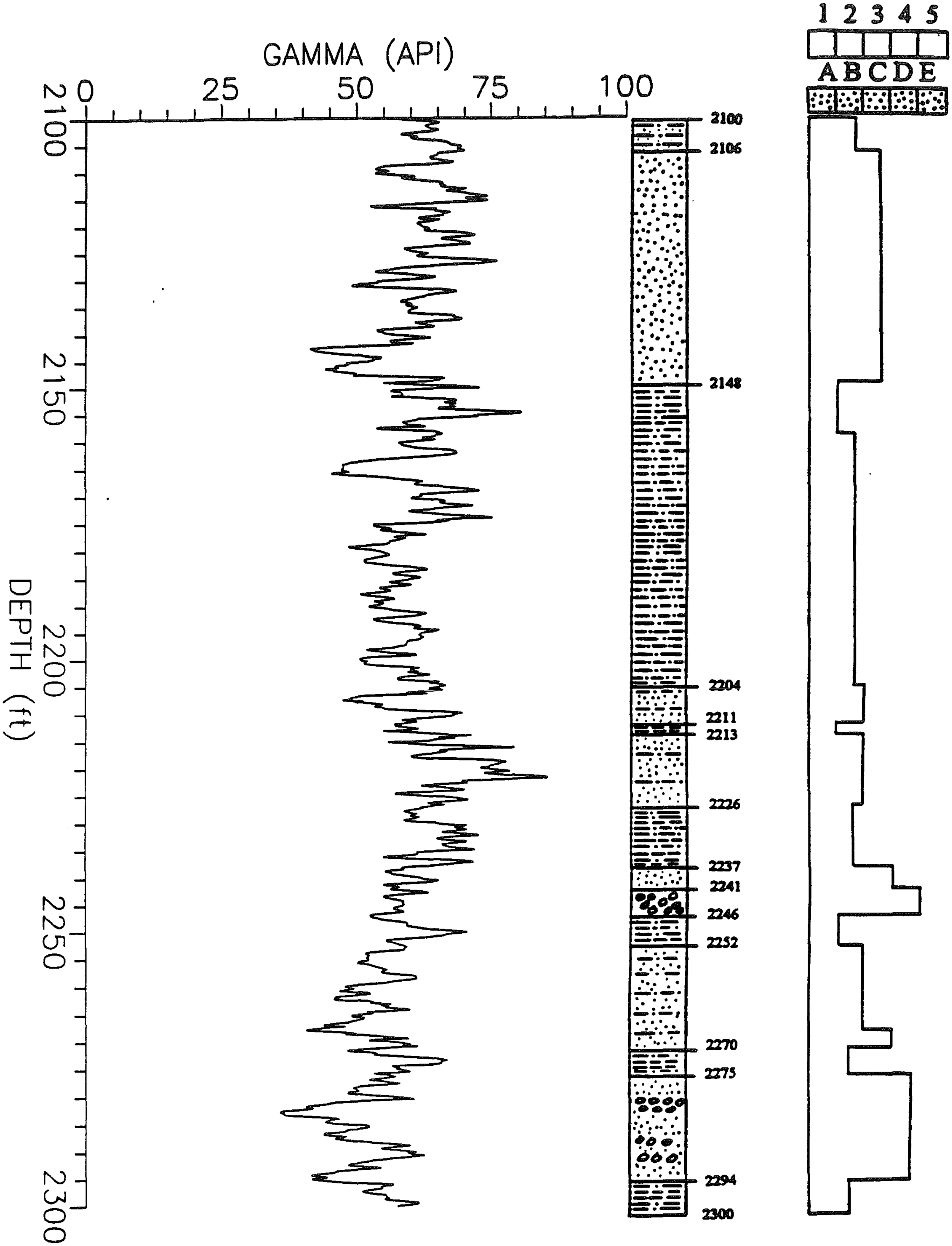

GAMMA (API)
0
25
50
75
100
2100
2150
2200
2250
2300
DEPTH (ft)
2100
2106
2148
2204
2211
2213
2226
2237
2241
2246
2252
2270
2275
2294
2300
1 2 3 4 5
A B C D E

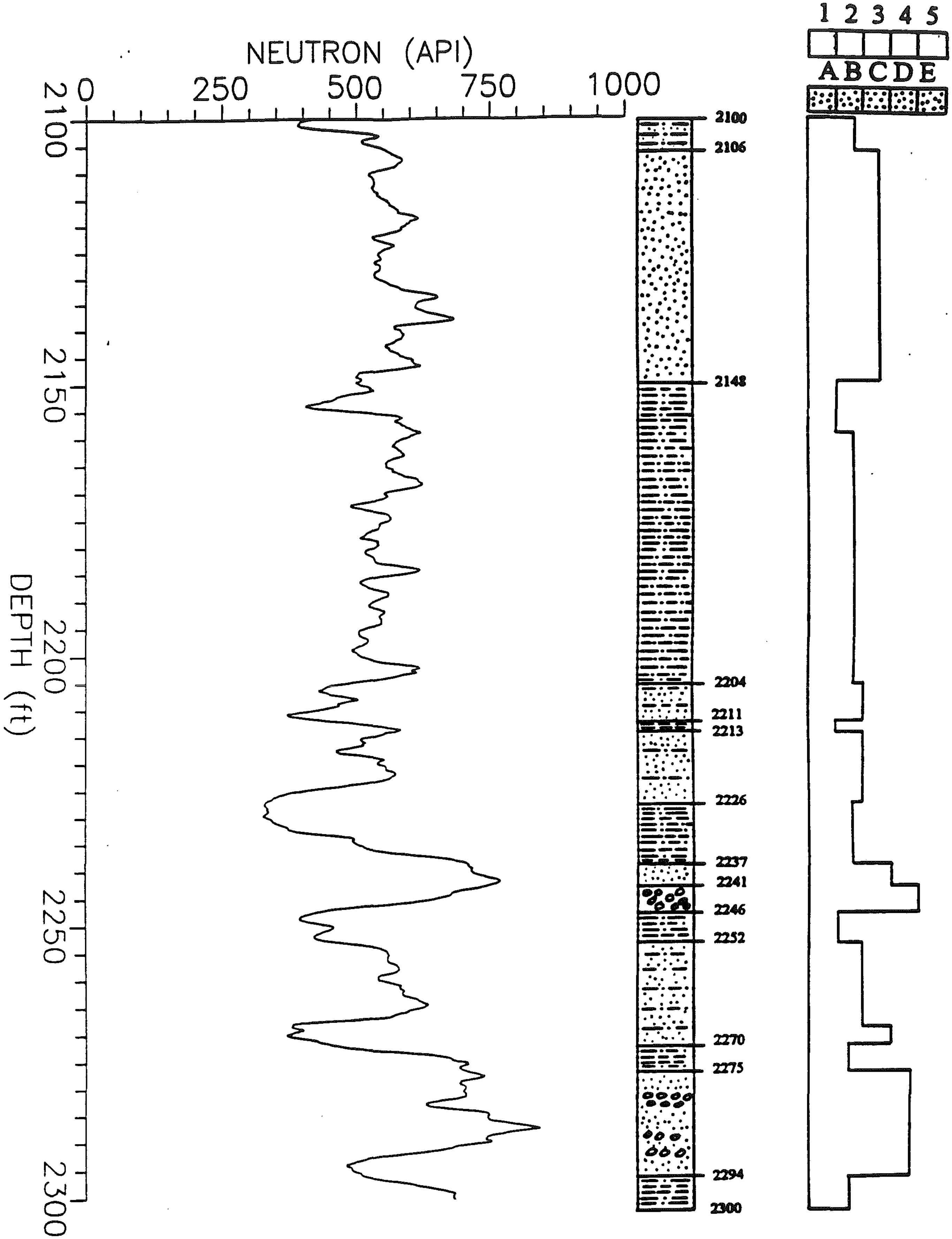
NEUTRON (API)
0
250
500
750
1000
2100
2150
2200
2250
2300
DEPTH (ft)
2100
2106
2148
2204
2211
2213
2226
2237
2241
2246
2252
2270
2275
2294
2300
1 2 3 4 5
A B C D E

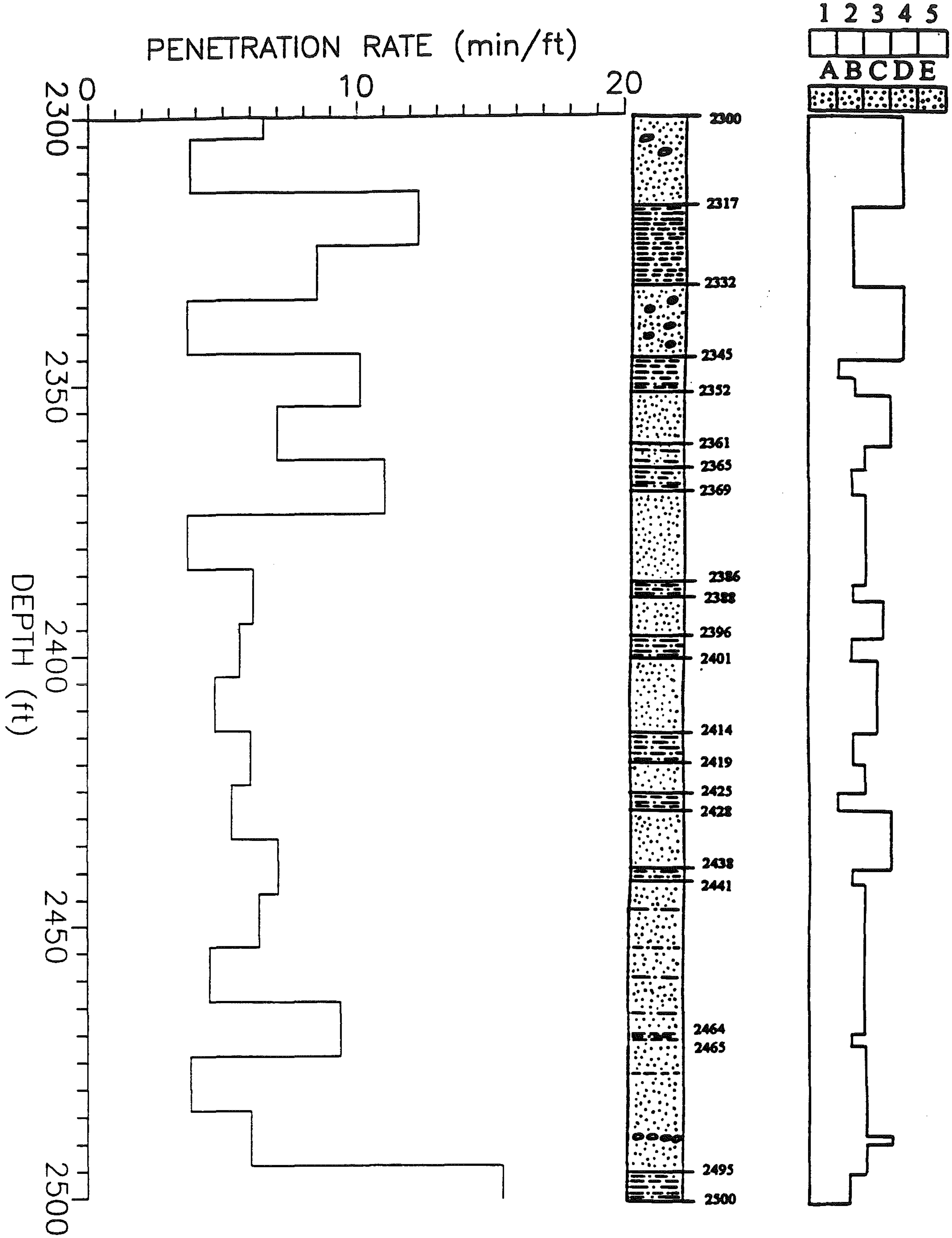

PENETRATION RATE (min/ft)
0
10
20
2300
2350
2400
2450
2500
DEPTH (ft)
2300
2317
2332
2345
2352
2361
2365
2369
2386
2388
2396
2401
2414
2419
2425
2428
2438
2441
2464
2465
2495
2500
1 2 3 4 5
A B C D E

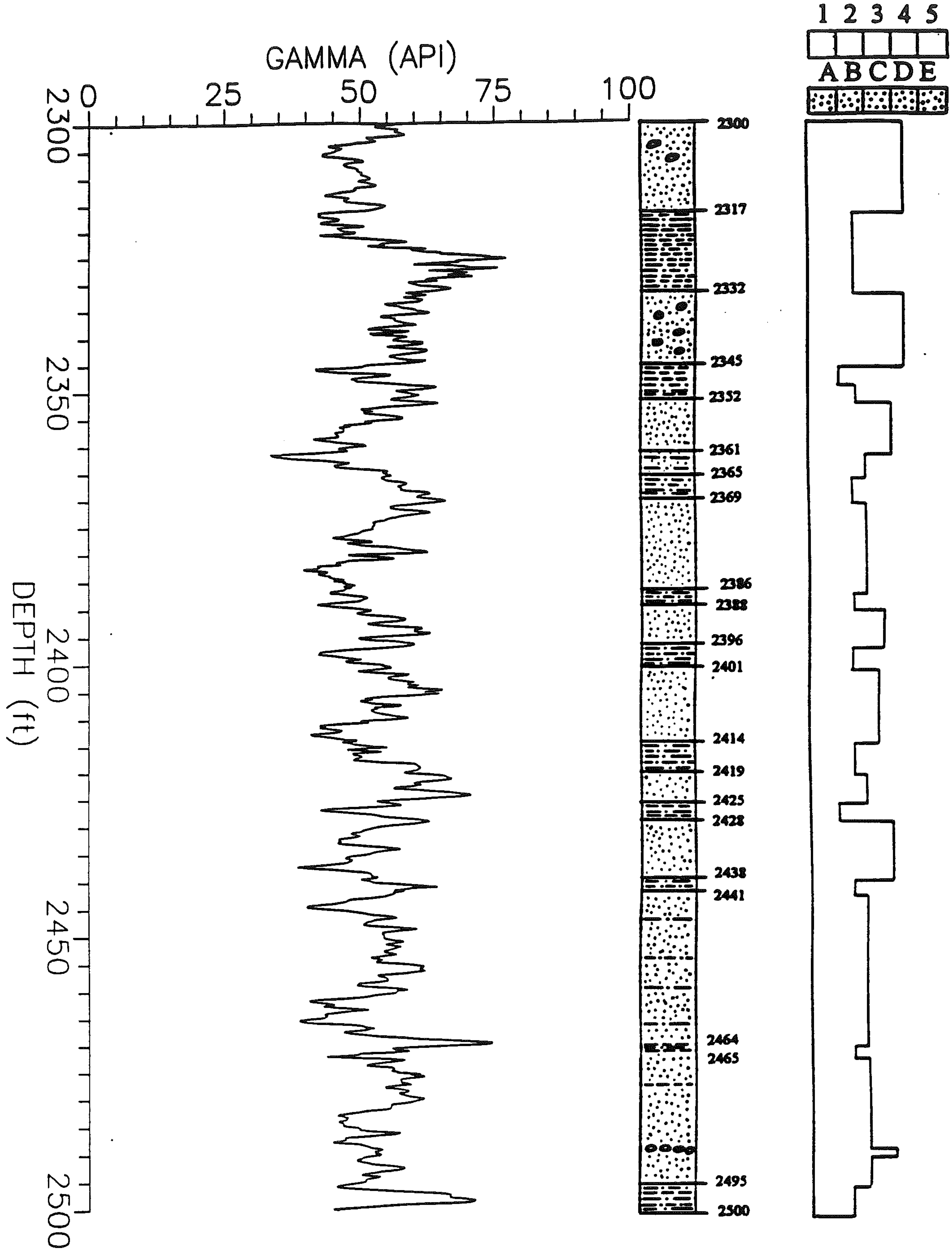

GAMMA (API)
0
25
50
75
100
2300
2350
2400
2450
2500
DEPTH (ft)
2300
2317
2332
2345
2352
2361
2365
2369
2386
2388
2396
2401
2414
2419
2425
2428
2438
2441
2464
2465
2495
2500
1 2 3 4 5
A B C D E

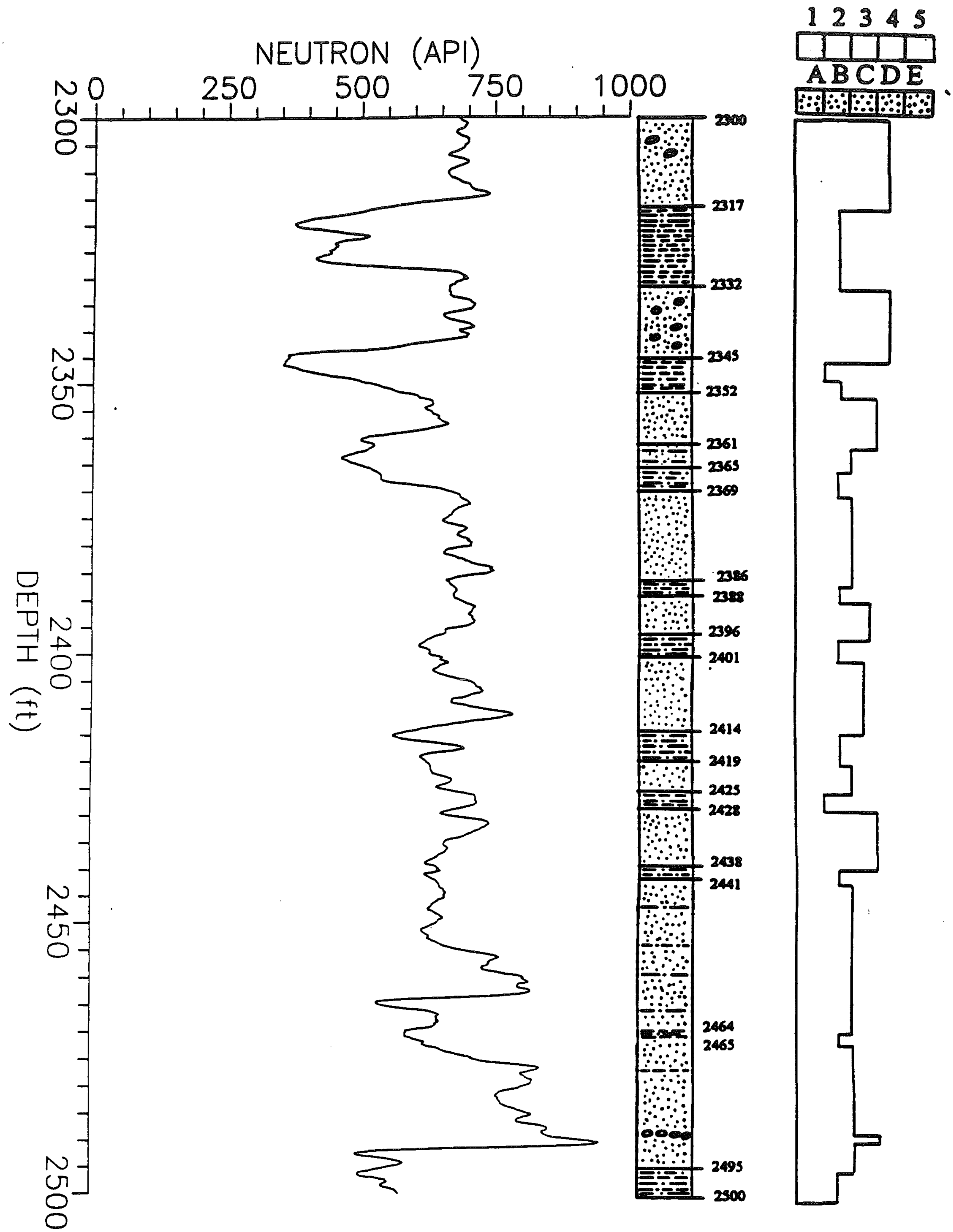
NEUTRON (API)
0
250
500
750
1000
DEPTH (ft)
2300
2350
2400
2450
2500
2300
2317
2332
2345
2352
2361
2365
2369
2386
2388
2396
2401
2414
2419
2425
2428
2438
2441
2464
2465
2495
2500
1 2 3 4 5
A B C D E

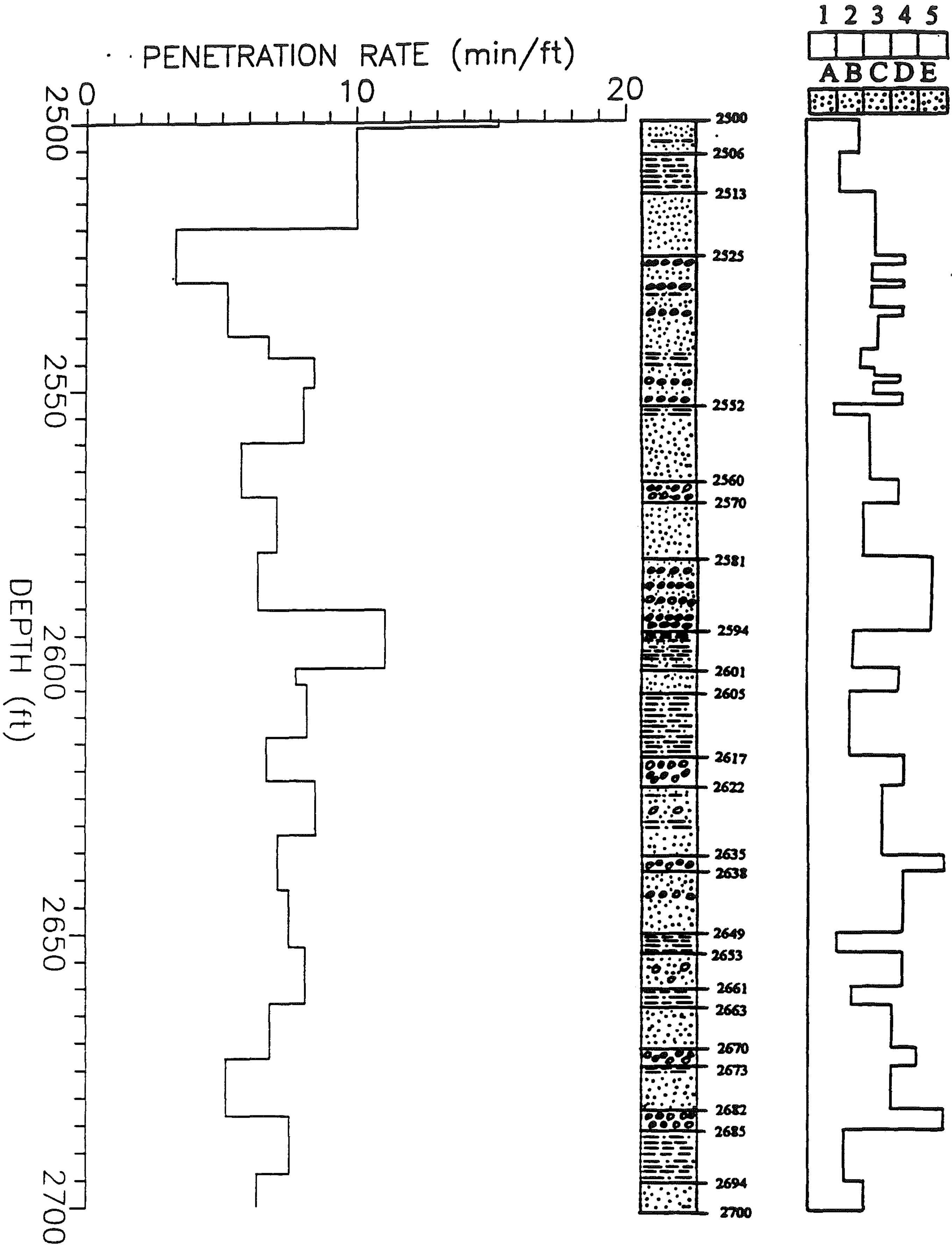
PENETRATION RATE (min/ft)
0
10
20
DEPTH (ft)
2500
2550
2600
2650
2700
2500
2506
2513
2525
2552
2560
2570
2581
2594
2601
2605
2617
2622
2635
2638
2649
2653
2661
2663
2670
2673
2682
2685
2694
2700
1 2 3 4 5
A B C D E

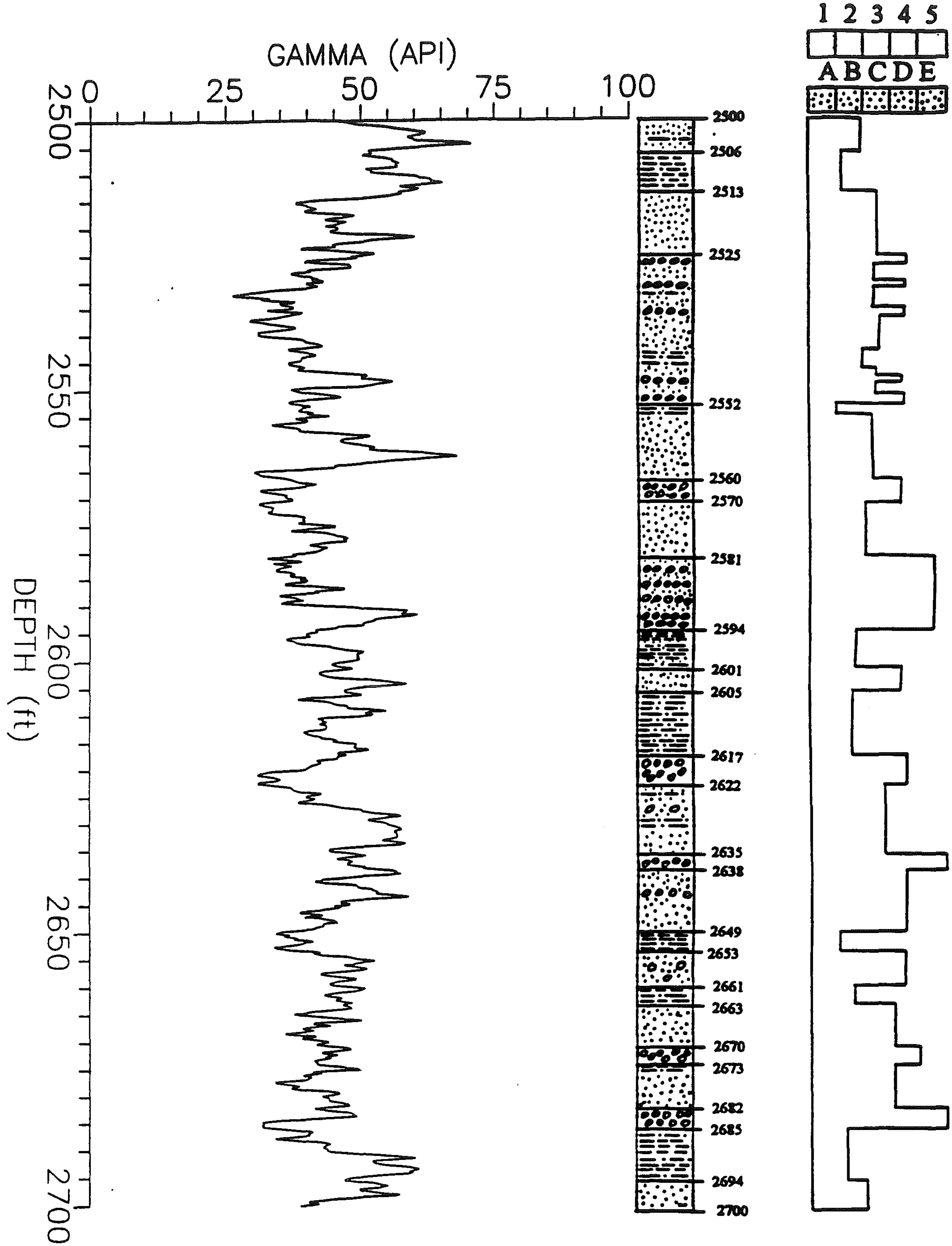
GAMMA (API)
0
25
50
75
100
2500
2550
2600
2650
2700
DEPTH (ft)
2500
2506
2513
2525
2552
2560
2570
2581
2594
2601
2605
2617
2622
2635
2638
2649
2653
2661
2663
2670
2673
2682
2685
2694
2700
1 2 3 4 5
A B C D E

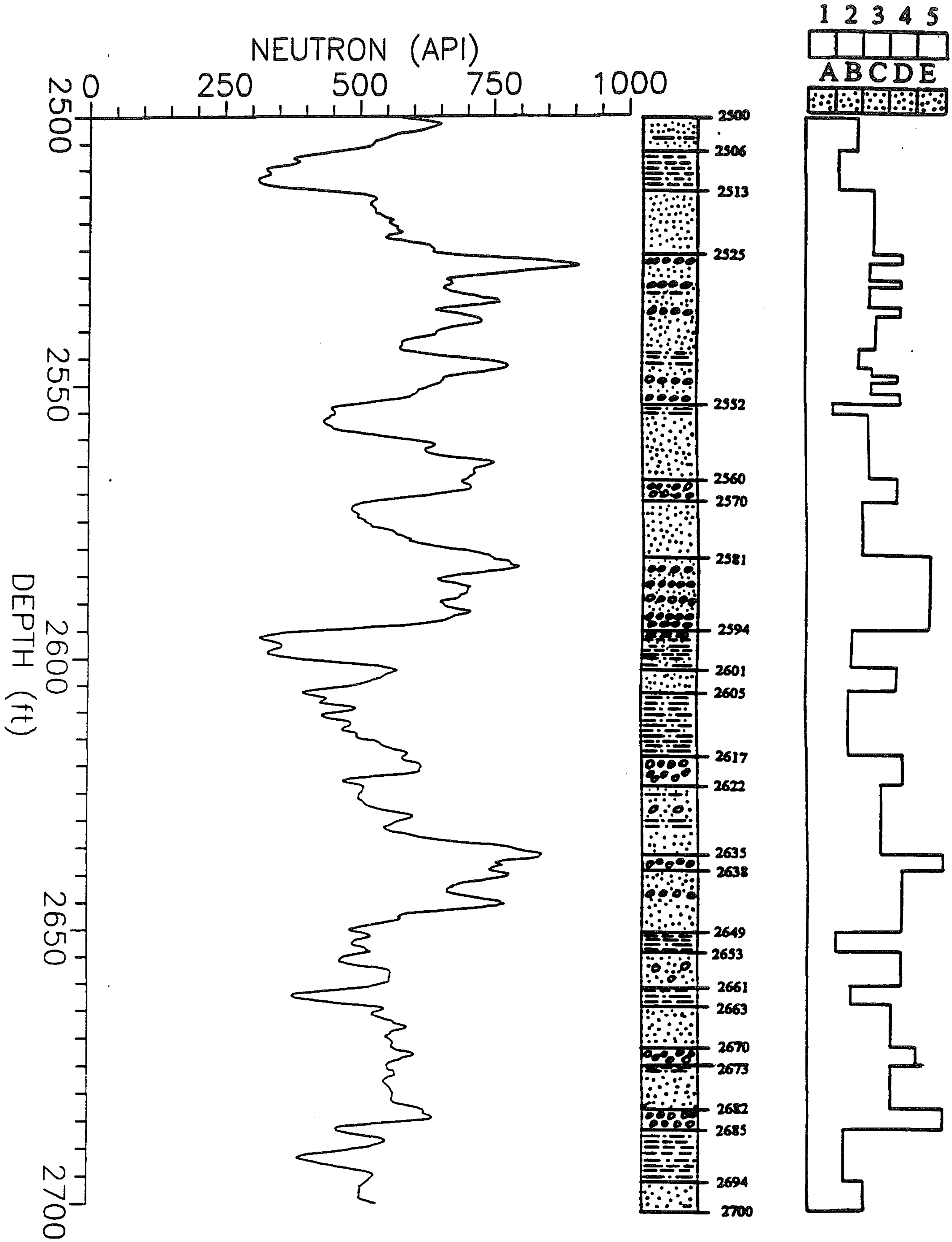
NEUTRON (API)
0
250
500
750
1000
DEPTH (ft)
2500
2550
2600
2650
2700
2500
2506
2513
2525
2552
2560
2570
2581
2594
2601
2605
2617
2622
2635
2638
2649
2653
2661
2663
2670
2673
2682
2685
2694
2700
1 2 3 4 5
A B C D E

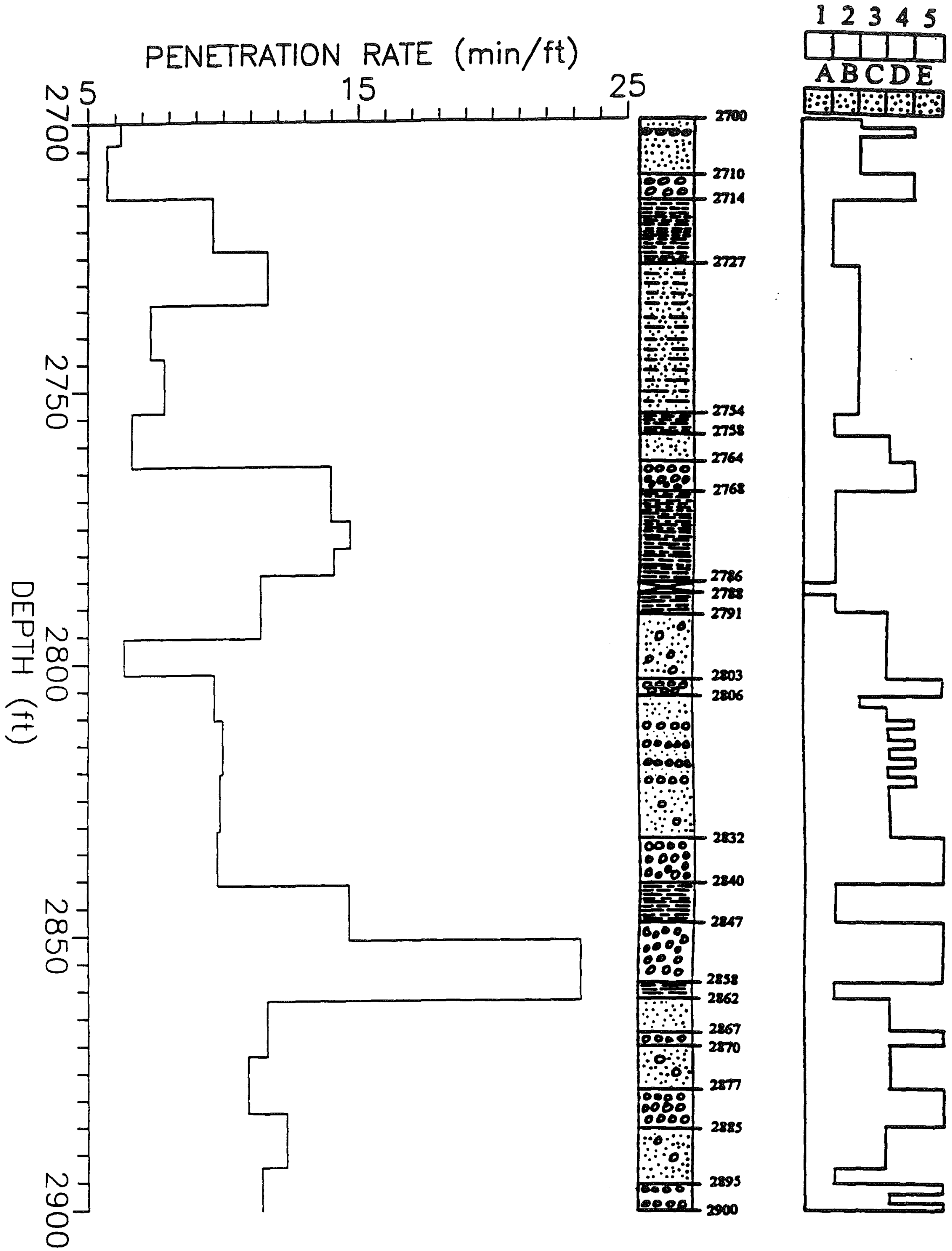

PENETRATION RATE (min/ft)
5
15
25
DEPTH (ft)
2700
2750
2800
2850
2900
2700
2710
2714
2727
2754
2758
2764
2768
2786
2788
2791
2803
2806
2832
2840
2847
2858
2862
2867
2870
2877
2885
2895
2900
1 2 3 4 5
A B C D E

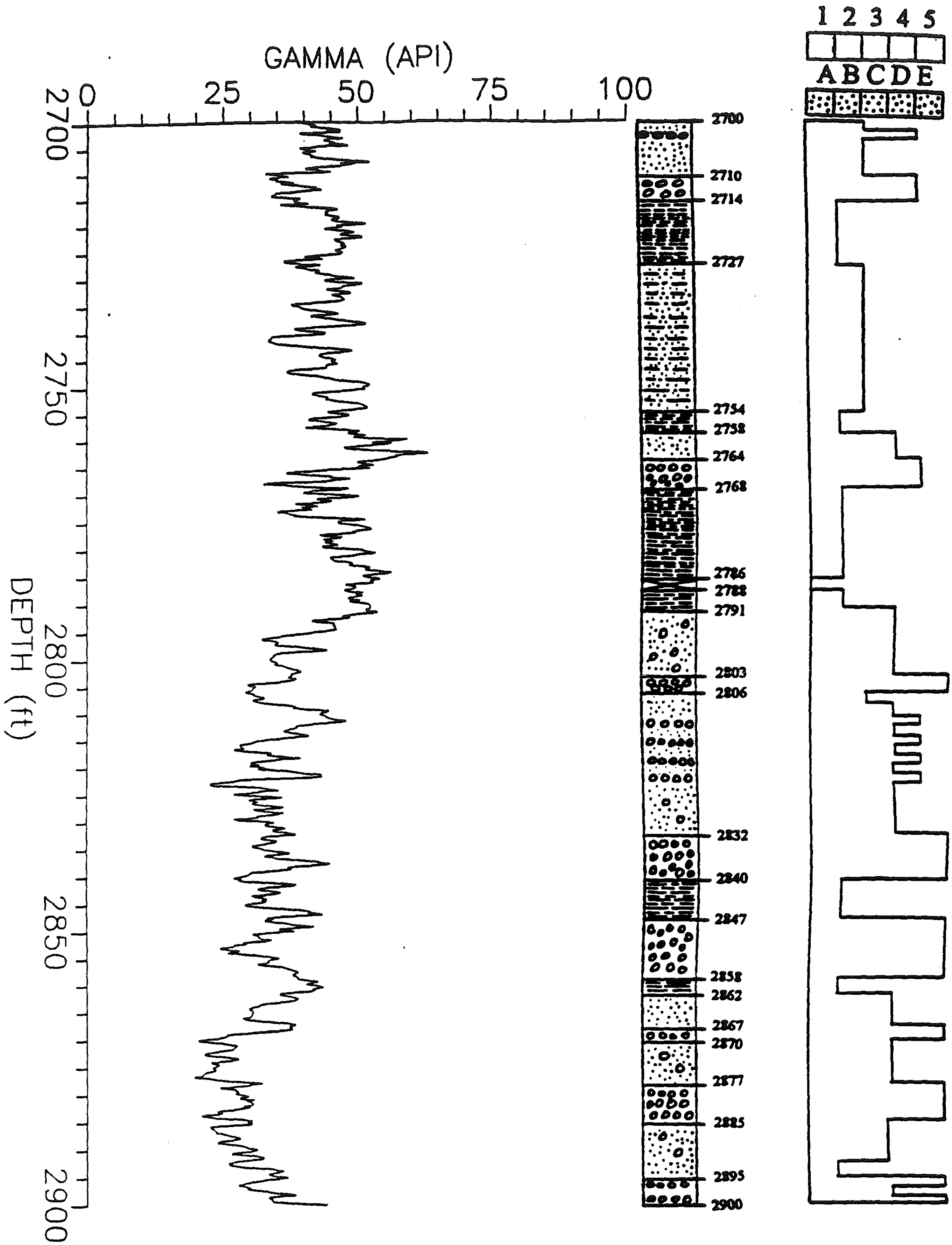
GAMMA (API)
0
25
50
75
100
2700
2750
2800
2850
2900
DEPTH (ft)
2700
2710
2714
2727
2754
2758
2764
2768
2786
2788
2791
2803
2806
2832
2840
2847
2858
2862
2867
2870
2877
2885
2895
2900
1 2 3 4 5
A B C D E

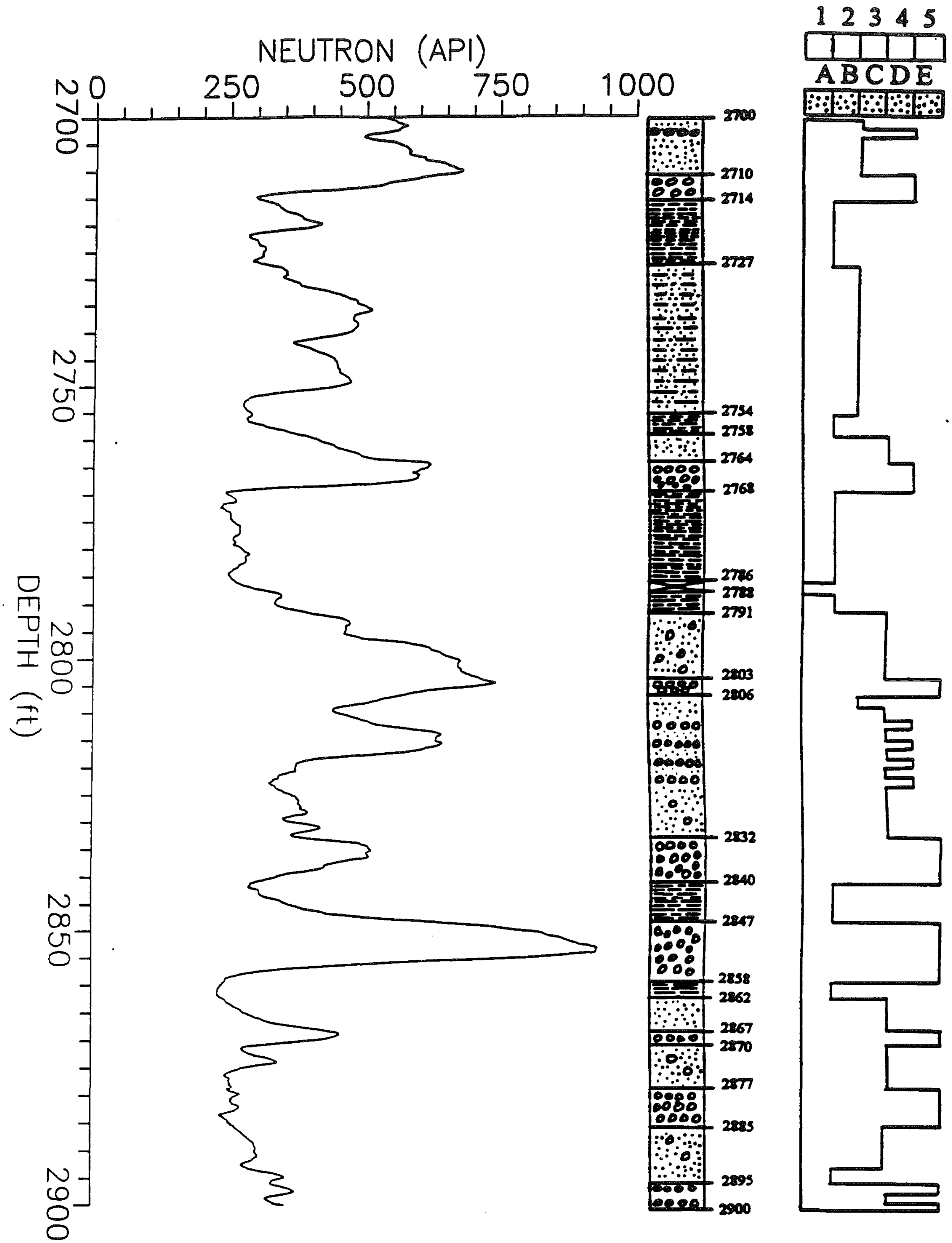
NEUTRON (API)
0
250
500
750
1000
DEPTH (ft)
2700
2750
2800
2850
2900
2700
2710
2714
2727
2754
2758
2764
2768
2786
2788
2791
2803
2806
2832
2840
2847
2858
2862
2867
2870
2877
2885
2895
2900
1 2 3 4 5
A B C D E

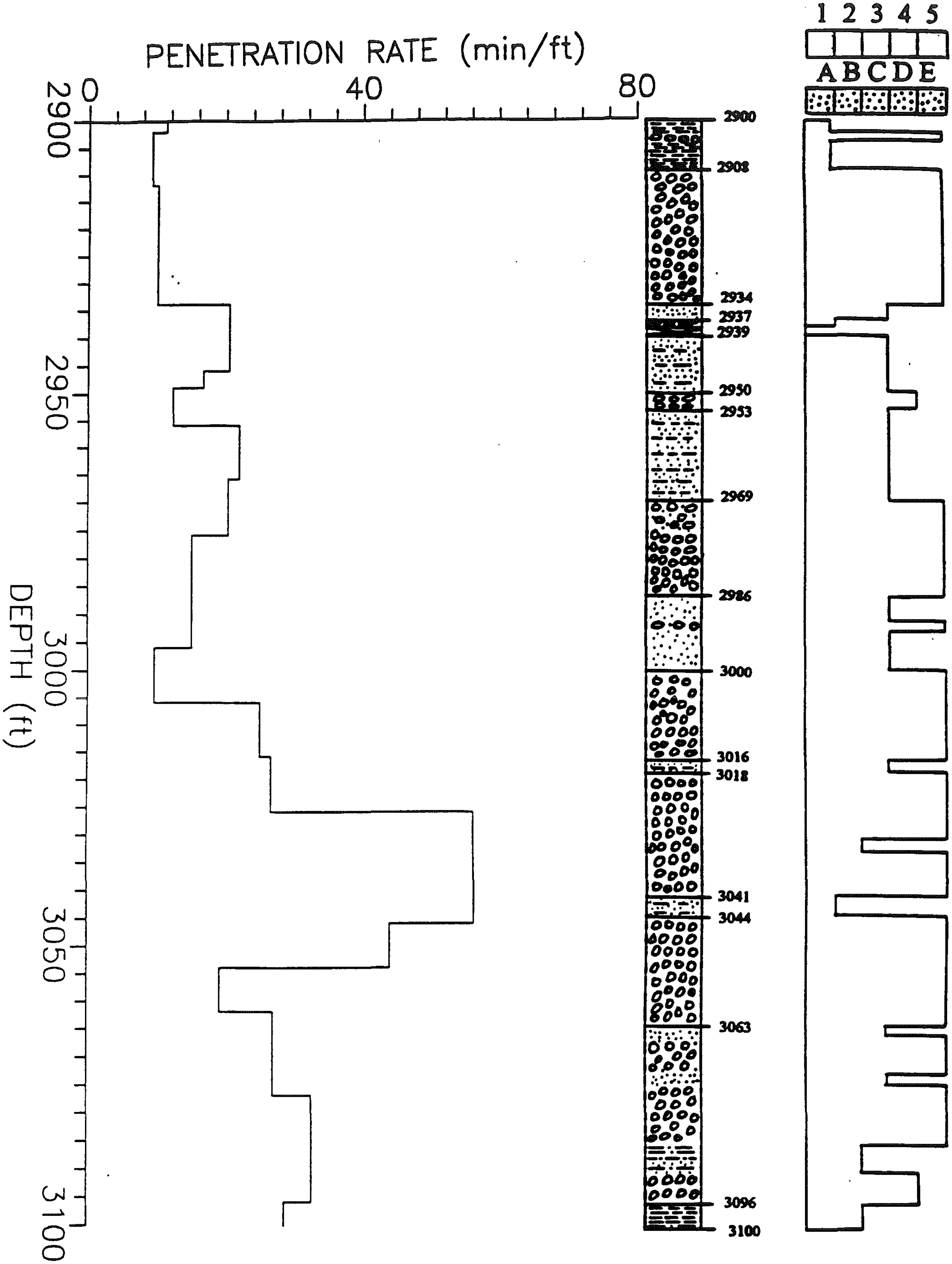

PENETRATION RATE (min/ft)
0
40
80
2900
2950
3000
3050
3100
DEPTH (ft)
2900
2908
2934
2937
2939
2950
2953
2969
2986
3000
3016
3018
3041
3044
3063
3096
3100
1 2 3 4 5
A B C D E

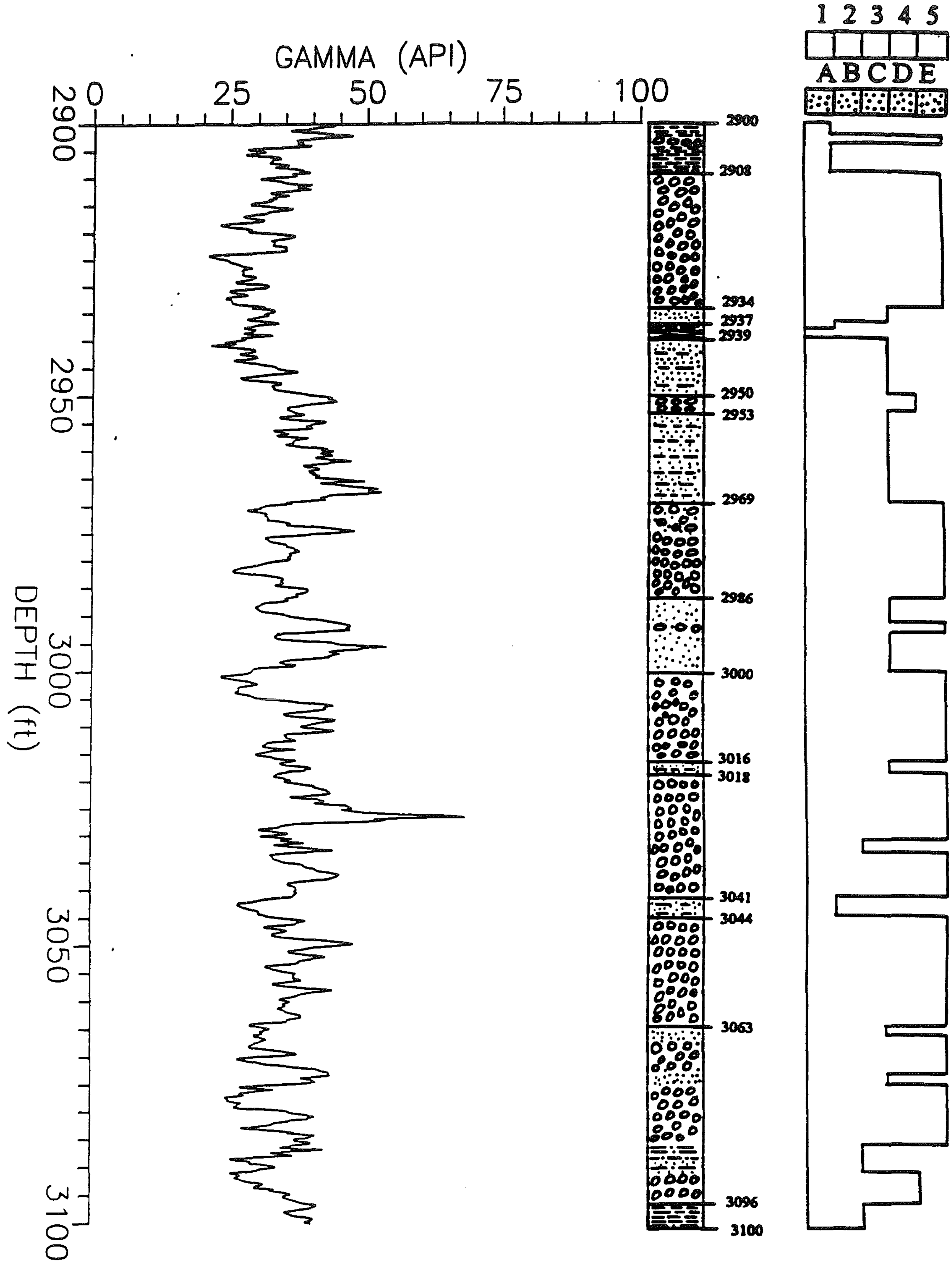
GAMMA (API)
0 25 50 75 100
DEPTH (ft)
2900 2950 3000 3050 3100
2900
2908
2934
2937
2939
2950
2953
2969
2986
3000
3016
3018
3041
3044
3063
3096
3100
1 2 3 4 5
A B C D E

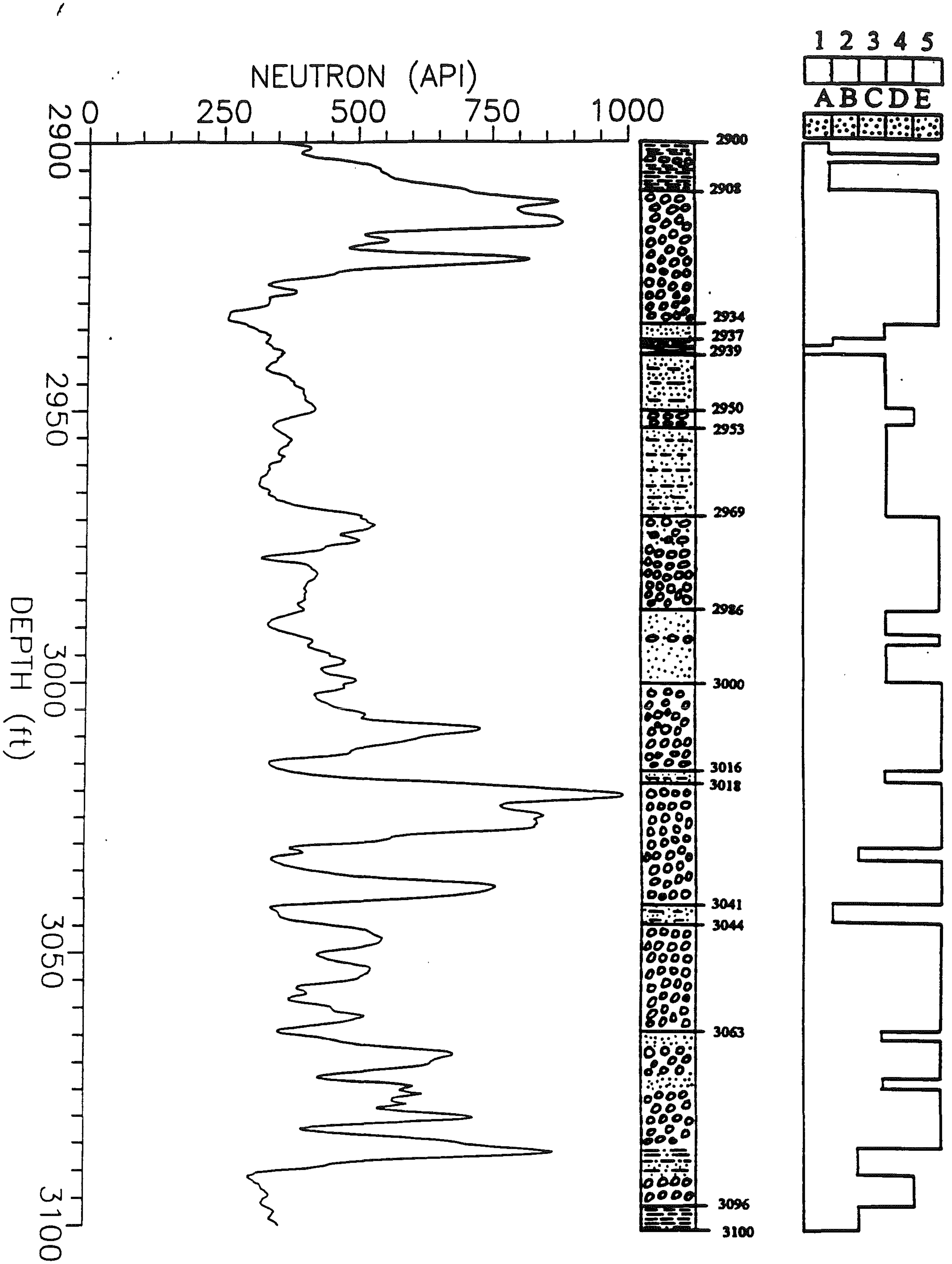
NEUTRON (API)
0
250
500
750
1000
DEPTH (ft)
2900
2950
3000
3050
3100
2900
2908
2934
2937
2939
2950
2953
2969
2986
3000
3016
3018
3041
3044
3063
3096
3100
1 2 3 4 5
A B C D E

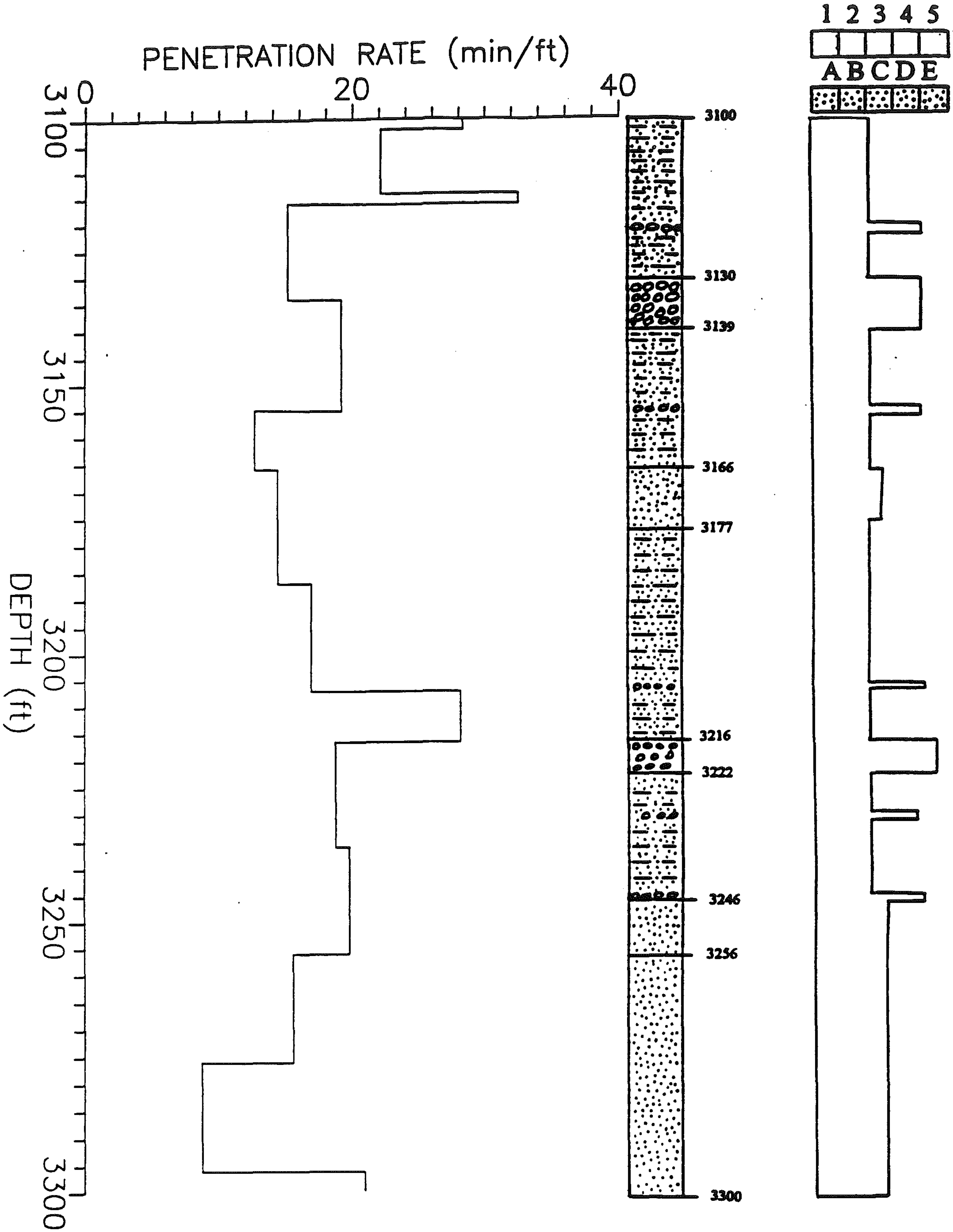
PENETRATION RATE (min/ft)
0
20
40
DEPTH (ft)
3100
3150
3200
3250
3300
3100
3130
3139
3166
3177
3216
3222
3246
3256
3300
1 2 3 4 5
A B C D E

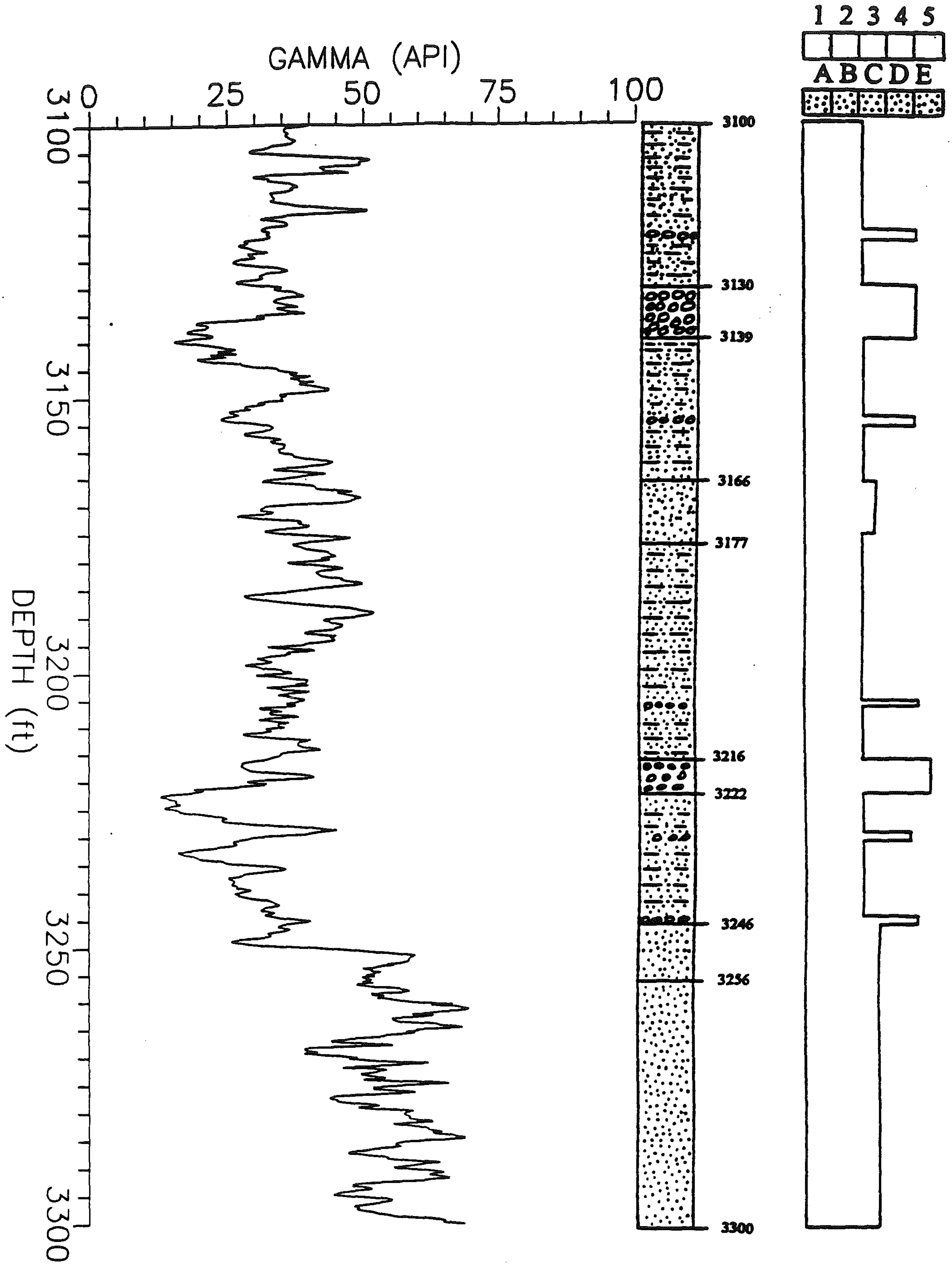
GAMMA (API)
0
25
50
75
100
3100
3150
3200
3250
3300
DEPTH (ft)
3100
3130
3139
3166
3177
3216
3222
3246
3256
3300
1 2 3 4 5
A B C D E

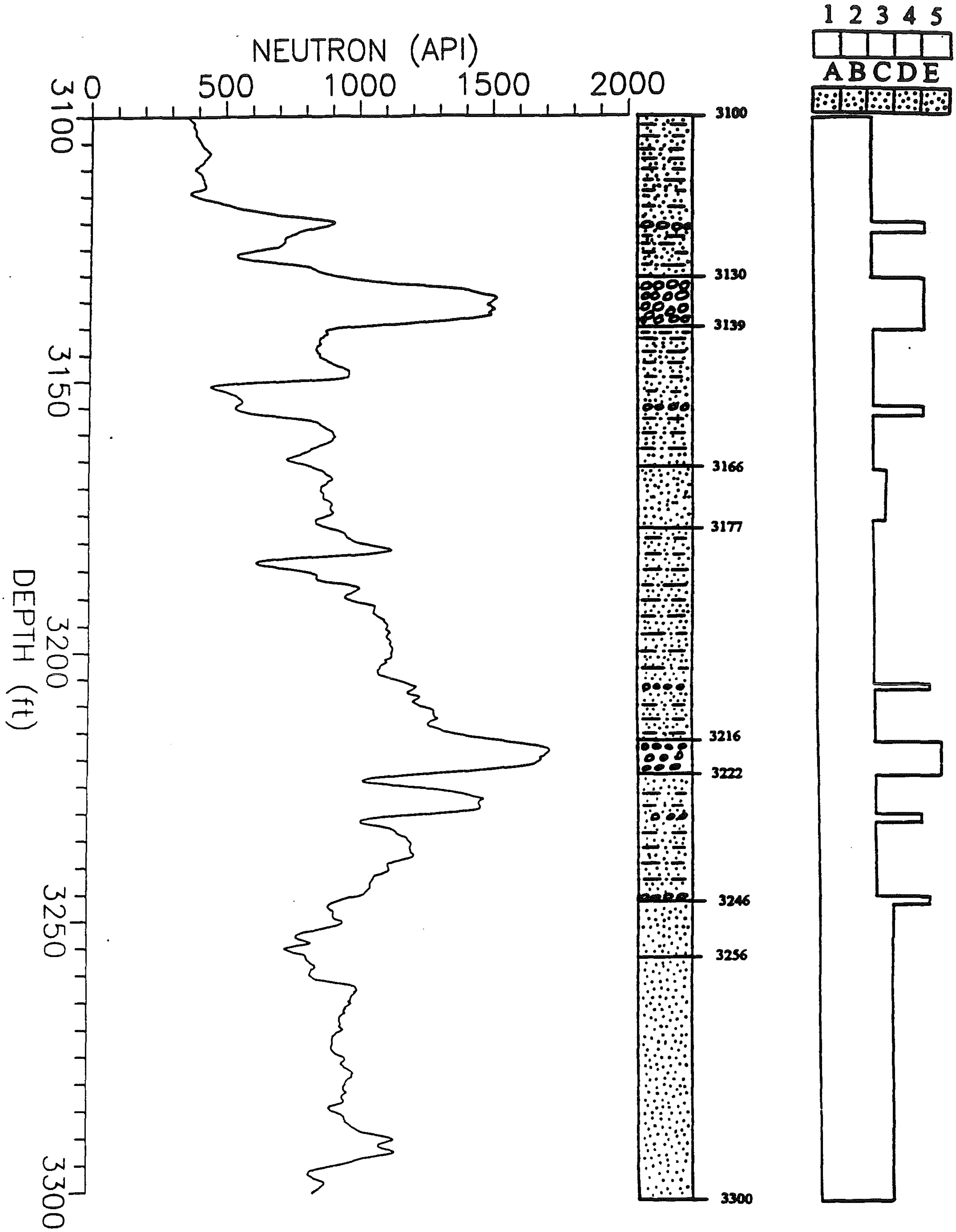
NEUTRON (API)
0
500
1000
1500
2000
3100
3150
3200
3250
3300
DEPTH (ft)
3100
3130
3139
3166
3177
3216
3222
3246
3256
3300
1 2 3 4 5
A B C D E

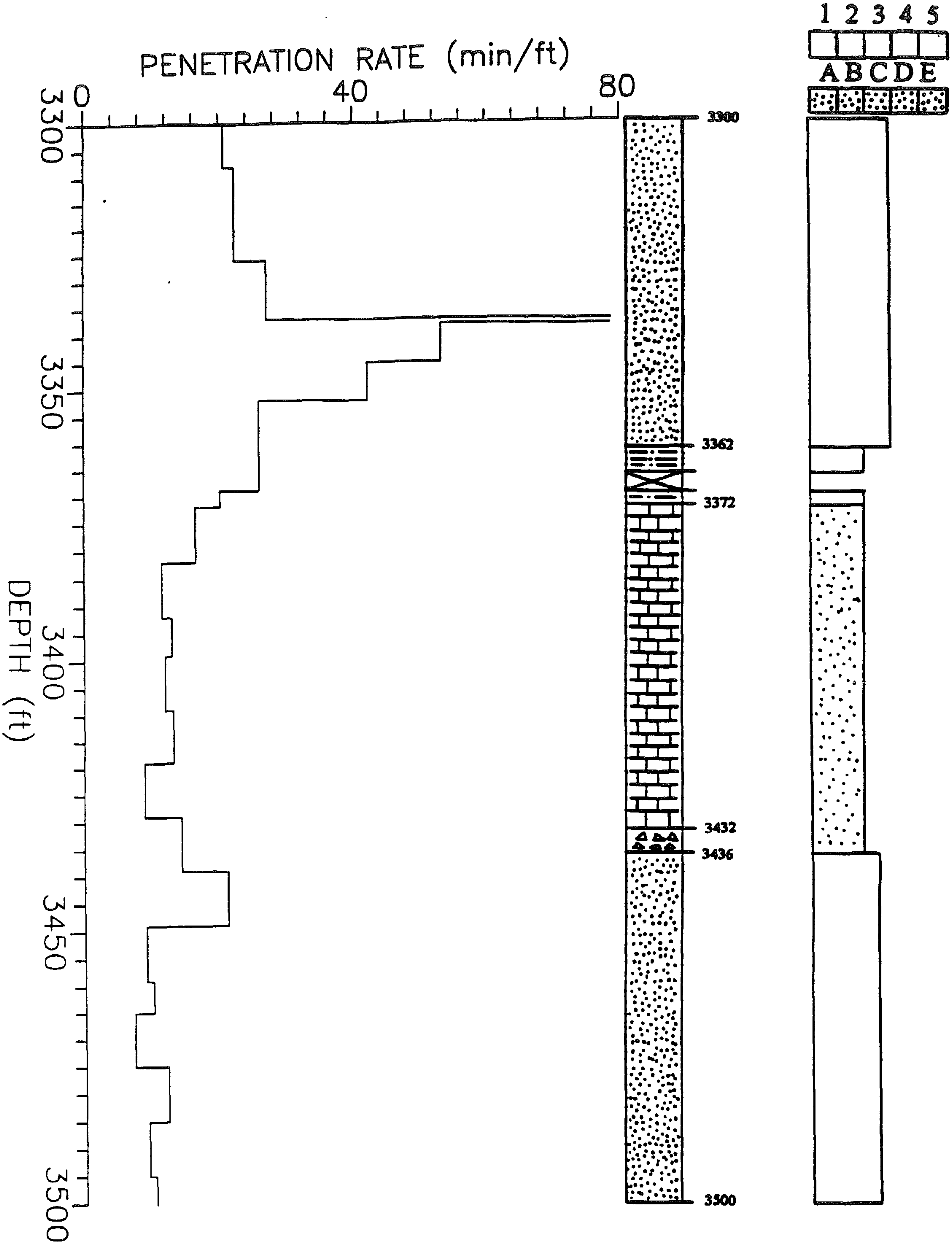

PENETRATION RATE (min/ft)
0
40
80
3300
3350
3400
3450
3500
DEPTH (ft)
3300
3362
3372
3432
3436
3500
1 2 3 4 5
A B C D E

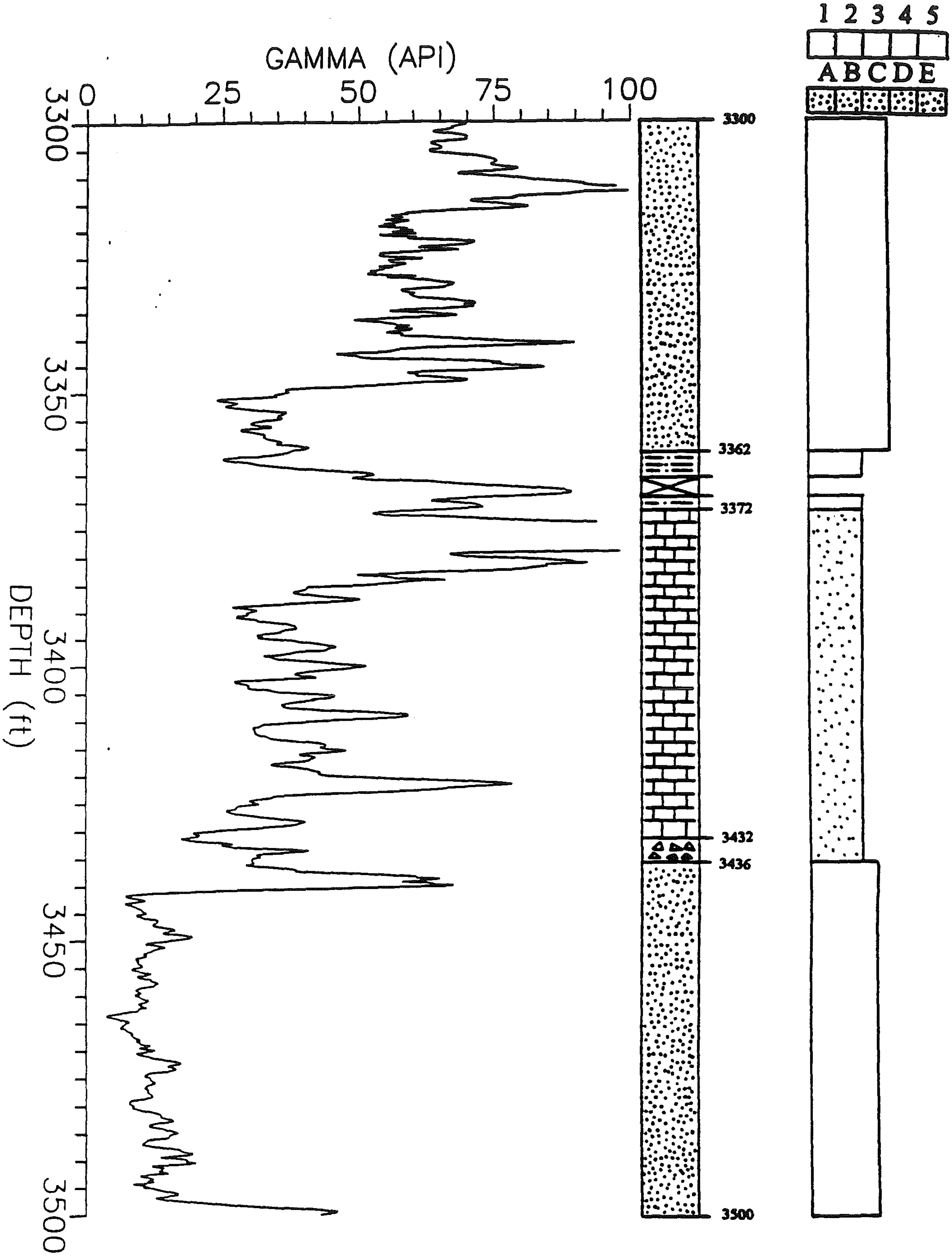
GAMMA (API)
0
25
50
75
100
3300
3350
3400
3450
3500
DEPTH (ft)
3300
3362
3372
3432
3436
3500
1 2 3 4 5
A B C D E

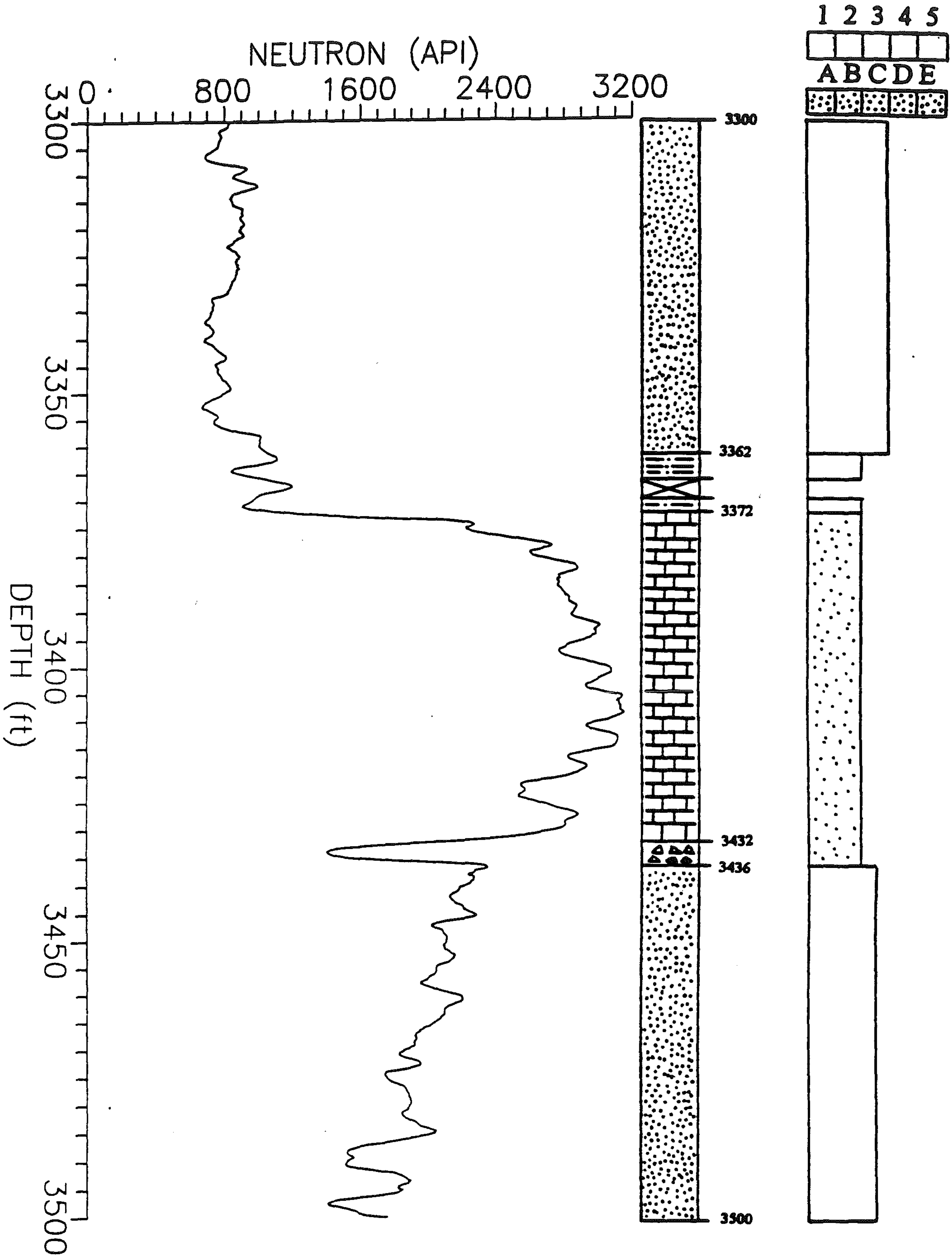
NEUTRON (API)
0
800
1600
2400
3200
3300
3350
3400
3450
3500
DEPTH (ft)
3300
3362
3372
3432
3436
3500
1 2 3 4 5
A B C D E

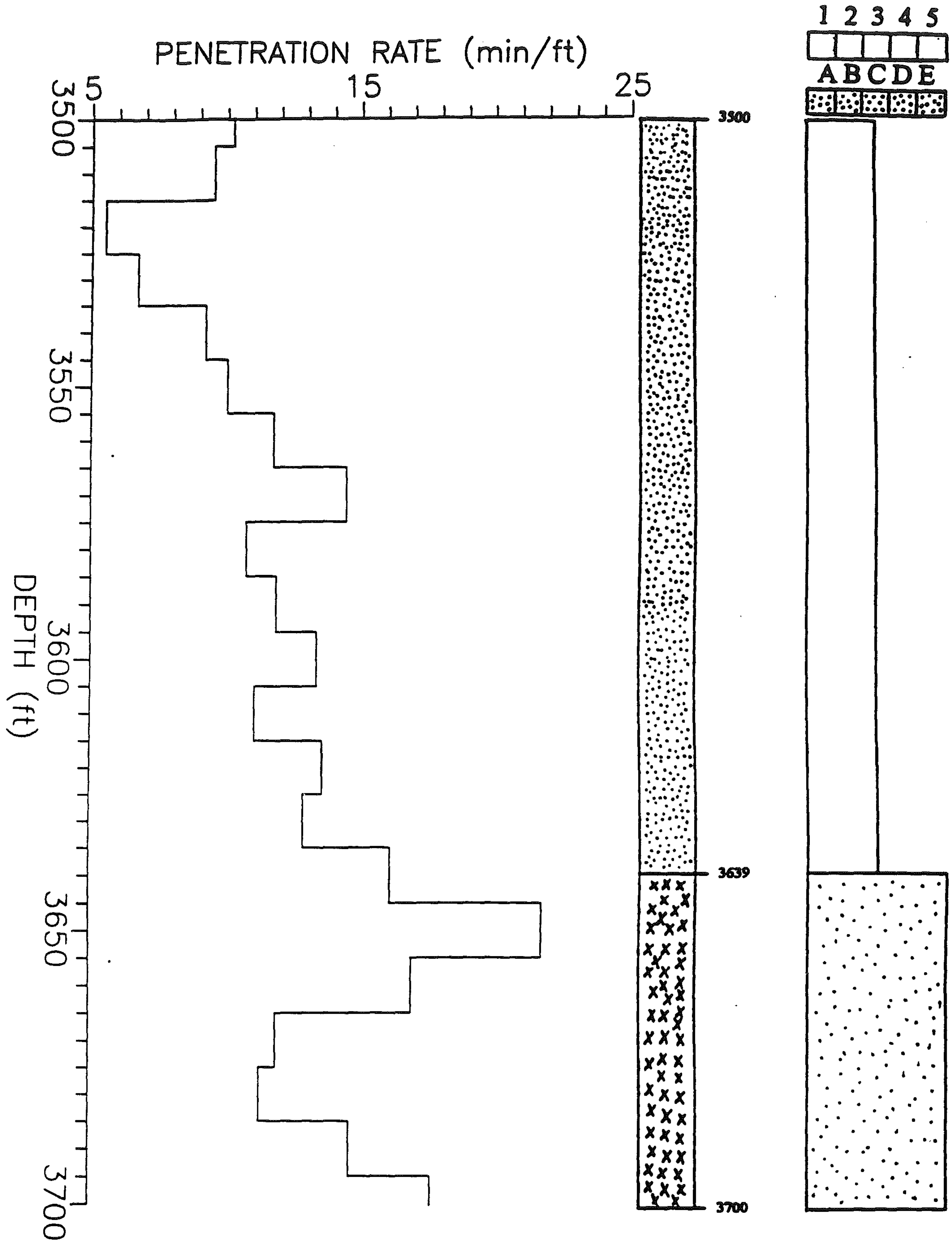
PENETRATION RATE (min/ft)
5
15
25
3500
3550
3600
3650
3700
DEPTH (ft)
3500
3639
3700
1 2 3 4 5
A B C D E

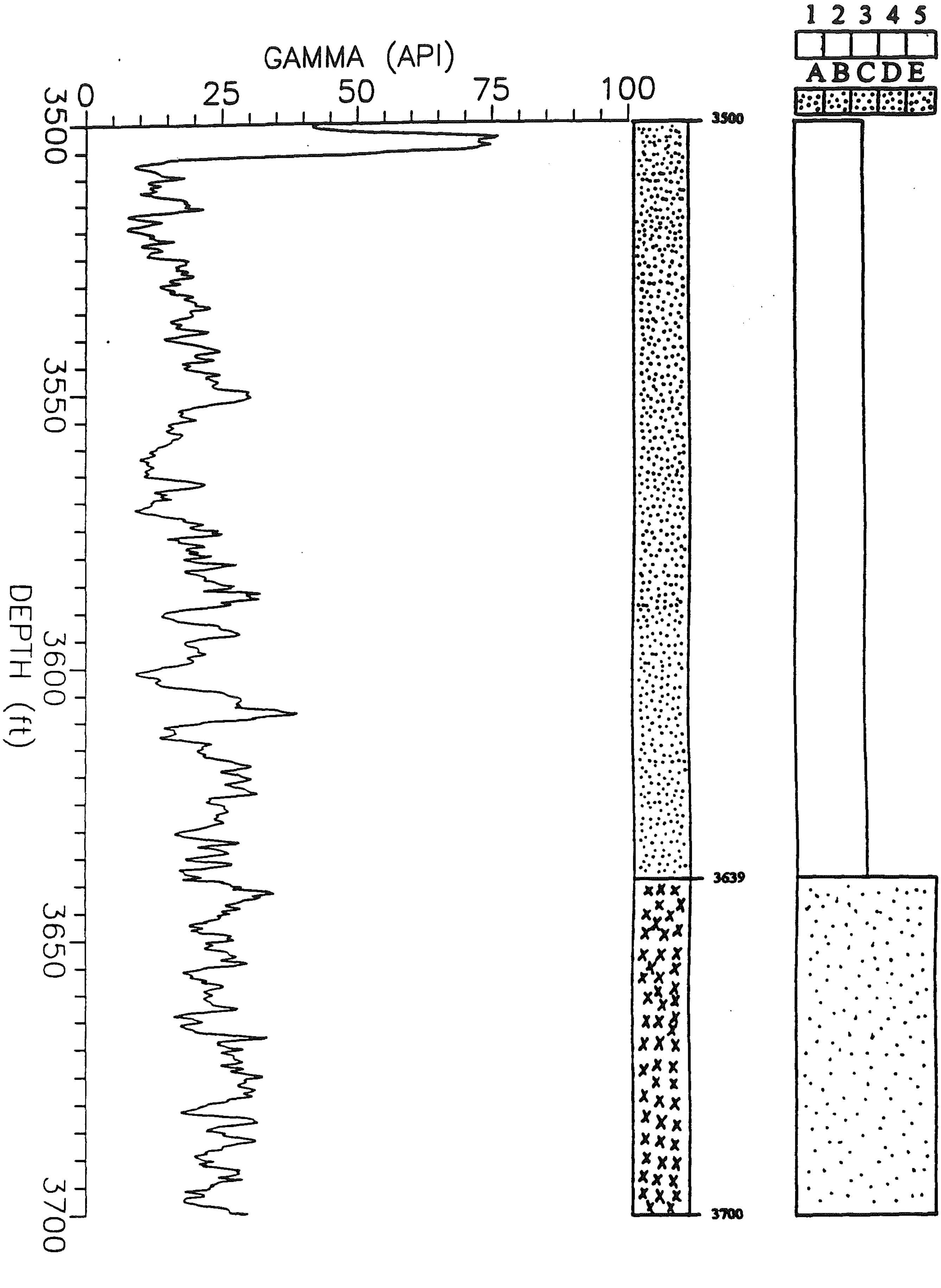
GAMMA (API)
0
25
50
75
100
3500
3550
3600
3650
3700
DEPTH (ft)
3500
3639
3700
1 2 3 4 5
A B C D E

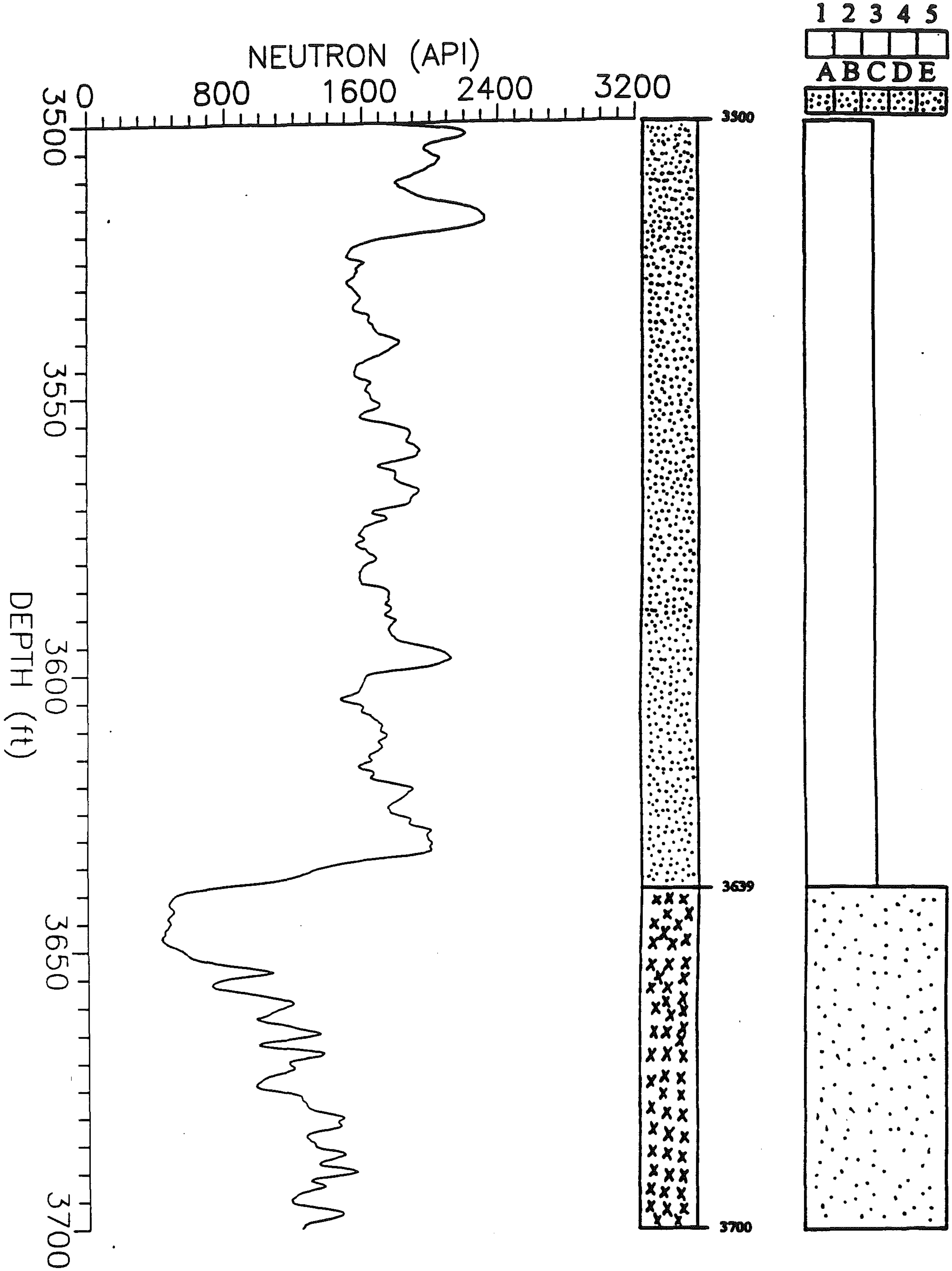
NEUTRON (API)
0
800
1600
2400
3200
3500
3550
3600
3650
3700
DEPTH (ft)
3500
3639
3700
1 2 3 4 5
A B C D E

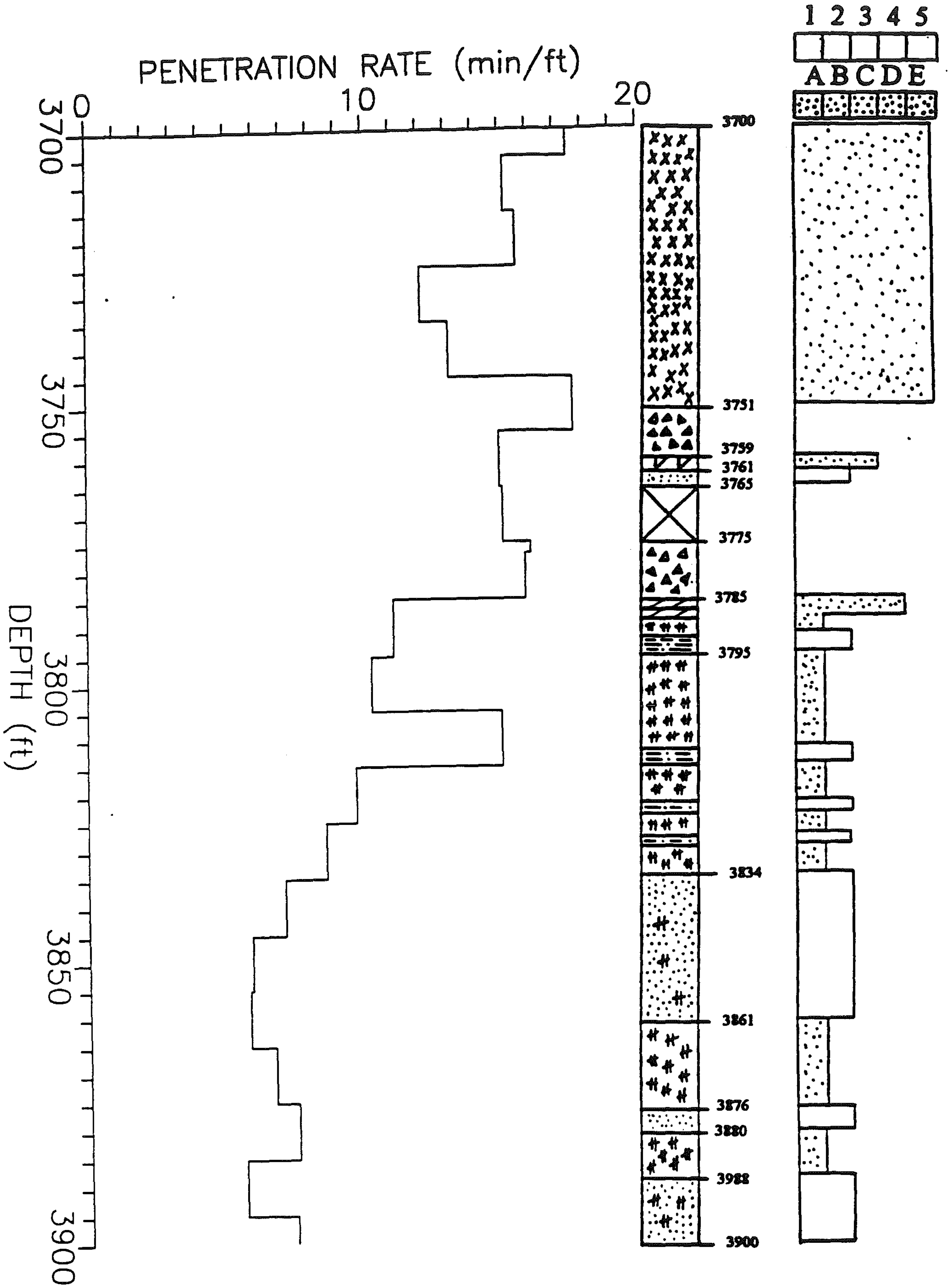
PENETRATION RATE (min/ft)
0
10
20
DEPTH (ft)
3700
3750
3800
3850
3900
3700
3751
3759
3761
3765
3775
3785
3795
3834
3861
3876
3880
3988
3900
1 2 3 4 5
A B C D E

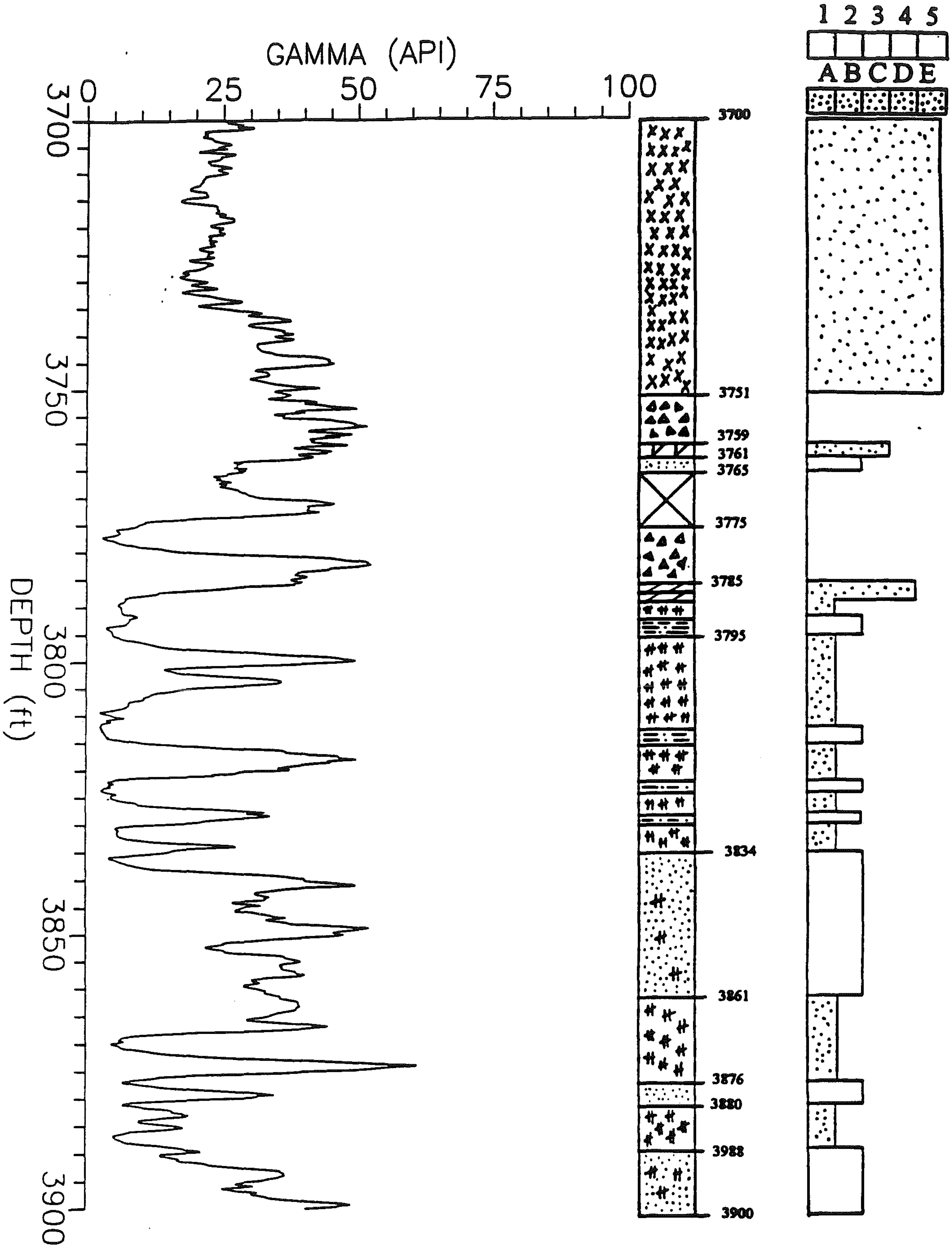

GAMMA (API)
0
25
50
75
100
3700
3750
3800
3850
3900
DEPTH (ft)
3700
3751
3759
3761
3765
3775
3785
3795
3834
3861
3876
3880
3988
3900
1 2 3 4 5
A B C D E

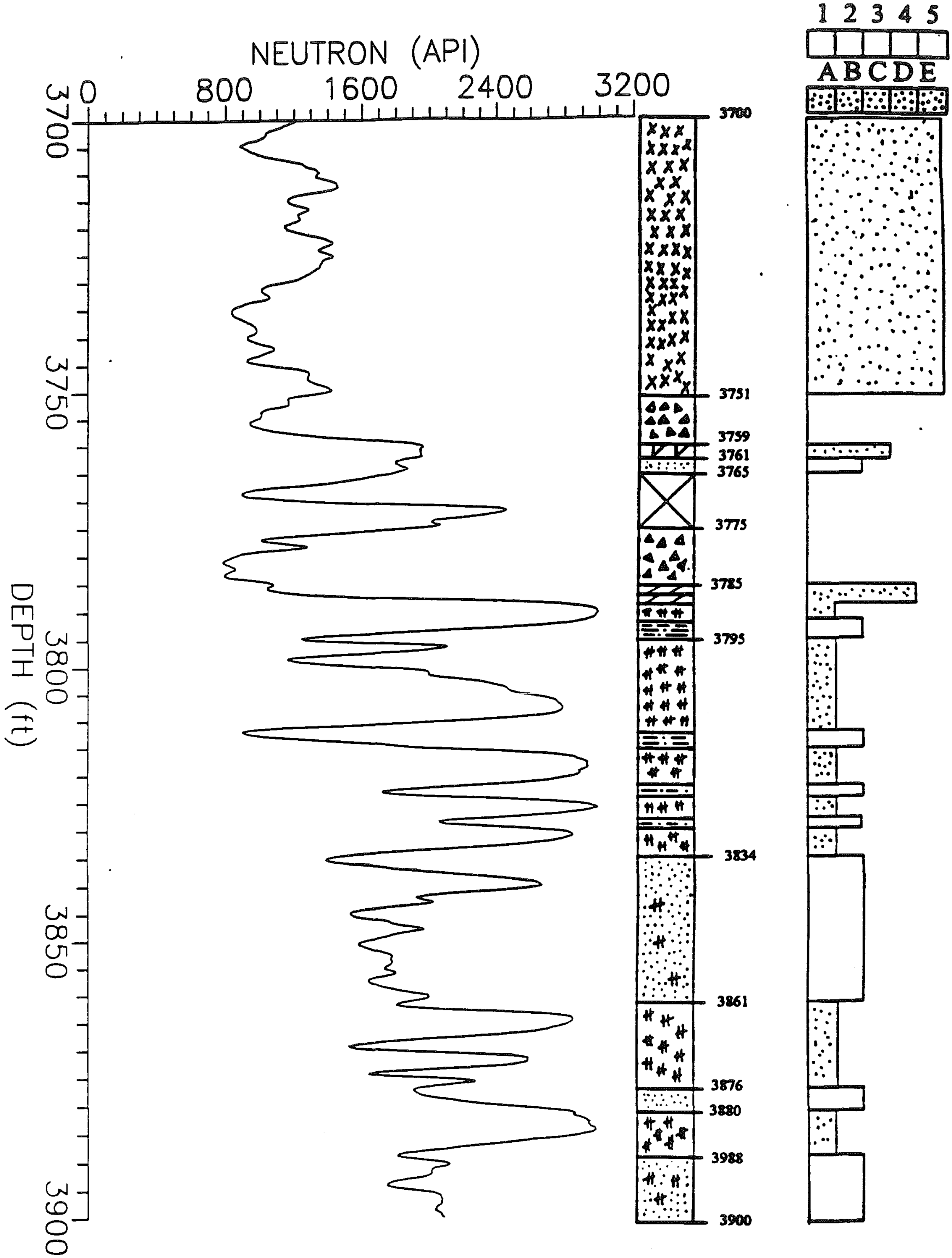

NEUTRON (API)
0
800
1600
2400
3200
DEPTH (ft)
3700
3750
3800
3850
3900
3700
3751
3759
3761
3765
3775
3785
3795
3834
3861
3876
3880
3988
3900
1 2 3 4 5
A B C D E

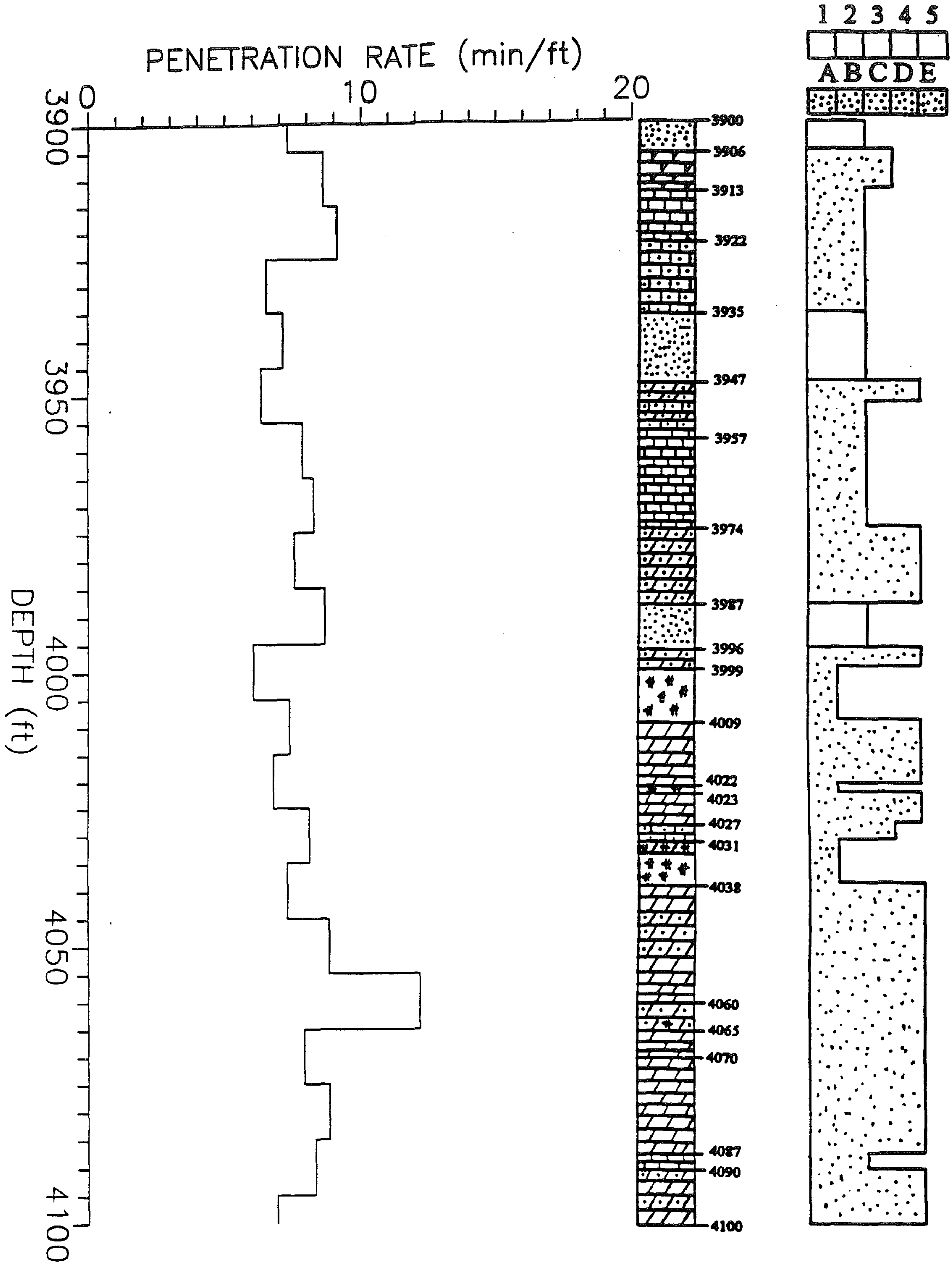

PENETRATION RATE (min/ft)
0
10
20
3900
3950
4000
4050
4100
DEPTH (ft)
3900
3906
3913
3922
3935
3947
3957
3974
3987
3996
3999
4009
4022
4023
4027
4031
4038
4060
4065
4070
4087
4090
4100
1 2 3 4 5
A B C D E

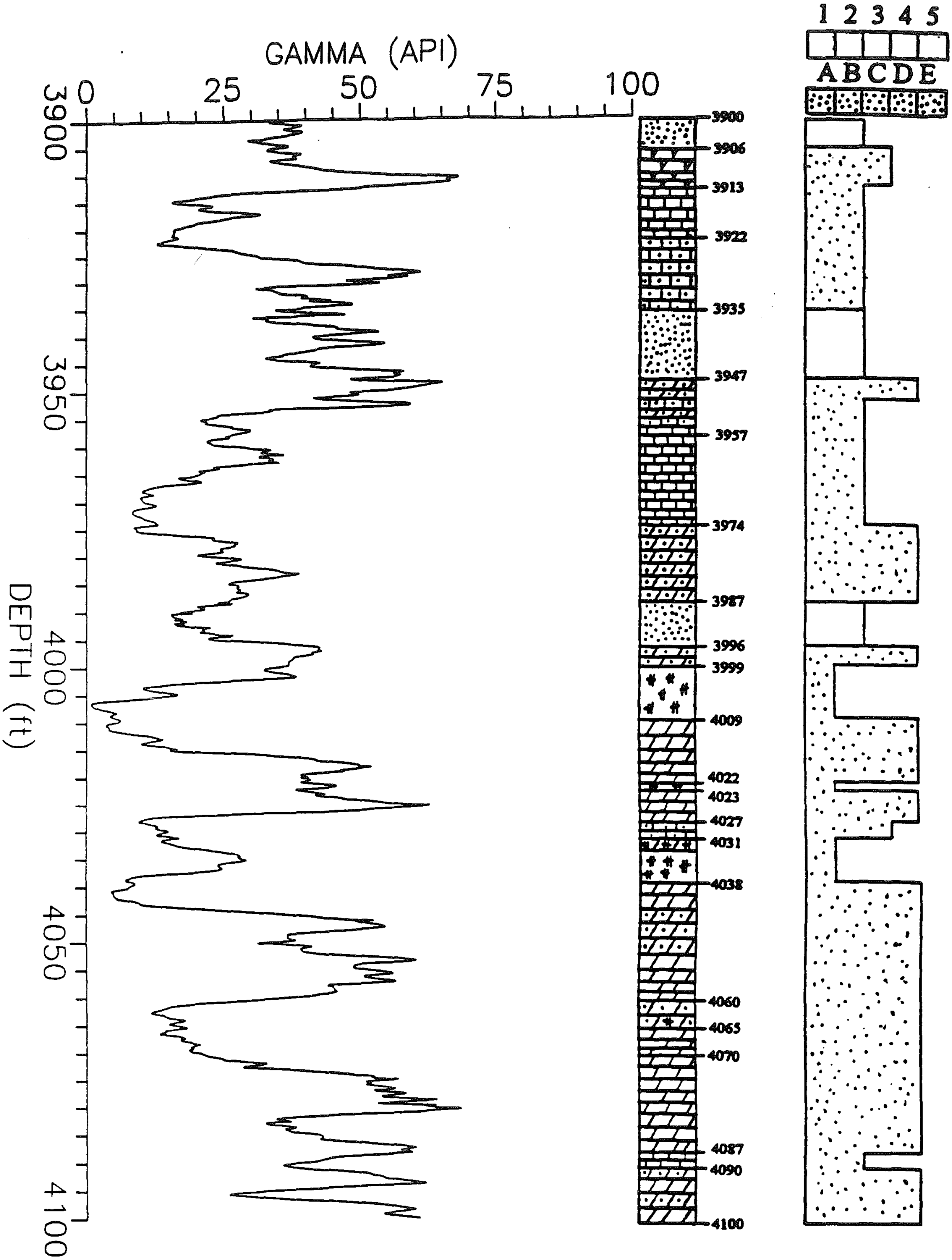
GAMMA (API)
0
25
50
75
100
3900
3950
4000
4050
4100
DEPTH (ft)
3900
3906
3913
3922
3935
3947
3957
3974
3987
3996
3999
4009
4022
4023
4027
4031
4038
4060
4065
4070
4087
4090
4100
1 2 3 4 5
A B C D E

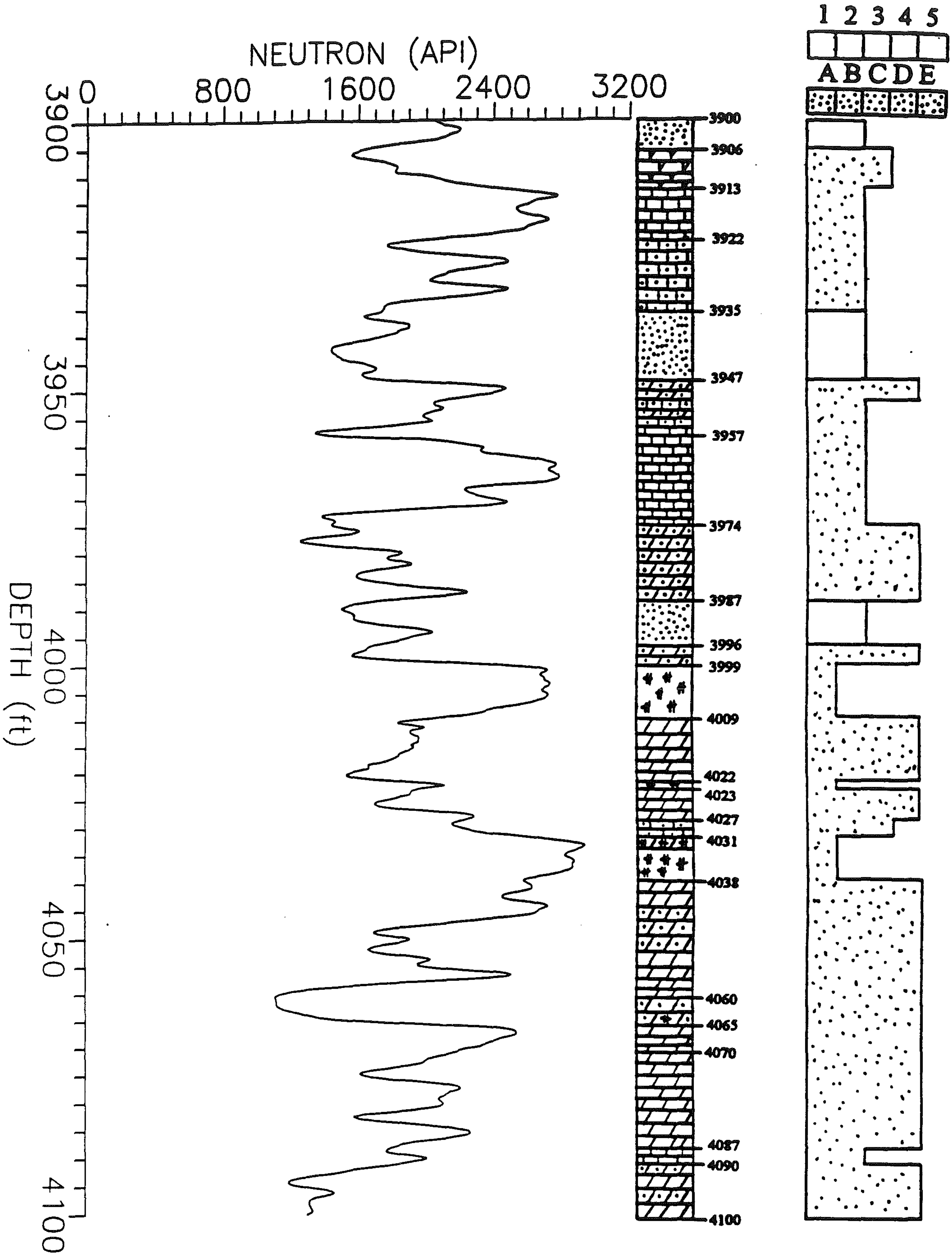

NEUTRON (API)
0
800
1600
2400
3200
3900
3950
4000
4050
4100
DEPTH (ft)
3900
3906
3913
3922
3935
3947
3957
3974
3987
3996
3999
4009
4022
4023
4027
4031
4038
4060
4065
4070
4087
4090
4100
1 2 3 4 5
A B C D E

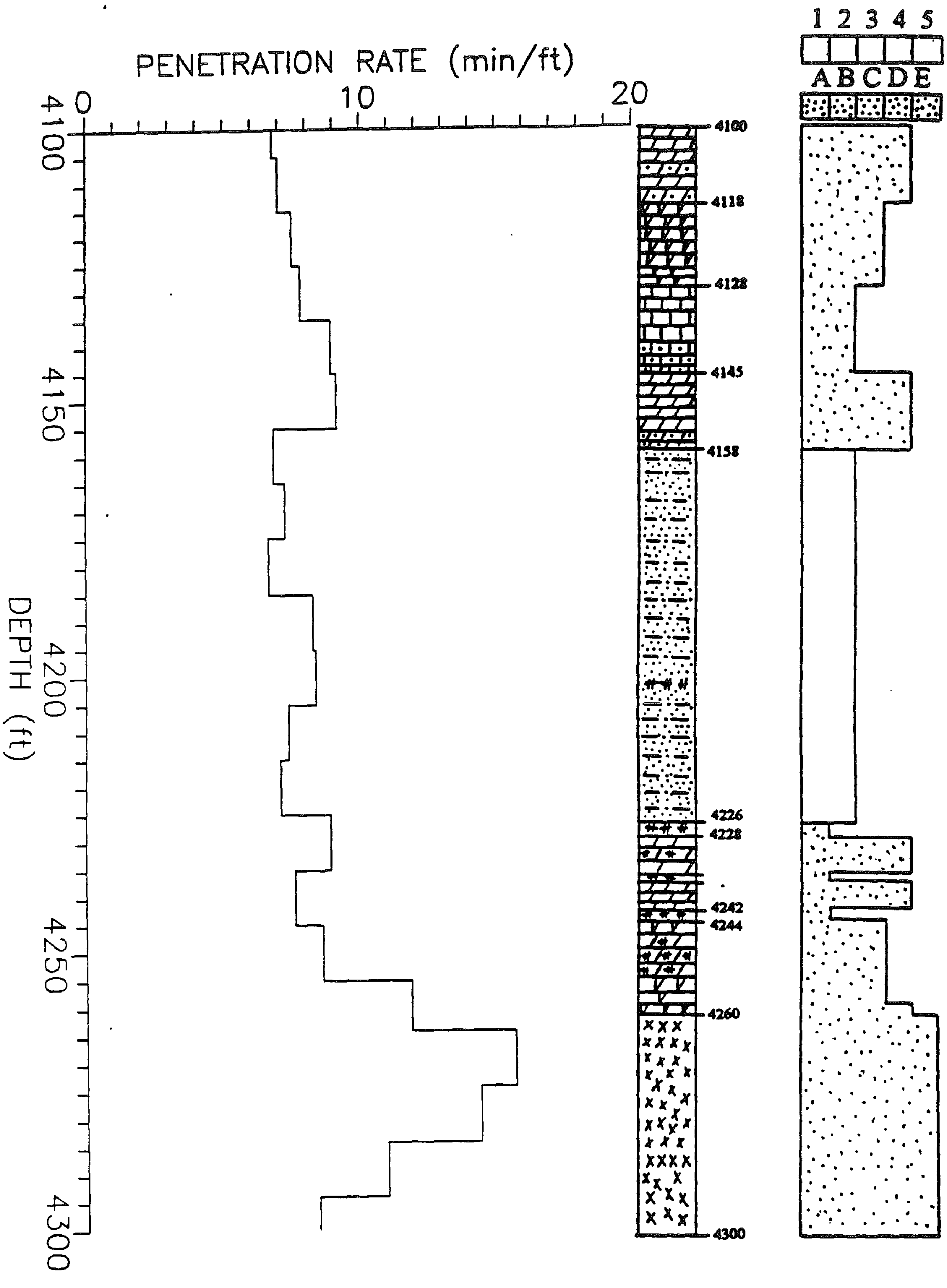
PENETRATION RATE (min/ft)
0
10
20
DEPTH (ft)
4100
4150
4200
4250
4300
4100
4118
4128
4145
4158
4226
4228
4242
4244
4260
4300
1 2 3 4 5
A B C D E

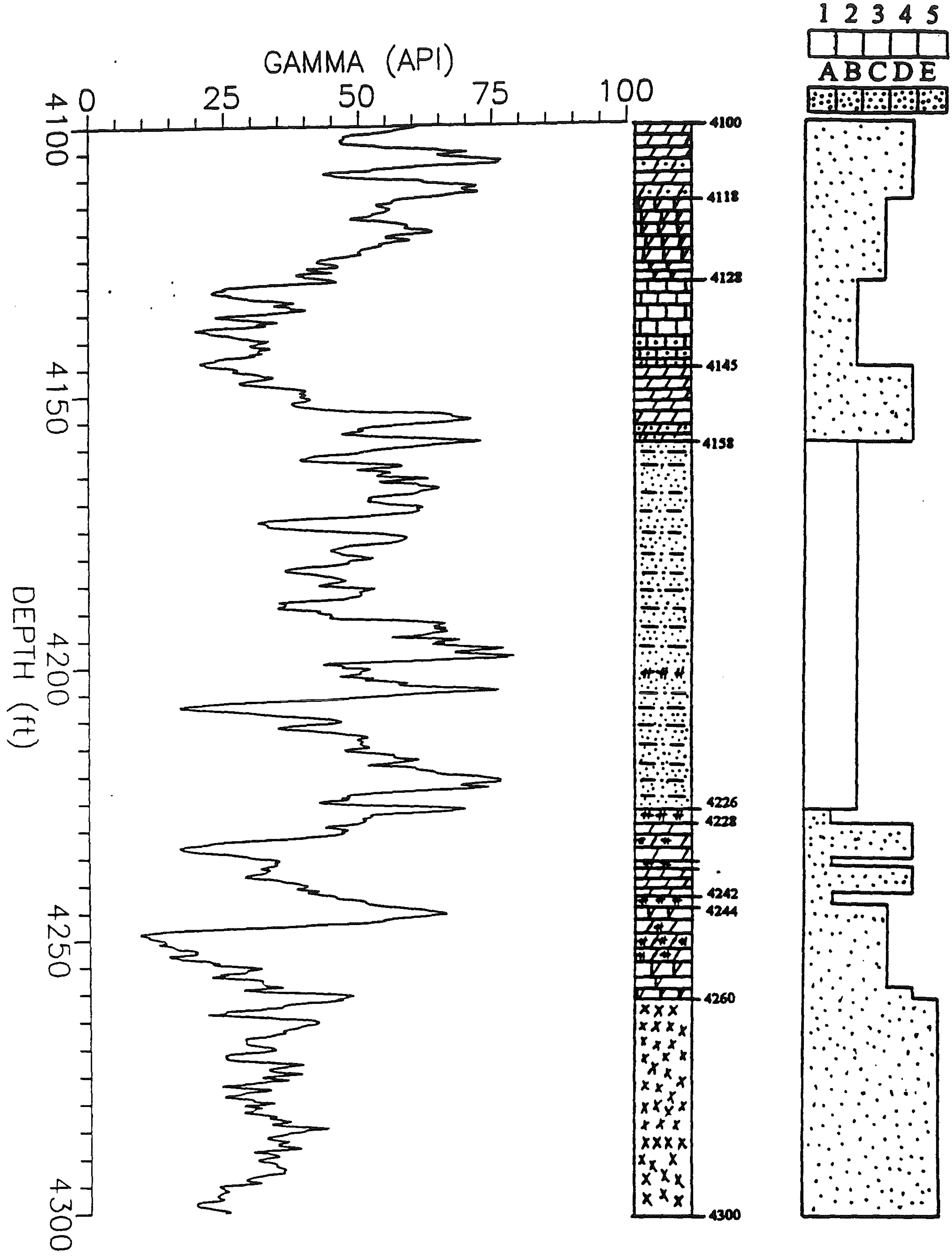

GAMMA (API)
0
25
50
75
100
4100
4150
4200
4250
4300
DEPTH (ft)
4100
4118
4128
4145
4158
4226
4228
4242
4244
4260
4300
1 2 3 4 5
A B C D E

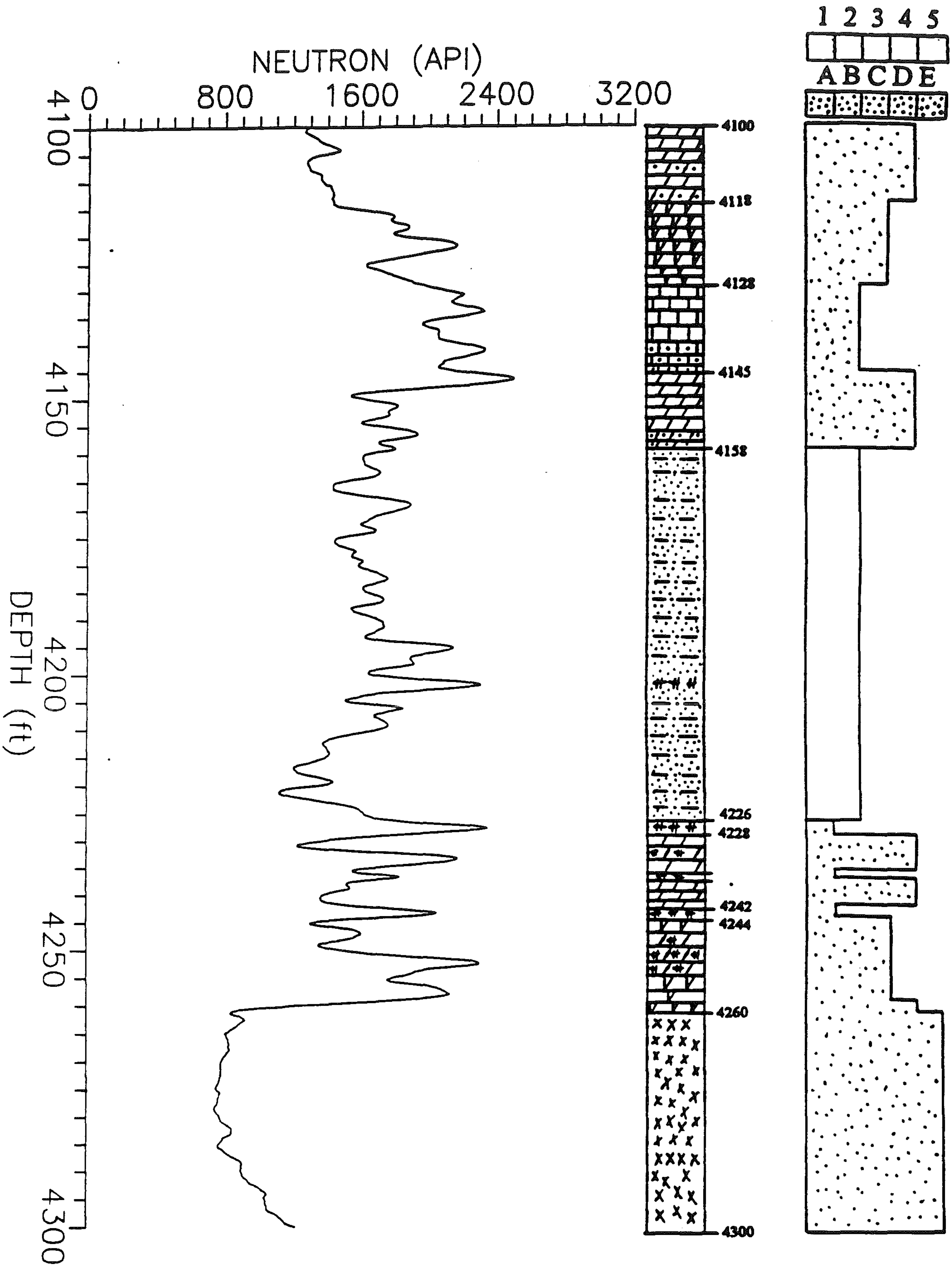

NEUTRON (API)
0
800
1600
2400
3200
4100
4150
4200
4250
4300
DEPTH (ft)
4100
4118
4128
4145
4158
4226
4228
4242
4244
4260
4300
1 2 3 4 5
A B C D E

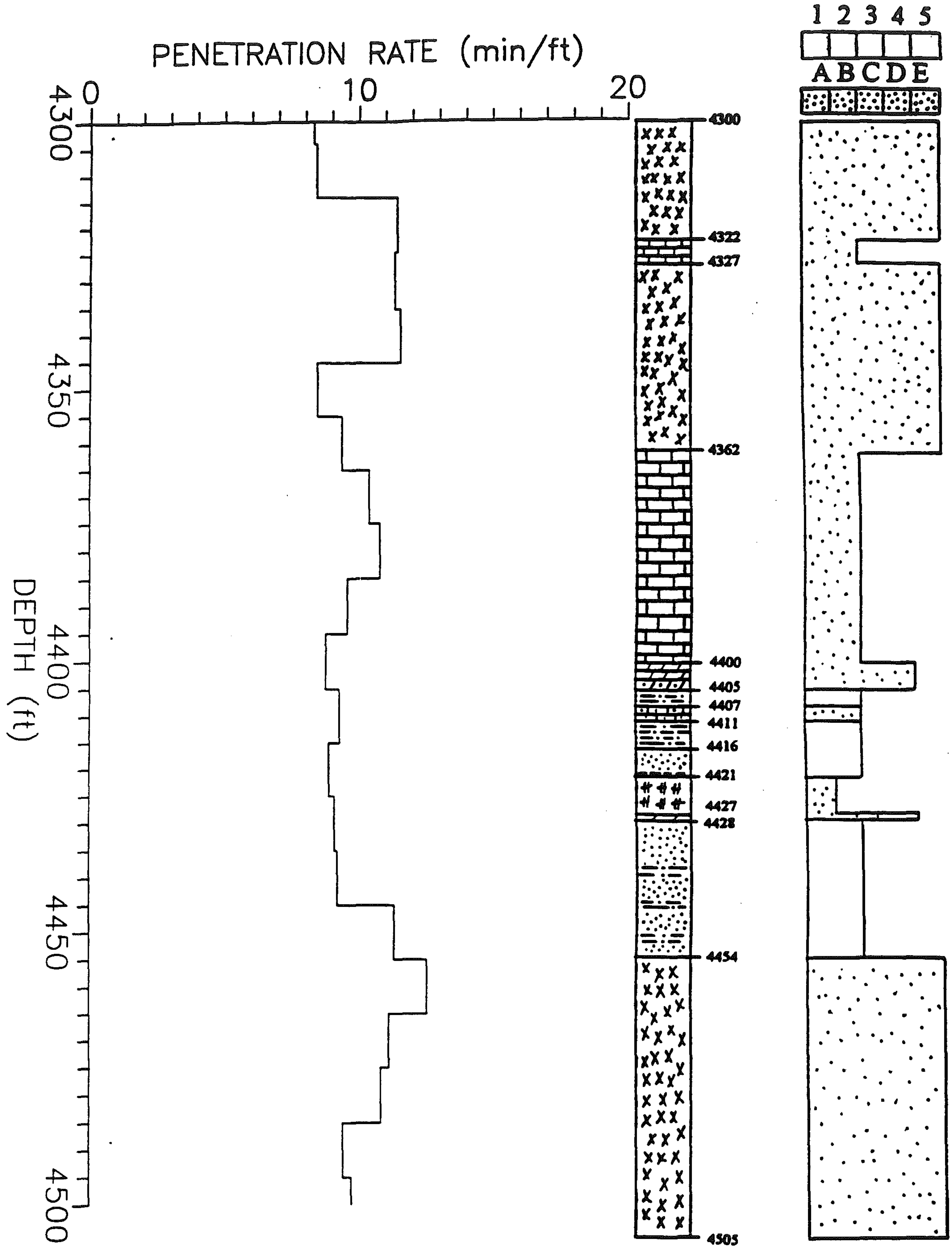
PENETRATION RATE (min/ft)
0
10
20
DEPTH (ft)
4300
4350
4400
4450
4500
4300
4322
4327
4362
4400
4405
4407
4411
4416
4421
4427
4428
4454
4505
1 2 3 4 5
A B C D E

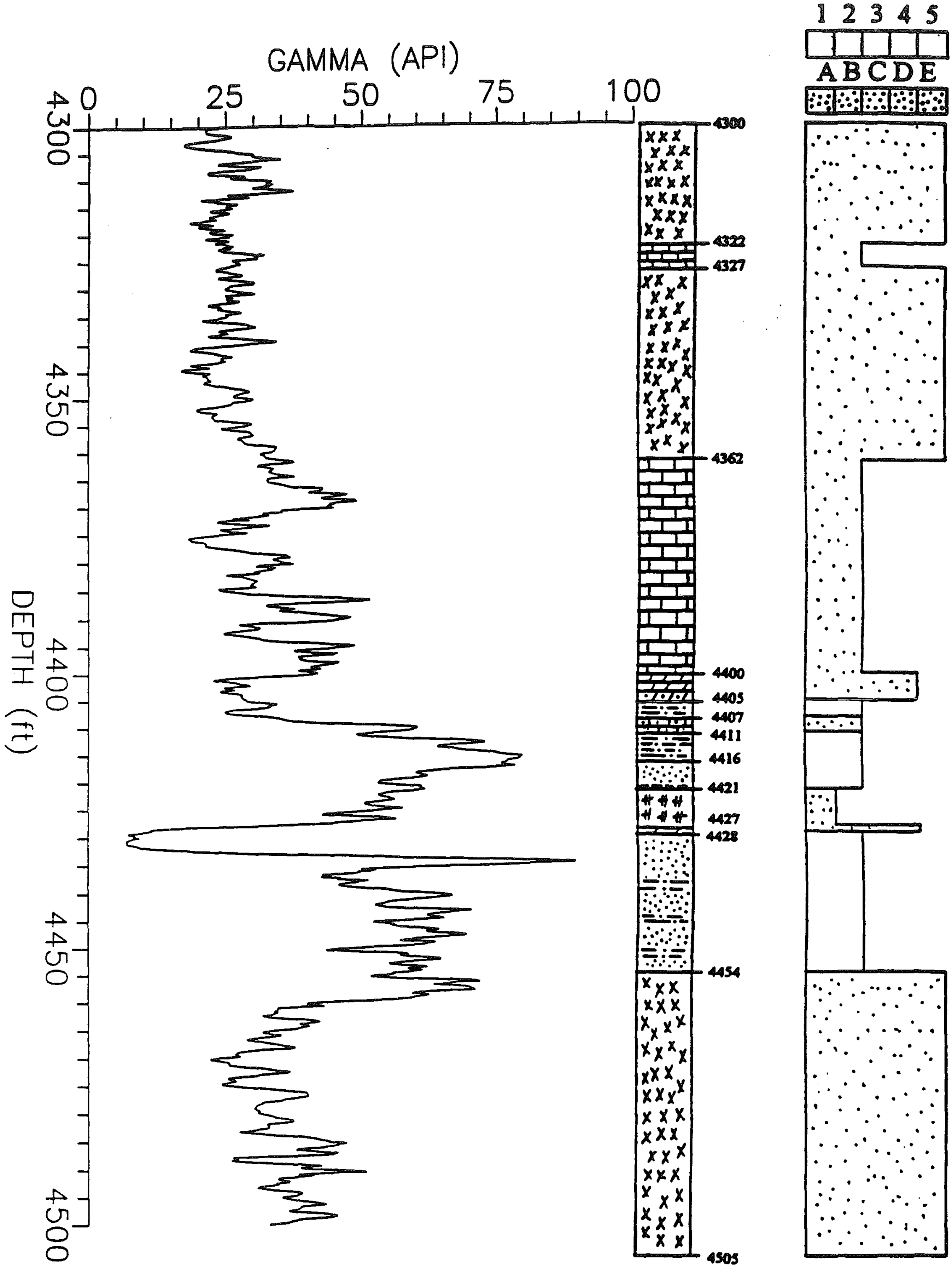
GAMMA (API)
0
25
50
75
100
4300
4350
4400
4450
4500
DEPTH (ft)
4300
4322
4327
4362
4400
4405
4407
4411
4416
4421
4427
4428
4454
4505
1 2 3 4 5
A B C D E

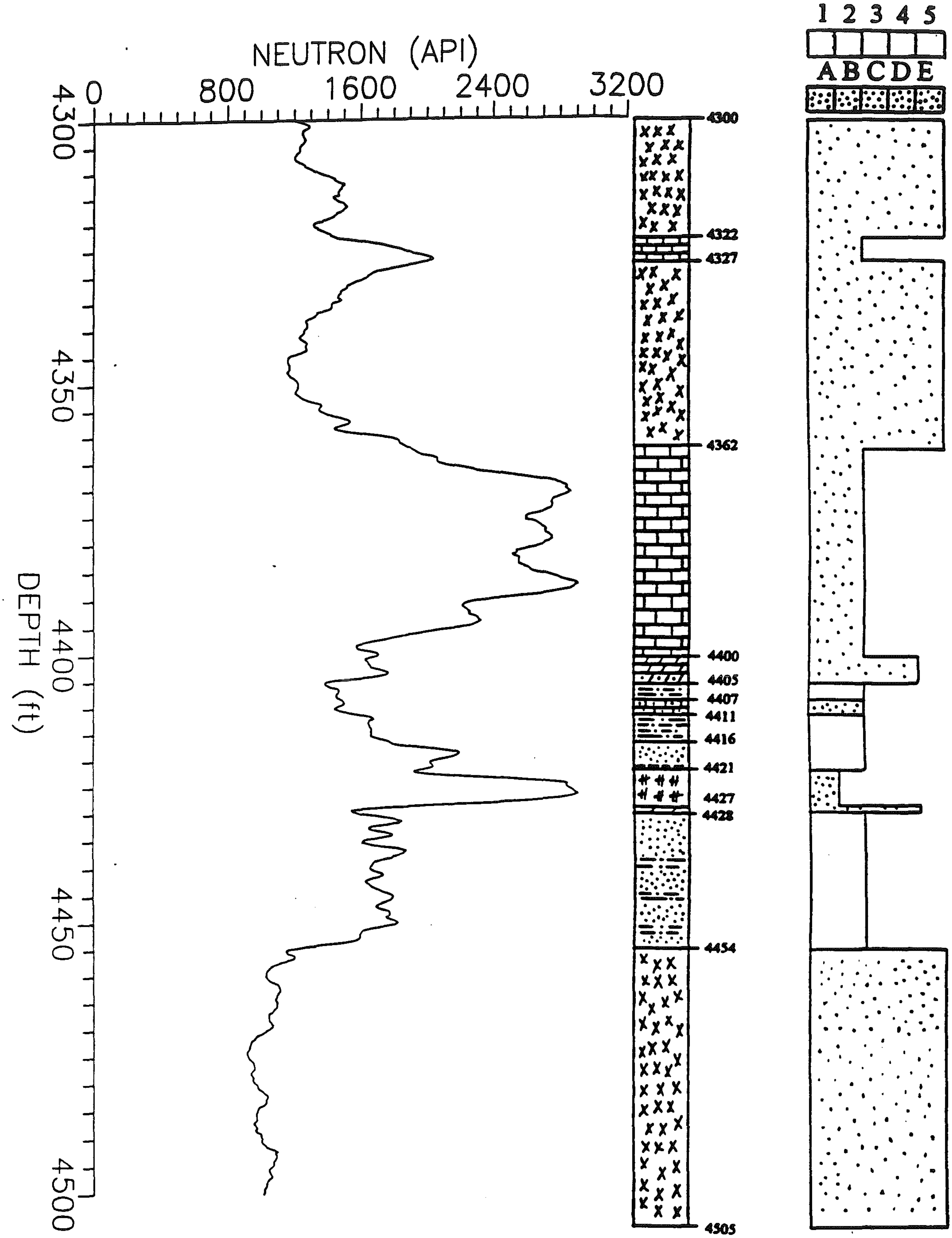
NEUTRON (API)
0
800
1600
2400
3200
DEPTH (ft)
4300
4350
4400
4450
4500
4322
4327
4362
4400
4405
4407
4411
4416
4421
4427
4428
4454
4505
1 2 3 4 5
A B C D E

APPENDIX 10

SUMMARY EQUILIBRIUM TEMPERATURE VERSUS DEPTH AT 25 FEET INTERVALS FOR THE ALPINE1/FEDERAL BOREHOLE

DEPTH ft	TEMPERATURE F	DEPTH m	TEMPERATURE C
25	47.51	7.62	8.62
50	51.64	15.24	10.91
75	51.51	22.86	10.84
100	51.81	30.48	11.01
125	52.44	38.10	11.36
150	53.16	45.72	11.76
175	53.89	53.34	12.16
200	54.72	60.96	12.62
225	55.59	68.58	13.11
250	56.53	76.20	13.63
275	57.32	83.82	14.07
300	58.13	91.44	14.52
325	58.91	99.06	14.95
350	59.93	106.68	15.52
375	60.88	114.30	16.04
400	61.77	121.92	16.54
425	62.69	129.54	17.05
450	63.55	137.16	17.53
475	64.66	144.78	18.14
500	65.53	152.40	18.63
525	66.66	160.02	19.26
550	67.56	167.64	19.76
575	68.60	175.26	20.33
600	69.66	182.88	20.92
625	70.60	190.50	21.44
650	71.64	198.12	22.02
675	72.71	205.74	22.62
700	73.53	213.36	23.07
725	74.62	220.98	23.68
750	75.65	228.60	24.25
775	76.77	236.22	24.87
800	77.70	243.84	25.39
825	78.60	251.46	25.89
850	79.50	259.08	26.39
875	80.35	266.70	26.86
900	81.16	274.32	27.31
925	81.96	281.94	27.76
950	82.85	289.56	28.25
975	83.84	297.18	28.80
1000	84.66	304.80	29.26
1025	85.54	312.42	29.74
1050	86.55	320.04	30.31
1075	87.42	327.66	30.79
1100	88.36	335.28	31.31
1125	89.17	342.90	31.76
1150	89.85	350.52	32.14
1175	90.63	358.14	32.57
1200	91.34	365.76	32.97

DEPTH ft	TEMPERATURE F	DEPTH m	TEMPERATURE C
1225	92.01	373.38	33.34
1250	92.69	381.00	33.72
1275	93.25	388.62	34.03
1300	93.87	396.24	34.37
1325	94.70	403.86	34.83
1350	95.89	411.48	35.49
1375	96.10	419.10	35.61
1400	96.36	426.72	35.76
1425	96.90	434.34	36.06
1450	97.34	441.96	36.30
1475	97.89	449.58	36.61
1500	98.46	457.20	36.92
1525	99.12	464.82	37.29
1550	100.10	472.44	37.83
1575	100.62	480.06	38.12
1600	101.36	487.68	38.53
1625	102.23	495.30	39.02
1650	103.12	502.92	39.51
1675	103.97	510.54	39.98
1700	104.90	518.16	40.50
1725	105.70	525.78	40.94
1750	106.59	533.40	41.44
1775	107.40	541.02	41.89
1800	108.21	548.64	42.34
1825	108.96	556.26	42.76
1850	109.88	563.88	43.27
1875	110.63	571.50	43.68
1900	111.32	579.12	44.07
1925	112.15	586.74	44.53
1950	112.86	594.36	44.92
1975	113.70	601.98	45.39
2000	114.24	609.60	45.69
2025	115.02	617.22	46.12
2050	115.84	624.84	46.58
2075	116.65	632.46	47.03
2100	117.53	640.08	47.52
2125	118.24	647.70	47.91
2150	119.04	655.32	48.36
2175	119.69	662.94	48.72
2200	120.46	670.56	49.14
2225	121.26	678.18	49.59
2250	122.06	685.80	50.03
2275	122.86	693.42	50.48
2300	123.80	701.04	51.00
2325	124.55	708.66	51.42
2350	125.18	716.28	51.77
2375	126.06	723.90	52.26
2400	126.78	731.52	52.66

DEPTH ft	TEMPERATURE F	DEPTH m	TEMPERATURE C
2425	127.49	739.14	53.05
2450	128.13	746.76	53.41
2475	129.15	754.38	53.97
2500	129.89	762.00	54.38
2525	130.87	769.62	54.93
2550	131.49	777.24	55.27
2575	132.20	784.86	55.67
2600	132.82	792.48	56.01
2625	133.71	800.10	56.51
2650	134.69	807.72	57.05
2675	135.27	815.34	57.37
2700	135.76	822.96	57.64
2725	136.20	830.58	57.89
2750	136.65	838.20	58.14
2775	137.18	845.82	58.43
2800	137.71	853.44	58.73
2825	138.25	861.06	59.03
2850	138.88	868.68	59.38
2875	139.58	876.30	59.77
2900	139.96	883.92	59.98
2925	140.76	891.54	60.42
2950	141.48	899.16	60.82
2975	142.16	906.78	61.20
3000	142.61	914.40	61.45
3025	143.41	922.02	61.89
3050	144.03	929.64	62.24
3075	144.65	937.26	62.58
3100	145.27	944.88	62.93
3125	145.81	952.50	63.23
3150	146.58	960.12	63.66
3175	147.32	967.74	64.07
3200	147.88	975.36	64.38
3225	148.74	982.98	64.86
3250	149.51	990.60	65.28
3275	150.20	998.22	65.67
3300	150.79	1005.84	65.99
3325	151.35	1013.46	66.31
3350	151.95	1021.08	66.64
3375	152.56	1028.70	66.98
3400	153.01	1036.32	67.23
3425	153.37	1043.94	67.43
3450	153.72	1051.56	67.62
3475	154.02	1059.18	67.79
3500	154.67	1066.80	68.15
3525	155.50	1074.42	68.61
3550	156.03	1082.04	68.91
3575	156.57	1089.66	69.21
3600	157.09	1097.28	69.49

DEPTH ft	TEMPERATURE F	DEPTH m	TEMPERATURE C
3625	157.46	1104.90	69.70
3650	157.91	1112.52	69.95
3675	158.25	1120.14	70.14
3700	158.59	1127.76	70.33
3725	158.86	1135.38	70.48
3750	159.14	1143.00	70.63
3775	159.68	1150.62	70.93
3800	160.75	1158.24	71.53
3825	161.55	1165.86	71.97
3850	161.92	1173.48	72.18
3875	162.35	1181.10	72.42
3900	162.74	1188.72	72.63
3925	163.12	1196.34	72.84
3950	163.53	1203.96	73.07
3975	163.99	1211.58	73.33
4000	164.48	1219.20	73.60
4025	164.89	1226.82	73.83
4050	165.28	1234.44	74.04
4075	165.90	1242.06	74.39
4100	166.20	1249.68	74.56
4125	166.52	1257.30	74.73
4150	166.99	1264.92	74.99
4175	167.70	1272.54	75.39
4200	168.04	1280.16	75.58
4225	168.47	1287.78	75.82
4250	169.02	1295.40	76.12
4275	169.40	1303.02	76.33
4300	169.82	1310.64	76.57
4325	170.26	1318.26	76.81
4350	170.73	1325.88	77.07
4375	171.24	1333.50	77.36
4400	171.83	1341.12	77.68
4425	172.22	1348.74	77.90
4450	172.65	1356.36	78.14
4475	173.06	1363.98	78.37
4500	173.42	1371.60	78.57
4505	173.47	1373.12	78.59